Impact of protein, starch, and dietary fiber on functionality and protein matrix of faba bean and pea Texturized Vegetable Protein (TVP)

by

Amanda Lynn Buchko

A thesis submitted in partial fulfillment of the requirements for the degree of

Master of Science

in

Food Science and Technology

Department of Agricultural, Food and Nutritional Science
University of Alberta

Abstract

Low moisture extrusion is a complex scalable technology that uses heat, pressure and shear to texturize plant proteins into extrudates called texturized vegetable proteins (TVP) used in the development of meat analogue products. Increasing interest in meat analogues and the rise of new sources of plant proteins requires understanding of internal interactions by protein, starch and fiber to develop highly functional and nutritional TVP. This thesis investigates the impact of moisture, protein, starch, and dietary fiber on faba bean and/or pea TVP to improve extrudate functionality and structure. Firstly, the impact of moisture (50%, 55%) and extrusion on the protein conformation and the melt rheological properties and microstructure was studied at increasing protein content (60%, 70%, 80%) as analyzed by Fourier transform infrared spectroscopy (FTIR), rheometer, confocal and scanning electron microscopy (SEM). Analysis performed correlated to TVP functionalities like expansion ratio, bulk density, water holding capacity (WHC), and oil holding capacity (OHC). Lower moisture content at 50% improved expansion of TVP with good WHC and OHC by forming a protein melt matrix with increased storage modulus (G'). As protein content increased from 60% to 70%, an appropriate level of separation of the protein phase and the starch phase allowed the formation of a relatively homogeneous protein matrix, which facilitated TVP expansion. Whereas further increasing protein content to 80%, the oblong shaped air pocket microstructure shifted to a dense protein matrix with large sporadic air pockets resulting in decreased WHC.

Secondly, the inclusion of pea starch, pea hull insoluble dietary fibers and oat β-glucan (soluble fiber) were assessed to determine improvement on TVP microstructure and functionality, while increasing the overall value-added health benefits. Inclusion of 7.5%-20% pea starch improved expansion and microstructure of pea protein and faba bean protein based TVP with

larger pores and thicker cell walls, as well as WHC. Resistant starch (RS) and slowly digestible starch (SDS) in pea was mostly converted to readily digestible starches (RDS) after extrusion treatment. Insoluble fiber (5%, 10% at 100μm and 150μm sizes) had a negative effect on expansion and disrupted the TVP microstructure but did improve WHC. Whereas soluble fiber (5%, 10%, 20%) improved TVP expansion, WHC, and OHC at all inclusion levels. At 10% inclusion and above, the blending of soluble fiber into the protein phase might help TVP expansion, leading to a decrease in bulk density. Both faba bean and pea were shown to produce TVP from a protein concentrate, and the expansion and WHC were improved upon the addition of starch and soluble fiber. Faba bean TVP was more prone to aggregation, thus showed slightly lower expansion but had similar WHC and OHC as the pea TVP. The findings from this research can help to provide understanding of microstructure and TVP functionality by modulating moisture, protein content, starch and dietary fiber inclusion to improve TVP quality and to expand TVP source protein options like faba bean in the market.

Preface

This thesis is an original work by Amanda Buchko under the supervision of Dr. Lingyun Chen of the Department of Agriculture, Food, and Nutritional Science at the University of Alberta. This thesis consists of four chapters: Chapter 1 provides a literature review and the research rationale related to the thesis topic, Chapter 2 focuses on the effect of moisture and protein content on faba bean and pea protein TVP structure and functionality, Chapter 3 compares the effect of starch and dietary fiber on TVP structure and functionality, lastly chapter 4 provides a conclusion to the thesis, study innovations and future work.

A version of Chapter 2 of this thesis has been submitted as "Buchko, A., Han, J., and Chen, L. (2024) Effects of Moisture and Protein Content on Protein Structure and Protein-starch Phase Separation in Relation to the Functional Properties of Faba Bean and Pea Texturized Vegetable Protein" to Food Research International. I was responsible for: Conceptualization, Methodology, Formal analysis, Investigation, Data curation, Writing - original draft, and Writing - review & editing. Dr. Lingyun Chen was the supervisory author responsible for: Conceptualization, Resources, Writing - review & editing, Supervision, Project administration, and Funding acquisition. Dr. Jay Han was responsible for: Conceptualization and Resources.

Chapter 2 has been presented in part as "Effect of protein and moisture content on physiochemical and structural attributes of Pea Texturized Vegetable Protein (TVP)" at the IFT FIRST Conference in Chicago, U.S. on July 16-19, 2023.

Chapter 3 is in preparation for submission to a peer reviewed international journal.

Acknowledgements

I would very much like to express my deepest gratitude to my supervisor Dr. Lingyun Chen for her dedication, knowledge, patience and guidance for me along this journey. Your generous encouragement and support has given me so many opportunities within the University of Alberta and the greater scientific community that would not have been achievable otherwise.

Words cannot express my gratitude and appreciation to Dr. Jay Han for being my committee member and lifelong mentor. I would not be where I am without your guidance and advice which has shaped my career path and personal growth.

This endeavor could not have been possible without my colleague's support and encouragement at the Food Processing Development Centre. My sincerest thank you to Dindo Quiambao for your extrusion expertise and friendship as well as to all the scientists, technologists, and management at FPDC for your help and encouragement along the way.

I would also like to thank everyone involved with the NSERC-CAPTURE CREATE program which has given me both technical and professional opportunities to grow and explore.

Finally, I would like to thank my family and friends. My parents Phyllis and Don, sisters Vanessa and Monica, and Braden for their love, support, and encouragement. And to Emily for being there wholeheartedly and sharing in this journey along the way.

Table of Contents

List of Tables

List of Figures

List of Abbreviations

AMG	Amyloglucosidase
BD	Bulk density
CV	Convicilin
DD	Degree of double helix
DO	Degree of order
ER	Expansion ratio
FTIR	Fourier transform infrared spectroscopy
G’	Storage modulus
G”	Loss modulus
HME	High moisture extrusion
L-A	Legumin A
L-α	α-Legumin
L-B	Legumin B
L-β	β-Legumin
LME	Low moisture extrusion
MS	Minor subunits
MW	Molecular weight
OHC	Oil holding capacity
PAA	Pancreatic α-amylase
RS	Resistant starch
RDS	Readily digestible starch
SDS	Slowly digestible starch

SDS-PAGE	Sodium dodecyl-sulfate poly-acrylamide gel electrophoresis
SEM	Scanning electron microscope
SM	Starting materials
SME	Specific mechanical energy
TDS	Total digestible starch
TVP	Texturized vegetable protein
V	Vicilin
WHC	Water holding capacity
XRD	X-ray Diffraction

Chapter 1: Literature Review

1.1 Plant protein based foods

The current landscape for protein-based foods consists mainly of animal-based products, though over the last two decades there has been a shift towards plant protein-based food products that have come to be termed as meat alternatives or meat analogues. Protein is an important macronutrient required for various biological functions like muscle maintenance and growth. Proteins are comprised of up to 20 essential and non-essential amino acids which can be broken down into their nitrogen sources. These proteins are found in both animal meats (myofibrillar proteins like myosin or actin) and in plants (storage proteins like globular legumin) which can be extracted from plants and used to develop meat analogues (Damodaran, 2008a). The purpose of a plant-based meat analogue is to mimic sensory qualities of meat like appearance, texture, and flavour while trying to keep the nutritional value the same or better (Sha et al., 2020). As the world population grows with a projected population of 8.5 billion by 2030 (United Nations, 2022), the need for additional sustainable sources of protein increases other than protein strictly from livestock animals and their derivatives like milk or eggs. Alternative sources of proteins from plants can help fill this gap but require additional processing and development into a variety of food products and ingredients. Consumption of alternative proteins is expected to grow from 13 to 97 million metric tons by 2035 reaching $290 billion USD with the largest increase in compound annual growth rate of 16% between 2025-2030 of plant-based alternatives (Morach et al., 2021). Flexitarians choose to substitute meat in their diets with alternative sources of proteins including plant-based meat analogues and have become one of the main driving forces behind the growth of the alternative protein market, providing opportunity for new sources of plant proteins and plant-based meat analogues (Vatansever et al., 2020; Baune et al., 2022).

Other alternative sources of protein for meat analogues are not limited to but include insects, cultured meat, and fermentation based mycoproteins from fungi, though they may have negative consumer perceptions based on cultural preferences, political views, specific food aversions, or are too costly to produce, are not yet commercially available, or have negative impacts on the environment (Van Loo et al., 2020; Green et al., 2022; Dekkers et al., 2018a). Proteins extracted from plants naturally high in protein are a more accepted source of protein for use in meat analogues. Soy and wheat are typically used to develop meat analogue structural qualities due to their ability to form gels and provide elasticity needed to achieve the desired meat-like texture, but soy and wheat are both known allergens and consumers negatively associate soy with genetic modification (Kurek et al., 2022). As new sources of plant proteins become available, equipment and techniques need to be adapted to accommodate these changes in protein sources and become relevant again. Therefore, the importance of developing meat analogues with other plant-based sources of protein like faba bean or pea must be stressed in order to provide product developers with alternative sources of protein to meet consumers' needs.

The use of plant protein from pulse crops like faba bean or pea can benefit the environment directly or from an industry perspective, making plant proteins a more sustainable source of protein. By fixing nitrogen into the soil and implemented into crop rotations, it can promote biodiversity, conservation agriculture and decrease the use of fertilizers (Boukid, 2021). Environmental life cycle assessments of faba bean and pea have shown that the negative impact on climate in CO_2 equivalents per kg of legumes (0.55-0.57kg CO_2-eq/kg) were substantially lower than that of meat from ruminant animals (19-38kg CO_2-eq/kg) and even slightly lower than cereal grains (0.66-0.72kg CO_2-eq/kg) in all dried and intermediate forms as well as in finished products (Svanes et al., 2022). The incorporation of plant-based proteins can also improve overall human

diet quality by increasing intake of fiber and vitamins while decreasing the intake of total fat and cholesterol and can reduce the risk of cardiovascular disease or diabetes (Sokolowski et al., 2020; Boukid, 2021). Therefore, plant proteins can provide many benefits over animal-based proteins on a societal and personal scale.

Development of meat analogues are catered to consumers like flexitarians that typically eat meat products but want to consume protein from plant-based sources for a variety of social, ethical, and environmental reasons (Green et al., 2022). Therefore, these products are expected to mimic the flavour, texture, mouthfeel, and even nutritional value of animal meat products. This presents a challenge to product developers because the protein composition, structure, and functionality of plant proteins are very different than animal proteins. For example, juiciness is an attribute of meat-based products that requires water binding capabilities which is difficult to achieve without modification of plant proteins or processing by either chemical or physical means (Kurek et al., 2022). Various technologies and techniques have been developed to facilitate transformation of plant-based proteins into meat analogue products that have similar structures and properties to meat, but each technique has its own benefits and drawbacks.

Meat analogues can generally be split into two categories: i) whole muscle meats like steaks, pulled pork or whole chicken contain fibrous protein strands, or ii) reconstructed meats like burger patties, sausage, deli meats, and chicken nuggets which are generally spongy in texture. Whole muscle meat analogues can be produced by wet spinning based on plant protein solvent precipitations, electrospinning based on plant protein electrode-based principles, shear cell technology based on plant protein cooling and cone shearing, and lastly extrusion based on plant protein cooling and linear protein alignment. Reconstructed meats can be produced from ingredients made by mixing plant proteins and hydrocolloids based on cation precipitation

principles, resulting in a weak structure and limited use in products. Or by extrusion based on plant protein alignment around expanded air pockets, which can result in a stronger product capable of withstanding mixing during the development of reconstructed meat analogues (Dekkers et al., 2018a). 3-D printing can be used to produce either whole muscle or reconstructed meats by hydro-gel forming principles but has geometric limitations (Prabha et al., 2021). Extrusion is the only commercially available option that's scalable of these techniques to create fibrous whole muscle like analogues as well as sponge like products used in reconstructed meat analogue products (Dekkers et al., 2018a).

1.2 Extrusion

1.2.1 Use of extrusion for low moisture TVP

Extrusion can be defined as the process of plasticizing and texturizing proteinaceous and/or starchy materials through the use of mechanical shear, pressure, heat, and moisture to produce an expanded food product or ingredient (Vatansever et al., 2020). Extrusion uses high temperature under shear force and pressure in combination to melt and alter the structural characteristics of mainly starch and proteins. Although there are other techniques to produce meat analogues such as wet and electro-spinning, shear cell technology, 3-D printing and mixing proteins with hydrocolloids as mentioned above, extrusion is the only technology that is widely commercially available, scalable, has a low environmental impact, and also produces layered fibrous products that mimic animal meats (Dekkers et al., 2018a). Meat analogues like texturized vegetable proteins can be produced through the utilization of plant proteins undergoing a texturizing process within an extruder under high heat, pressure, and shear force. The resulting TVP can be further processed and used in various products to replicate or replace animal meats (Ek, et al., 2020a; Zhang et al., 2022a). The TVP process can be broken down into two types based mainly based off of moisture

content and temperature to control the degree of expansion and alignment of proteins to form distinct textures, low moisture extrusion (LME) and high moisture extrusion (HME).

High moisture extrusion typically uses moisture contents between 40%-80% and barrel temperatures of 100°C -150°C with a cooling die at the end of the extruder (Akdogan, 1999; Zhang et al., 2022a) to create a meat whole muscle meat like texture with fibrous protein strands aligned in the same direction as the extruder barrel. Fiber formation in HME is heavily dependent on having at least a two-phase matrix (protein, polysaccharides, and/or lipids), protein alignment and the protein's ability to form strong bonds like covalent disulfide bonds to hold the fibrous structure. Briefly, proteins hydrate, denature, and unfold from the heat and shear within the extruder to create a laminar flow where proteins re-align down the length of the barrel. Upon cooling in the long die, the newly aligned proteins or protein aggregates form noncovalent interactions but more importantly, form crosslinking between proteins with disulfide bonds to maintain a fibrous, anisotropic structure. Although to achieve both a layered and orientated fibrous structure, the protein aggregation speed must equal the phase separation speed when exiting the die (Zhang et al., 2022b).

Low moisture extrusion typically uses moisture contents between 20%-40% (Zhang et al., 2022a) and higher barrel temperatures of 130°C-180°C, though temperatures of up to 200°C have been previously investigated (Beck et al., 2017b; Lyu et al., 2023). Low moisture TVP needs higher barrel temperatures to be able to melt and plasticize the proteins since the moisture content is lower. LME can produce a range in extrudate sizes of TVP with expansion and porous structures to mimic cooked animal meats (Akdogan, 1999). For example, large extrudates (15-20mm) can mimic cooked nuggets or large meat chunks, smaller extrudates (2-15mm) can mimic minced meats like ground beef or chicken, whereas flaked or fine extrudates can be used as a binder in

products like sausage and patties (Vatansever et al., 2020). Degree of expansion and resulting porous structures can be controlled in the melt through manipulation of nucleation sites (starting points of expansion), bubble growth (increasing bubble size), coalescence (merging of bubbles), and shrinkage (decreasing bubble size), and when exiting the die through fixation (solidification of the melt and strength of the protein network). These mechanisms are largely governed by ingredient properties, barrel temperature, moisture content, and shear, which in turn effect melt elasticity and viscosity (Kristiawan et al., 2020).

The final product moisture content of HME can vary but is typically above 30% and is ready-to-eat but requires packaging and refrigeration or freezing to preserve the product and extend the product's shelf life. HME products can be consumed as-is or as an ingredient in food products, but still requires further technological development and adaptation in industry. LME on the other hand is dried after extrusion and has a final moisture content at or below 12%, making it shelf stable and greatly extending the shelf life compared to HME products. Conversely, LME is not ready to eat and requires hydration prior to consumption but is typically used as an ingredient in further food products and has more versatility with regards to shape, size, texture and food product applications (Zhang et al., 2022a). In addition, HME products need high levels of protein content generally above 60% to form a fibrous network, whereas LME products tend to have lower protein (50%-70%) content and are higher in starch to promote the desired expanded structure (Zhang et al., 2022a; Zhang et al., 2019).

1.2.2 Utilizing TVP as a food source

TVP produced via high moisture extrusion mimics the fibrous structure of whole muscle meats, with long protein chains aligned in the same direction parallel to each other and can be further processed by shredded or cut but are meant to be less processed and resemble whole muscle

meat products (Ryu, 2020). Currently, HME analogues require substantially more development and are considered an immature market, while LME analogues have mature developed markets around the globe sourced from soy, wheat, and pea though faba bean and canola sources are emerging (Baune et al., 2022; Zhang et al., 2022a). Low moisture TVP can provide a wider range of products over high moisture TVP and can be utilized in a wide variety of food products and have extended application beyond 100% plant-based products with typical inclusion rates of 30% before negative sensory attributes are reached (Baune et al., 2021; Hidayat et al., 2018). For example, TVP can be incorporated into meatballs to decrease animal meat proportion while simultaneously increasing fiber content, beneficial omega-fatty acids, and lowering environmental impact through life cycle assessment studies (Baune et al., 2021). Hidayat et al., (2018) found inclusion of low moisture TVP made from soy protein up to 40% in beef sausage increased the water holding and cook yield of sausage while decreasing the fat content, though an increase in TVP resulted in a softer product. Low moisture TVP comes in a variety of sizes and altered texture, making low moisture TVP a shelf stable versatile product (Zhang et al., 2022a). Based on the size of TVP and the expected texture of subsequent food products, low moisture TVP can be used in meat analogue products such as meat chunks, meatballs, burgers, chicken nuggets, sausage and as how ground meat would be used in products like chili, dumplings, or as taco meat (Baune et al., 2021; Baune et al., 2022; Zhang et al., 2022a; Ryu, 2020; Hidayat et al., 2018). Low moisture TVP can be sold and stored as dry products which have a longer shelf life than high moisture TVP, although low moisture TVP needs to be rehydrated with water for typically 15 minutes before consuming or further processing (Zhang et al., 2022a; Hidayat et al., 2018).

1.2.3 Screw configuration and extrusion zones

Typically, low moisture TVP is produced using a twin-screw extruder (Fig 1.1) because they are more adaptable, efficient at mixing and kneading the protein melt, and have more versatile processing capacities compared to a single screw extruder. The extruder barrel length can be roughly divided into three sections based on the structural transformation of the protein melt in the extruder. The three zones are: i) the feeding zone, ii) the mixing zone, and iii) the melting zone. Each zone has different functional elements that make up the screw configuration. Screw

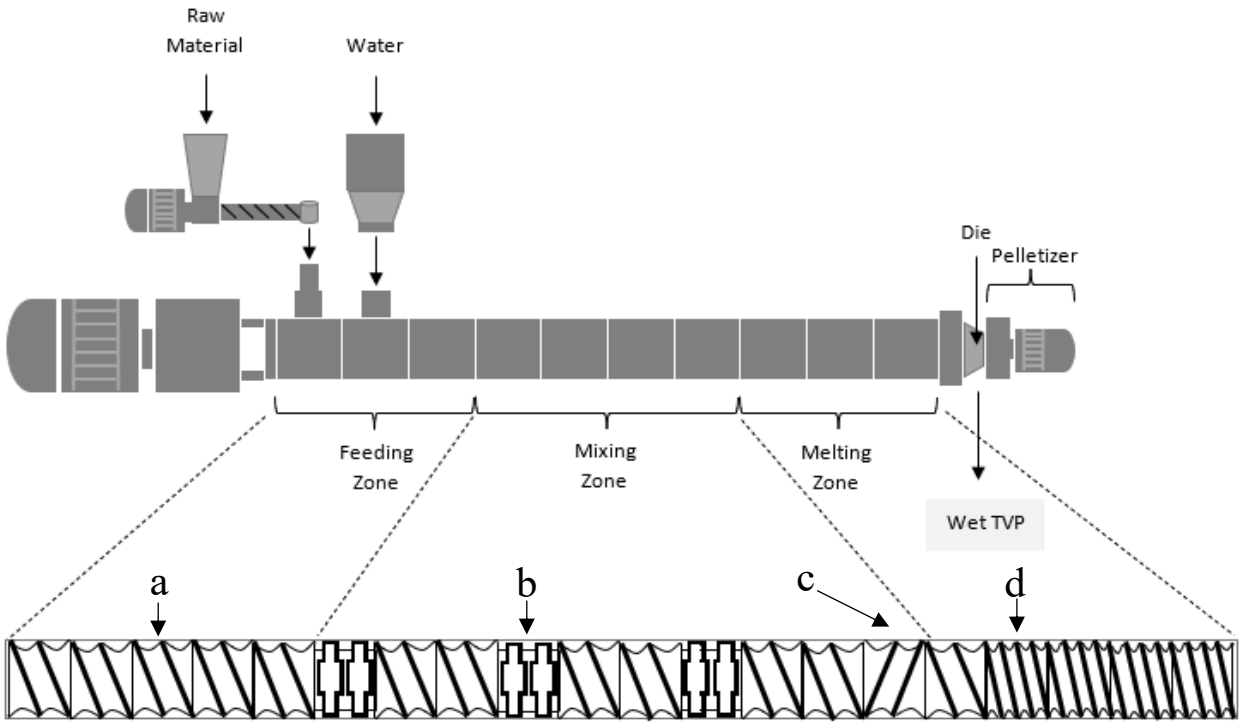

Fig. 1.1 Extrusion configuration and typical screw configuration of a low moisture TVP including a feeding zone with forward conveying elements (a), a mixing zone with forward conveying, mixing (b) and backwards (c) elements, a melting zone with forward elements of shortened pitch (d), and pelletizer.

configuration has a large impact on textural outcomes of low moisture TVP and must be tailored by removing or adding elements to each functional zone of the extrusion screw profile to achieve desired cook, texturization, and resulting expansion (Ek et al., 2020a; Chen et al., 2022). Development of a screw profile (Fig 1.2) is essential to produce TVP with desirable qualities by factoring in the amount and placement of single flight forward conveying elements, mixing blocks, reverse elements and double flight forward conveying elements with half the pitch of a standard forward conveying element (Yacu, 2020).

Fig. 1.2 Screw profile developed for production of TVP rotating clockwise with the protein melt flowing from the feeding zone (left) to the die end (right).

Firstly, preconditioning of starting materials is important for uniform mixing of components like starch, fiber, and protein as well as for uniform moisture distribution prior to entering the extruder barrel to provide not only stability to the extruder, but to also provide proper alignment of proteins from uniform moisture penetration of components resulting in an enhanced finished product (Vatansever et al., 2020). Preconditioning is the mixing of raw materials with moisture prior to extrusion and will also help limit negative effects of extrusion on starting materials such as protein aggregation or starch dextrinization from shearing by pre-hydrating the raw materials (Lazou, 2022).

The feeding zone is where the raw material is fed into the extruder and a predetermined amount of water is injected further down the extrusion barrel to incorporate into the mixture and hydrate the raw material to a specified moisture content. In this section, forward conveying

elements under low pressure are used to build volume of materials entering the extruder and to convey the material down the extruder barrel (Yacu, 2020).

The mixing zone is where the material is mixed under high temperatures and shear to transition from a solid state to a highly viscous state to partially unfold proteins, gelatinize starches, and start to cook and plasticize the mixture (Kristiawan et al., 2020). This step is where retention time is interrelated to screw speed and screw configuration with the bulk of mixing elements are located. Mixing elements not only help to mix and create shear force but also help to slow product flow and increase retention time spent in the extruder (Yacu, 2020). Adequate mixing must be performed under increasing temperatures and pressure to unfold proteins leading them to melt and denature, which will later allow for protein cross-linking to form and create an expanded or fibrous structure. Unfolding of proteins could result in loss of tertiary and/or secondary structure (Lazou et al., 2022) which could be observed using fourier transform infrared spectroscopy (FTIR) or sodium dodecyl-sulfate poly-acrylamide gel electrophoresis (SDS-PAGE) analysis of extrudates compared to their respective starting materials. In addition, backwards conveying elements restrict flow and increase the mixing intensity, retention time, and energy which assists in building more pressure in the extruder barrel (Yacu, 2020). Enough back-pressure must be built up to aid in expansion but not too much pressure such that the protein melt does not have enough force from the forward conveying elements to overpower the pressure built up from the reverse elements.

Lastly, the melting zone is where the viscous mixture melts and starts to realign the protein and starch structures with the direction of the barrel creating an expanded and/or fibrous texture when expelled from the extruder to a lower temperature and pressure (Kristiawan et al., 2020). Under higher temperatures, proteins undergo physical and chemical changes, making this zone the

functional area of the extruder in which weak hydrogen bonds and hydrophobic interactions breakdown, polymerization occurs to form protein aggregates, and unfolded proteins can realign to cross-link and form new protein-protein or protein-starch interactions (Guyuny et al., 2023; Zhang et al., 2019; Kristiawan et al., 2020). Once the protein melt reaches the extrusion die, the drop in pressure and temperature causes evaporation of trapped water vapour resulting in expansion of the melt, where pores are formed and the extrudate structure is held by protein cross-linking and setting of gelatinized starch (Zhang et al., 2019).

1.2.4 Process and system parameters

Expansion and protein alignment of extrudates is affected by the extruder parameters and the plant source material or product formulation. Extrusion uses multiple unit operations in one system to cook food materials in a short time inside the extruder (Ek et al., 2020a). Extrusion parameters can be interrelated or independent and can change extrudate characteristics (Sahu et al., 2022). Extruder parameters consist of: i) processing parameters which remain independent and, ii) system parameters which are dependent on process parameters (Morales, 2020; Lazou, 2022). Final product outcomes or product characteristics such as functionality and structure are heavily dependent on the complex interactions of process and system parameter that take place throughout the extrusion process (Lazou, 2022), making the development of extruded products from novel sources difficult.

Processing parameters refer to set parameters of the extruder machine itself such as feed rate, water rate (impacts moisture content), screw configuration, screw speed, barrel temperature and die size, and the formulation of raw materials and their characteristics (Morales, 2020). Feed rate, water rate, screw speed, and barrel temperature are all process parameters that can be easily changed during extrusion quickly whereas changes to screw configuration and die size/shape

require halting the extrusion process. Although changing the die is less labour and time intensive than changing the screw configuration, barrel temperature and moisture content are both significant variables that impact final characteristics of extrudates (Brishti et al., 2021a). These processing parameters are easily controlled and are often altered in literature research to observe the changes in desired product characteristic. Barrel temperature must be high enough to melt the input materials to create texturization and expansion but not so high that expanded structures become unstable and collapse. Beck et al. (2017b) observed that pea protein at 81.5% produced a stable expanded product between 140°C-150°C, where at less than 140°C no expansion was found, and above 150°C expansion started to decrease. Below 140°C there may not have been enough texturization, meaning not enough proteins were able to unfold enough to reform around air pockets and cross link to solidify and hold the structure, resulting in less expansion. Above 150°C, too much protein denaturation may have caused protein degradation or aggregation which can limit the flexibility of a protein to form around air pockets, again resulting in decreased expansion. Moisture content can also influence expansion such that at 150°C, as moisture content increases from 26% to 35% expansion decreases because additional moisture will decrease the shear force put on the proteins, thus less texturization will occur and fewer proteins will unfold enough to solidify around air pockets. These results indicate that expansion is dependent on both temperature and moisture content (Beck et al., 2017b). The formulation of raw materials including protein source, starch, and fiber interact in the extruder barrel and can have a wide impact on microstructure and functionalities of extrudates (Duque-Estrada et al., 2023; Webb et al., 2023). For example, a review by Webb et al. (2023) of protein sources in extrudates such as soy, wheat, pea, chickpea, faba bean, lentil, and mungbean found that protein composition of amino acids, protein Osbourne classes (e.g. globulins, albumins, prolamin and glutelin) and protein extraction

techniques all had an impact on extrudate structure like porosity and extrudate functionalities like water and oil holding capacities. Therefore, new and emerging starting materials will have different structures and properties of their starches, proteins, and fibers, but exact product parameters may not be easily reproducible between starting material sources or formulations with additional ingredients (Lazou, 2020). Therefore, extrusion parameters must be determined specific to each new plant protein and extrudate formulation. Continued research into extrusion of new plant protein sources or ingredients must be conducted to expand vital knowledge on extrusion processing.

System parameters determine the product characteristics by measuring and describing the physiochemical and rheological properties that the starting materials are going through within the extruder barrel. System parameters are dependent on the process parameters and refer to residence time, mechanical and thermal energy, melt temperature and pressure, and melt viscosity. Mechanical energy can be defined as the specific mechanical energy (SME) which factors in screw speed and flow rate process parameters to determine the overall mechanical energy input (Morales, 2020). Finally, differences in melt temperature, pressure, and viscosity are subjected mostly to changes in starting material formulations and their characteristics, but viscosity can also be influenced by set extruder processing parameters such as moisture content (Guyony et al., 2023). For example, an increase in protein content (starting formulation) may require more moisture to hydrate and therefore result in an increased viscosity. Too much protein could cause negative effects on extrusion parameters like malfunction from uneven water distribution causing surging. Whereas an increase in moisture content by increasing the water rate (processing parameter) can result in decreased viscosity (Day et al., 2013). Changes in one or more system parameters may

alter other system parameters which could alter product parameters directly, or may require alterations to processing parameters, emphasizing the complexity of the extrusion process.

Parameter optimization studies can employ surface response methodology to reveal overall trends on product characteristics based on some system parameters (Brishti et al., 2021a) but optimization is not always transferable due to differences in protein source, formulation, or extruder designs. Therefore, optimization of system and process parameters must be conducted while developing an experimental plan based on desired product characteristics.

1.2.5 Product characteristics

Product characteristics are the measurable physical and chemical properties of the extrudates which affect textural, sensory and nutritional qualities and can often be referred to as product functionalities. Generally, processing and system parameters are intentionally altered to transform the starting material physically and chemically to fit the desired product characteristics (Morales, 2020) such as expansion, texture, microstructure, oil holding capacity and water holding capacity (Brishti et al., 2021a). The water holding capacity of TVP relies mainly on pore size and exposed hydrophilic pockets of proteins (Hidayat et al., 2018). The oil holding capacity of TVP also relies on pore size as well as the unfolding of proteins to expose hydrophobic pockets that may have been hidden prior to extrusion (Han et al., 2023). WHC and OHC both help to contribute to the juiciness of a meat analogue, resulting in better quality and texture (Hidayat et al., 2018; Han et al., 2023). A good microstructure with sufficient expansion and pores contribute to the desired chewiness and texture of a meat analogue (Fiorentini et al., 2020). Without adequate water and oil holding capacities or an appropriate microstructure, meat analogues would taste dry and tough rather than tender and juicy without the mouthfeel of traditional animal meat products (Han et al., 2023; Fiorentini et al., 2020). Most parameters are interrelated causing changes in system

and product parameters, which in turn change based on processing parameters, extrusion contains complex relationships in which general assumptions can be made to changes in parameters (Lazou, 2010). For example, expansion and bulk density can be altered by adjusting temperature, moisture content and screw speed which creates a structural protein matrix that can be visualized through photographic images, scanning electron microscopy (SEM), and confocal laser scanning microscopy (Chen et al., 2022). Water holding and oil holding capacities are strongly influenced by protein source and starting material composition but also by the extruder temperature, moisture and screw speed. These product characteristics often determine quality, which is not easy to express, but can also provide insight to physiochemical changes of the starting materials happening during the extrusion process (Lazou, 2022).

1.3 Protein Sources

Generally, beef and chicken products are commonly replicated meat analogues (Green et al., 2022), using TVP. Not only can TVP quality be affected by extrusion parameters, but it can also be affected by the raw materials like source of protein or additives like starch or dietary fiber which can undergo denaturation, aggregation, degradation, and changes in molecular conformations. Soy protein makes up approximately 63.3% of the meat analogue market followed by wheat, pea, and rice protein, which all differ in physiochemical composition and functional properties (Boukid, 2021). New sources like faba bean, potato, mung bean, and lupin are gaining interest for their sustainable and functional characteristics as well as their ability to combat known allergens like wheat or soy while diversifying an analogues' nutrient profile (Boukid, 2021; Green et al., 2022; Kurek et al., 2022). As the market segment grows for meat analogue products, so must the options of plant protein sources to meet these demands.

1.3.1 Pulses

There has been increasing research interest in pulse proteins, with publications quadrupling in the past decade specifically on categories like pulse flours, pulse concentrates, protein extraction, and pulse protein technology, which are correlated to other searched terms like fiber, diet and digestibility (Rajpurohit et al., 2023). Pulses are the dried edible seeds of the legume family typically higher in protein content (~20-30%) and slightly lower in fat content (~1-4%) than cereal grains (~6.6-17.7% protein and 1.7-5.1% lipids) making pulses an excellent alternative source of protein (Rajpurohit et al., 2023; Guerrieri et al., 2017; Stone et al., 2019). For example, Stone et al. (2019) compared the macro nutrient profile of typical Canadian pulses and cereals showing that pea and faba bean were higher in protein (24.5% and 33.2%), and lower in lipids (1.2% and 1.5%) than wheat, barley, and oat at 13.1%, 11.9% and 13.3% in protein and 1.9%, 2.4% and 5.1% in lipids respectively. In addition, pulses and cereals differ in the main type of protein which can be classified using the Osborne classification scheme into globulins (salt soluble), albumins (water soluble) and prolamins (soluble in ethanol). Cereal grains were most dominant in prolamins (33.1%-47.5%) followed by globulins (33.8%-43.5%) and albumins (17.9%-23.4%), whereas pea and faba bean are generally higher in globulins (pea 41.9% and faba bean 47.0%) and albumins (pea 52.3% and faba bean 47.3%) with minimal prolamins (pea 5.8% and faba bean 5.6%) (Stone et al., 2019). Although albumins are generally reported lower for pea and faba bean (pea 15%-25% and faba bean 20%) and higher in globulins (pea 50%-70% and faba bean 60%) than reported by Stone et al (2019) (Tripathi et al., 2021; Grossmann, 2023). While small albumins (MW 5-80kDa) are present in pulses and consist mainly of metabolic proteins, the dominant storage proteins are larger globulins consisting mainly of legumins (MW 300-400kDa) and vicilins (MW 145-190kDa) (Tripathi et al., 2021).

1.3.2 Faba bean and pea proteins

Faba beans (*Vica faba*) contain slightly higher protein content than peas ranging from 24%-32% protein, 57%-60% carbohydrates and 1.1%-4% lipids. Although faba bean may be higher in protein than pea, it does contain higher amounts of antinutritional factors like tannins, trypsin inhibitor, phytic acid, vicin and convicin (Tripathi et al., 2021) that range based on cultivars that may have slight negative effects. Antinutritional factors can be reduced through the extrusion process, most greatly trypsin inhibitor by 44% in faba beans and 59% in peas (Adamidou et al., 2011). As a legume, faba bean contains both globular proteins legumin (11s) and vicilin (7S) according to their sedimentation coefficients. Legumin is a hexamer held together non-covalently containing six subunit pairs (acidic subunit linked with a disulfide bond to the basic subunit) and contains methionine and cysteine (sulfur containing amino acids) which can form strong covalent disulfide bonds. Whereas vicilin is a trimer held together non-covalently because it lacks cysteine to form disulfide bonds (Tripathi et al., 2021). SDS-PAGE can help identify inter (within) and intra (between) bonding of subunits secondary and tertiary protein structures. Whereas FTIR can identify changes in secondary structures within the amide-I region like α-helix which could shift to β-sheets, β-turns and random coils (Yang et al., 2018) under protein denaturation from extrusion conditions.

Dried peas (*Pisum sativum*) composition is made up of 22%-31% protein, 52%-62% carbohydrates, and 1.1%-3% lipids (Tripathi et al., 2021). Pea contains both legumin (11S) and vicilin (7S) globular proteins as faba bean does, but also includes convicilin (70kDa), another 7S smaller globular protein. Convicilin is also a trimer with a similar basic structure to vicilin with no disulfide bonds, but it differs by containing a hydrophilic N-terminus that is highly charged and does not contain polar regions within the main protein (Grossmann, 2023).

1.3.3 Protein conformations

Storage proteins of pulses can change molecular conformation during processing and undergo loss of quaternary and tertiary structure to unfold and expose hidden polypeptide chains and functional groups (Fig. 1.3). For example, the surface of legumin protein in pea has α-chains that are hydrophilic but when denatured and unfolded, hidden hydrophobic regions become exposed and can interact with the given environment (Reinkenmeier et al., 2015). Alterations in these protein major components and their subunits from processing can be determined by using SDS-PAGE with or without reducing conditions. Although it is important to note that not all proteins present in the initial seed will be present proportionally in products like TVP since the protein extraction process can alter the presence and conformation of major and minor proteins and could ultimately alter the functional properties of proteins within food products. For instance, Grossmann (2023) explained the knowledge gap of protein processing data such that prolamins and glutelins will be retained in protein concentrates if air classification separation technique (dry fractionation) is used, whereas they would be mostly lost in protein isolates if isoelectric precipitation (wet fractionation) is used to separate the protein and starch fractions.

Proteins can interact with other proteins during processing to form homoprotein structures such as soluble or insoluble aggregates, and fibrils which have been linked mainly to globular proteins. For example, adverse environmental conditions like high temperatures common in extrusion can produce insoluble protein aggregates of various sizes. Small aggregates with higher surface hydrophobicity could adsorb faster to air-water interfaces of air pocket nucleation points during extrusion, helping to stabilize expansion (Grossman, 2023). The globular protein legumin has higher hydrophobicity and fewer negatively charged amino acids, and faba bean protein isolates tend to have higher legumin/vicilin ratios than pea protein isolates (Shi et al., 2022). More

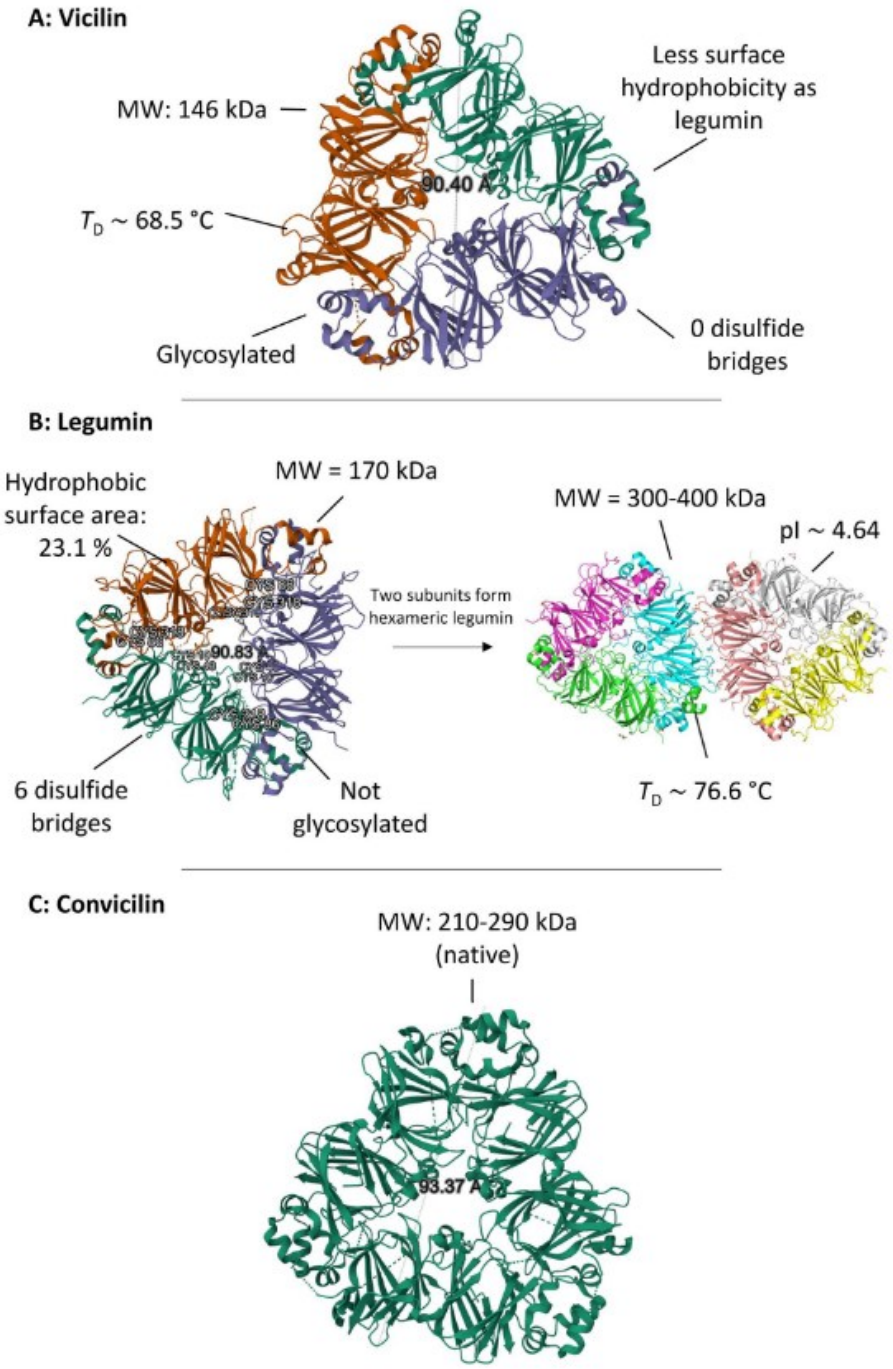

Fig 1.3. Molecular structure of vicillin, legumin and convicilin from pea with physiochemical properties, molecular weight (MW) and sulfur containing amino acids (Grossman, 2023).

hydrophobic groups exposed from extrusion conditions with fewer negatively charged amino acids could lead to protein aggregation, but with a higher molecular weight than vicilin could lead to slower adsorption to the air-water interface, thus decreasing air pocket stabilization of extruded pockets (Shi et al., 2022). These examples show that protein molecular weight and conformational changes of proteins can affect stability of proteins to hold air pocket structures in extrudates.

Different sources of protein like faba bean, pea or more traditionally soy and wheat can impact TVP functionality and structure. Protein source can determine protein flexibility and strength when formed around air pockets based on initial protein conformations and susceptibility to aggregation. For example, soy and wheat proteins traditionally in TVP may be more flexible and strong but are both known allergens. Whereas pea and faba proteins are not allergens and can provide acceptable TVP functional characteristics and structure. Literature on pea TVP tend to focus on extrusion parameter optimization whereas literature on faba bean TVP tends to focus on blending of faba bean with pea, soy, or wheat proteins to improve quality but does not look at improving faba bean TVP with other ingredients while keeping faba bean as the core protein. In addition, LME of faba bean or pea do not often explore changes in phase structure through imaging techniques or how that may be modulated by protein content or rheological properties brought on by moisture content. Though these interactions may be investigated individually, not often are they compared under the same conditions for different protein sources side by side.

1.4 **Starch Inclusion**

1.4.1 Amylose and amylopectin

Pulses contain about 60%-75% carbohydrates and are typically high in amylose content ranging from 24%-65% though peas have been known to range from 21%-58% and generally falling around 34% with amylose and from faba bean ranging slightly lower from 17%-42% and falling around 32% amylose content (Singh, 2021; Tripathi et al., 2021). Amylose and amylopectin make up the two types of starch polymers in our food (Magallanes-Cruz et al., 2017). Amylose is a long linear chain of glucosyl units (low MW) linked with α-(1-4) bonds, whereas amylopectin has both linear and highly branched glucosyl units with α-(1-6) bonds at the branch points and has shorter linear units but overall higher MW. Amylose and amylopectin starch chains can be hydrolyzed and broken down into its glucosyl monomers from the middle by α-amylase (endoamylase), along with amyloglucosidase which is an exoamylase that can hydrolyze both linear α-(1-4) bonds and branched α-(1-6) bonds releasing oligosaccharides which are eventually cleaved down into the glucosyl unit D-glucose (Lin et al., 2016). The crystalline domain of starches contain either double helices of amylopectin side chains (type A or B starch) or long amylose chains as a double helix with amylopectin (Pozo et al., 2018).

1.4.2 Use of starch in TVP formulations

Starch is a key factor in the expansion of extruded products and plays a major role in the formation of the three-dimensional structure of the TVP protein matrix (Guyony et al., 2023). Starches undergo degradation and physiochemical transformations (Fig 1.4) where the starch phase changes from a glassy stage (1) to melted (beyond the rubbery stage) (2) and back to a solid glassy state when cooled (3) is necessary for expanded extrusion products (Ek et al., 2020b). The final solid state is most likely gelatinized starch in an amorphous state but may contain some crystalline regions. Additional starch in the starting material can shift the starch transition curve up so that a higher temperature and moisture content is required to melt the starch (Ek et al., 2020b).

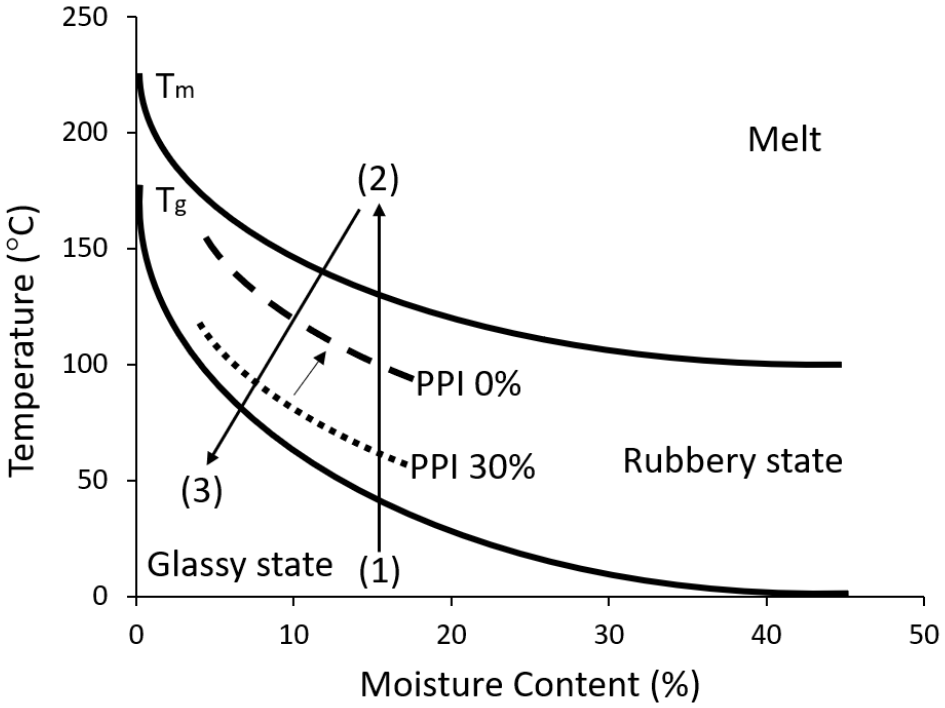

Fig 1.4. Phase change of starch states during extrusion from glassy (1) past the rubbery state to the melt (2) and back to the glassy state upon cooling (3). The addition of starch to pea protein isolate (PPI) can shift the starch transition curve up. Adapted from Ek et al., (2020b) and Philipp et al., (2018).

In addition, starch can help prevent protein unfolding and aggregation if they are imbedded within the protein phase (Lazou et al., 2022), which could benefit TVP structure by lowering protein aggregation.

1.4.3 Types of starch

Pulse starches generally consist of C-type starch which is comprised of a combination of both A-type (typically cereal starches) and B-type (typically tuber starches) (Singh, 2021). Figure 1.5 displays the crystalline packing structure and resulting helix formation of A-type and B-type polymorphs with water, and V-type complex with lipids. Differential scanning calorimetry could be used to assess short range order by disrupting the double helices to determine changes in enthalpy needed for ordered structure to gelatinize but can be misleading since it does not factor in hydration or swelling that also contribute to changes in enthalpy (Warren et al., 2016). Therefore, FTIR is better suited to determine short range ordered structures of the double helix by detecting bending of structures and bonds related to the CH_2 and COH groups of the glucose monomer to determine shifts in amorphous and crystalline regions of a sample (Kong et al., 2014; Pozo et al., 2018). The crystalline form of starches have been attributed to peaks at 995cm^{-1} and 1045cm^{-1} or in an amorphous form at 1022cm^{-1}, indicating the melting of crystalline regions which gelatinize (Warren et al., 2016). Although FTIR cannot differentiate between these typical starch polymorphs and V-type complexes, nor can FTIR accurately quantify the amount of starch type crystallinity (Kong et al., 2014).

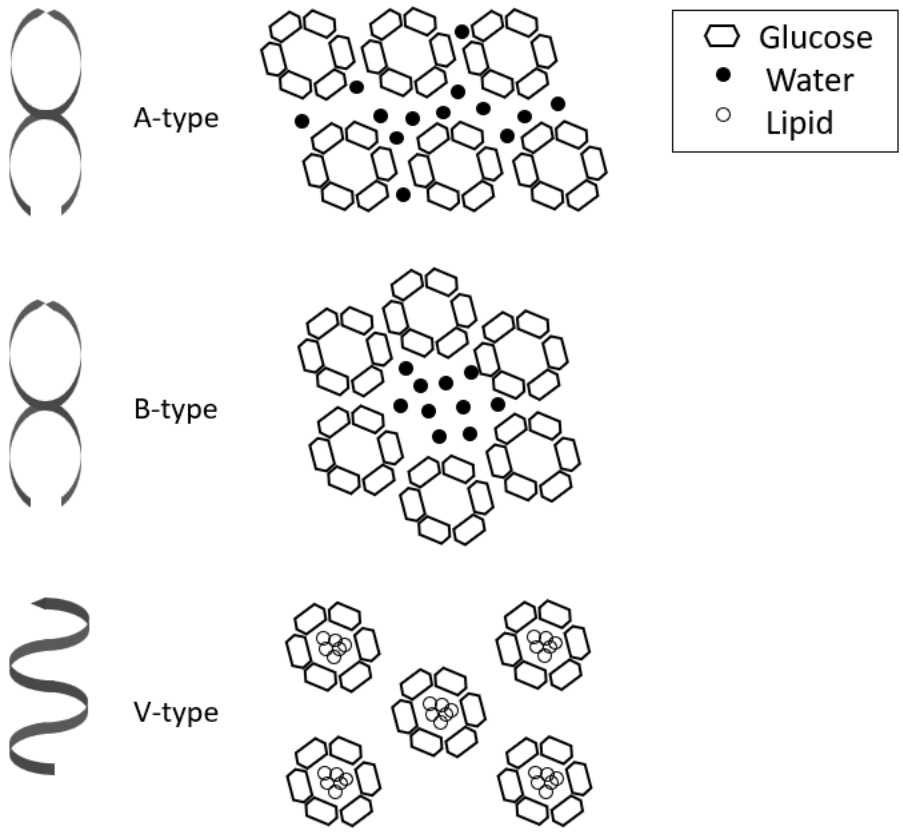

Fig. 1.5 Molecular model viewed from the top of crystalline structure and helix formation of A-type, B-type and V-type starch polymorphs. Adapted from Khatun et al., (2019) and Kong et al., (2014).

The degree of crystallinity and type of starch polymorph present and can be determined by using x-ray diffraction (XRD) which detects the long range ordered structure of the double helices linked to the packing structure of glucose monomers (Pozo et al., 2018). XRD can detect the characteristic peaks attributed to the starch type in a crystalline form (Singh, 2021) to differentiate A-type and B-type from C-type and V-type starch which differ based on their geometry of glucose monomers that dictate the double helical packing density which determine the amount of bound water within the crystalline structure (Wang et al., 1998). A-type starch crystal packing compacts tightly and has one water molecule between each double helix, whereas B-type starch crystals pack more openly and contain water in the center of the structure surrounded by six double helices (Fig.

1.4) (Pozo et al., 2018). Pea starch is typically described as a C-type starch pattern comprised of both A-type and B-type polymorphs. Typical indication peaks for starches indicating A-type crystallinity are at 2θ of 15°, 17°, 18° and 23°. B-type crystallinity displays a well-defined peak at 2θ of 17°, peaks at 22° and 24°, and sometimes peaks at 5.6° or 22° (Xu et al., 2023; Singh, 2021). Lastly, C-type starches have defined peaks at 2θ of 15°, 17° and 23° 2θ with a strong peak at 17° since both A-type and B-type crystallinity display peaks there that combine and amplify the intensity, and a shoulder peak at 18° (Wang et al., 2011; Xu et al., 2023). The shoulder peak at 18° is a defining feature of C-type crystallinity since A-type has a strong peak at 18° and B-type has no peak at 18° (Pozo et al., 2018). Although, retrogradation, protein-starch interactions and protein-protein interactions have been known to decrease the digestibility of starches which can be beneficial to reducing blood glucose levels and promoting prebiotic effects and healthy gut microbiota (Scott et al., 2023; Magallanes-Cruz et al., 2017).

Quantitative changes in internal structure can be calculated by using ratios of intensity to estimate the degree of order (DO) ($1045cm^{-1}/1022cm^{-1}$ ratio) representing the starch crystalline region to starch amorphous region, and the degree of double helix (DD) ($995cm^{-1}/1022cm^{-1}$ ratio) representing the change of double helical structure (Xu et al., 2023; Vatansever et al., 2021). When DD is higher than DO, the number of double helices is greater than the amount of crystallinity, meaning that the crystalline starch is undergoing conformational changes to increase in the amount of amorphous starch. Changes in DO and DD can indicate measurable changes in crystallinity from extrusion or between starch sources present in TVP ingredients like protein concentrates or isolates or added starch.

1.4.4 Digestible starch classification

Starches can also be classified based on digestibility into readily digestible starch (RDS), slowly digestible starch (SDS) (Magallanes-Cruz et al., 2017), total digestible starch (TDS) and resistant starch (RS). Specifically, digestible starch distribution in peas of total starch (e.g. 20.3%) is about 12.0% RDS, 2.0% SDS and 6.3% RS (Tripathi et al., 2021). These starch classifications are determined by Englyst method where the sample is subjected to enzymatic attack by α-amylase and amyloglucosidase to simulate digestion in the gut, after which hydrolyzed glucose is measured after 20 minutes (RDS), 2 hours (SDS) and 4 hours (RS) of digestion (Englyst et al., 1992). A-type starch polymorphs have been shown to exhibit levels of SDS whereas B-type starch exhibits levels of RS content (Zhang et al., 2006; Magallanes-Cruz et al., 2017), implying that C-type starch polymorphs from pulses may present both SDS and RS. Resistant starch is particularly interesting since it is more resistant to enzymatic hydrolysis and enters the colon for fermentation, making it beneficial to the gut as a prebiotic. It has a positive effect on prevention and management of diabetes by regulating postprandial glucose levels, and it's regulation of satiety signals for weight management (Bojarczuk et al., 2022).

Lin et al. (2016) found that starches higher in amylose content showed higher RS content in samples through several mechanisms according to Englyst's test. Firstly, the tight packing of amylose crystalline regions are more stable and less susceptible to enzymatic attack, intermediate components (long branched chains with lower MW than amylopectin) can associate tightly to hinder enzymatic attack, and lastly the formation of amylase-lipid complexes limits enzyme accessibility and hydration. Though long branched chains of amylopectin B-type double helices also resisted digestive enzymes (Lin et al., 2016). In addition, based on high amylose starch's ability to resist swelling under thermal treatment it has been reported to have a higher RS content

(Magallanes-Cruz et al., 2017). Specifically, the formation of amylose-lipid complexes (V-type starch) has been shown to resist digestion (Bhatnagar et al., 1994). Amylose-lipid complexes are formed by leached amylose during gelatinization that wind into helical structures entrapping lipids within, creating a stable structure that limits the infiltration of water and enzymatic attack. Extrusion has been shown to form amylose-lipid complexes at temperatures ranging from 110°C -156°C and up to 200°C (Lin et al., 2016). Although studies have reported thermal degradation of amylose between 140°C-170°C causing disentanglement of linear amylose, breaking of amylopectin branch points and scission of polymeric chains which can ultimately degrade the ordered crystalline phase to promote the amorphous phase (Todica et al., 2016).

Most literature on LME highlights a protein-in-starch network when investigating the effects of starch on extrusion, whereas TVP consists of a starch-in-protein network and could benefit from studies on the inclusion of starch to promote TVP quality. Papers investigating low moisture TVP focus on optimization of extrusion parameters or blending of protein sources but exclude the incorporation of starch and potential benefits on the comparison of different types of proteins. Based on previous work on protein-in-starch networks, the amylose starch in pea has been found more likely to form starch-lipid (V-type) complexes through extrusion known as a resistant starch and has been shown to promote regulation of blood glucose levels to benefit human health (Gulati et al., 2020; McCready et al., 1950) indicating starch could not only improve physical TVP quality but also health benefits.

1.5 Fiber Inclusion

The Food and Agriculture Organization defines dietary fiber as “carbohydrate polymers with ten or more monomeric units, which are not hydrolyzed by the endogenous enzymes in the small intestine of humans” (FAO, 1985). Most North Americans consume an average 17g of

dietary fiber per day and do not reach their daily recommended intake of fiber in a day (25g-30g), therefore the inclusion of both soluble and insoluble fiber sources in meat analogues such as TVP could promote fiber intake of products that would primarily be consumed for their protein content, thus adding value (McKeown et al., 2022). Dietary fiber is made up of both soluble and insoluble fiber as shown in figure 1.6.

Changes in rheological properties during extrusion can be affected by soluble and insoluble polysaccharides, rather than by protein-protein interactions when thermo-mechanically treated under temperature, pressure, and SME conditions that mimic extrusion in a closed cavity rheometer (Pietsch et al., 2019). Unlike starches that can undergo a phase transition from crystalline to amorphous states under extrusion heat and shear conditions, fibers are more rigid from additional hydrogen bonds in their polymer chains, and therefore undergo little or no transitions, specifically insoluble fibers. While soluble fibers could undergo a phase change based on their affinity for water and rigid structure under heat and shear, insoluble fibers would not, even though some molecular bonds of insoluble fibers can be altered on the particle surface causing fragmentation (Ek et al., 2020b). While studies have investigated the effects of soluble and insoluble fiber on direct expanded products, little work has been conducted on fiber inclusion of TVP where protein is the primary formulation ingredient focus.

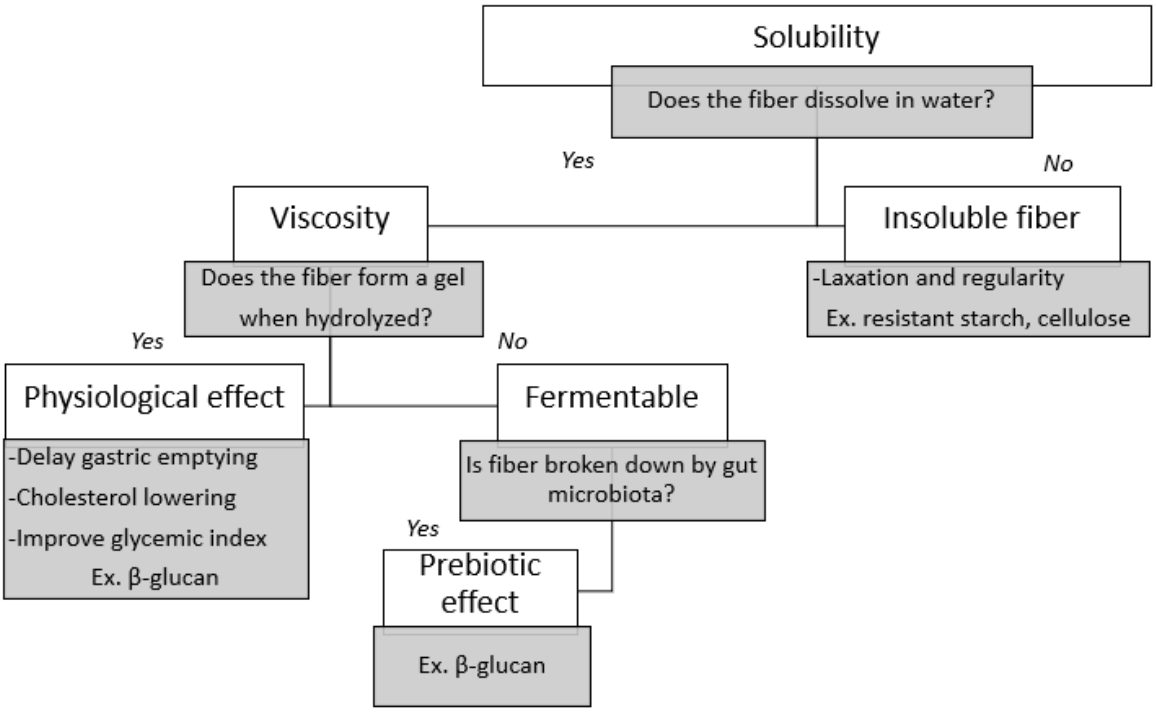

Fig 1.6. Physiological effect and examples of soluble and insoluble fiber. Adapted from McKeown et al., (2022).

1.5.1 Insoluble pea hull fiber

Pea hull fiber can be used as an insoluble fiber source to improve daily fiber content though have generally been known to reduce expansion of extrudates (Ek et al., 2020b), though additional isolated starch included in the formulation containing insoluble fiber could promote necessary expansion while allowing for increased nutritional benefits of added fiber content of a TVP extrudate. Pea hull fibers are often a byproduct from the protein extraction process but can be utilized as a value added upcycled ingredient in TVP to provide additional nutritional benefits. Insoluble pea hull fiber is generally incorporated into baked goods like bread, muffins, cakes, as batters or breading, but also in reconstructed meat products like sausages, hamburgers, and hams as a source of dietary fiber and for its water holding functionality (Martens et al., 2017).

Pea hull fiber is an excellent source of total dietary fiber (90.6%) compared to other pulses like soy bran (67.5%) or cereal brans like wheat (48.0%), barley (72.5%), rice (27%) or oat (24.7%). A large portion of total dietary fiber from pea hull is insoluble (85.3%) compared to other brans like soy (60.5%), wheat (45.6%), barley (69.4%), rice (24.5%) or oat (13.0%) (Robin et al., 2012). The insoluble portion of pea hull fiber generally consist of cellulose (65%), hemicellulose (4%) and lignin (1%) (Martens et al., 2017). Cellulose is comprised of linear β-(1-4) linkages between β-D-glucosyl units which can associate with each other over extended regions via hydrogen bonds to form fibrous bundles (Damodaran, 2008b). After extrusion, insoluble fiber content from pea hull fiber only has minimal decrease (2%-5% for raw hulls and 1.7% for ground hulls), indicating that although some of the polymers were indeed fragmented under extrusion conditions, majority of the insoluble fiber did not undergo extensive degradation and remained in the extrudate (Ralet et al., 1993). Inclusion of insoluble dietary fiber in soy based HME analogues up to 20% can increase the formation of a fibrous structure by acting as a discontinuous filler until the protein content is diluted too much to form enough crosslinks to hold the matrix together (Deng et al., 2023). Effects of dietary fiber on HME products could vary but similar principles could be applied to LME even though the melt would be under a larger difference in pressure drop when exiting the die. The size of insoluble fiber particles can also influence extrudate expansion. Previous reports have shown that a decrease in fiber particle size of sugar beet fiber and insoluble fiber from cherry pomace can actually have less negative impact on extrudate expansion at the same inclusion rate of a coarser fiber. This phenomenon has been explained by a few theories; i) coarse fibers prevent bubble development and collapse bubbles before maximum expansion, ii) higher water binding of fine fiber creates more nucleation sites for bubble development, iii) fine

particles are small enough to become trapped in the matrix of the bubble walls which remain intact (Lue et al., 1990; Wang et al., 2017).

Pea hull fiber has many health benefits similar to soluble fiber including but not limited to weight management and tolerance of postprandial glucose levels, relief of constipation, and a wide variety of bioactive compounds like phenolics, flavonoids, and antioxidants (Martens et al., 2017; Timm et al., 2023). Weight management could arise from a decrease in low-density lipoprotein cholesterol or body fat and by better regulating insulin response and glucose levels (Lambert et el., 2017). An increase in fecal bulk weight from increased water holding capacity with less gut fermentation than soluble fibers can help decrease constipation (Martens et al., 2017; Marcotorchino et al., 2021).

1.5.2 Soluble β-glucan fiber

A common soluble fiber used in foods is β-glucan due to its solubility, thickening properties, and health benefits. β-glucan has primarily been incorporated into food industry as a bioactive ingredient specifically in baked products like bread or muffins, dairy products like yoghurts or functional beverages and cheeses, reconstructed meat products like burgers, sausage, or meatballs, and in other food products like noodles or soups (Sridhar et al., 2023). The use of β-glucan has been shown to improve expansion in extruded snack products and to improve fiber content but little is known about how β-glucan inclusion affects the protein matrix in a TVP product, and how that structure may impact other functionalities (Brennan et al., 2013; Duque-Estrada et al., 2023).

Oats and barley both contain similar amounts of total β-glucan from cereal sources, though soluble β-glucan from oats is generally higher (4.19%) than barley (3.4%) (Lee et al., 1997). Oats

can range in soluble β-glucan content from 4-6% (Herrera et al., 2016). Extraction of β-glucan from oats can increase available dietary fiber content in foods but will contain other major components in the final fraction. For example, β-glucan rich fractions from wet extraction with and without defatting can contain not only β-glucan (28.5%-44.8%) but also other carbohydrates (11.7%-24.5%), starch (2.1%-18.2%) and protein (25.7%-53.1%) (Liu, 2014). β-glucan from oat consists of β-D-glucosyl units linked by 70% linear β-(1-4) bonds and 30% linear β-(1-3) bonds which allow for a viscous solution once solubilized (Bobade et al., 2022).

β-glucan is widely known for its many health benefits such as regulating blood glucose levels, hypertension, cardiovascular disease, and as a prebiotic among other health benefits (Bobade et al., 2021; Sridhar et al., 2023). Regulating blood glucose levels is beneficial to prevent or manage diabetes since β-glucan gives rise to viscosity that could physically interfere with glucose absorption, impair pancreatic amylase and thus regulate insulin levels. Again, the viscosity of β-glucans can influence various pathways and effects in the body such as insulin and lowering blood pressure, which all contribute to lower hypertension risk (Bobade et al., 2021). Prevention of cardiovascular disease is in part associated with β-glucans ability to decrease total cholesterol, low-density lipoproteins, and serum triglycerides with no side effects by binding to bile salts in the small intestine, preventing reabsorption and aiding in weight management (Sridhar et al., 2023; Bobade et al., 2021). The gut microbiota is largely governed by complex polysaccharides and can benefit from β-glucans though stimulating growth of helpful microorganisms like *Bifidobacteria* (Sridhar et al., 2023).

Contradicting literature on insoluble fiber particles effect on LME again are only investigated on starch based extrudates for LME products or on HME products, but not in low moisture TVP (Wang et al., 2017; Robin et al., 2012; Deng et al., 2023). Most work involving

soluble fiber and extrusion focuses on using extrusion as a treatment to improve the solubility of fiber but not on the physical and quality benefits of incorporating soluble fiber into low moisture TVP. The addition of insoluble and soluble fiber to diets has many well known beneficial health effects but is not often investigated in low moisture TVP even though some studies have reported positive outcomes on TVP structure and quality.

1.6 Research rationale and objectives

1.6.1 Research rationale

TVP is a LME product produced from well developed technology. Extrusion of TVP can include new and emerging sources of plant proteins, making this technology relevant again for emerging research and scientific literature. Therefore, the focus of this thesis will be on low moisture extrusion and the exploration of new plant protein sources (faba bean -*Vicia faba*) in TVP to increase protein content of TVP, and to further investigate starch and fiber (soluble and insoluble) inclusion on functionality and structure in a LME TVP.

Although low moisture extrusion production of TVP has been around since the 1960s, most work revolved around soy, wheat and more recently pea as protein sources (Guyony et al., 2023; Baune et al., 2022). But with the rise of the flexitarian consumers demanding alternative meat analogues high in protein with lower environmental impact, and with the global TVP market segment projected to increase to $2.1 billion USD by 2027, TVP is brought back again into the spotlight to fill this gap (Baune et al., 2022). The re-emergence of TVP brings opportunities to utilize new protein sources like faba bean to compete with rise of pea protein, though literature on the use of faba bean as an extruded TVP protein source is scarce, as is the impact of starch and fiber on the development of TVP structure relating to functional properties.

Extrusion is a “black box” technology, meaning in-line monitoring or analysis of interactions between components that comprise process and system parameters are limited. In addition, the design of extruded products and control over the extrusion process is largely based on empirical knowledge, even though the process has been studied for decades. Therefore, techniques to understand component interactions under thermomechanical treatments such as rheology, FTIR and SDS-PAGE can be employed (Chen et al., 2022). Since system and process parameters are heavily interconnected, the optimization of key parameters must be performed to provide consistent product results.

Pea starch was chosen for inclusion in this study due to its sustainability, potential health benefits and beneficial effect on TVP expansion. Pea starch is a more sustainable option of starch since it is a by-product from the protein extraction process and is not modified further. Pea starch has been shown to display good expansion capabilities in TVP (Rangira et al., 2020). It is higher in amylose content which has been known to form resistant starch with dense molecular packing, resisting enzymatic attack (Ye et al., 2018). In addition, amylose has been known to form amylose lipid complexes which are a resistant starch and can provide beneficial regulation of blood glucose levels (Gulati et al., 2020; McCready et al., 1950).

1.6.2 Prelimnary and optimization trials

Preliminary trials used pea protein isolate and concentrate with 10% moisture pre-conditioning to determine operating parameters by adjusting screw profile (4 profiles), protein content (60%-80%), final moisture content (45%-60%), and temperature (160°C-180°C). Screw speed was held constant and was determined by finding the optimal middle range of parameter variables based on visual TVP quality of typical yet adequate expansion and density. Screw profiles ranged from: i) insufficient mixing and lack of pressure buildup resulting in gelatinized

melt with a noodle like quality underexpanded, to ii) too many mixing and backward screw elements which caused water backup due to the melt not overcoming the pressure required to pass the backward screw elements. Extruder was operational within the 60%-80% protein content treatments which were taken forward to include in the study. Treatments at or below 45% moisture were too dry and crumbled since not enough mosture was available for proteins to hydrate and melt, whereas treatments at 60% moisture caused the extruder to surge, most likely due to inconsistant melt viscosity and increased pressure.

Based on results from preliminary trials, a full factorial optimization trial (Table. A1) was performed based on extruder limitations. Trials were run in triplicate to narrow down optimal temperature for the study and moisture contents to investigate based on the functionality results (expansion, waterholding capacity, and oilholding capacity). These functionality outputs were chosen based on known key sensory attributes of TVP for product texture (expansion), product tenderness (WHC/OHC), and product juiciness (WHC/OHC). Parameters included protein content (60% and 70%), moisture content (45%, 50%, and 55%), and extrusion barrel temperature (160°C, 170°C and 180°C). Results from the optimization trial that concluded the most optimal output combinations came from 50% and 55% moisture, and averaged 170°C for both 60% and 70% protein levels. Therefore barrel temperature remained constant at 170°C in the study.

1.6.3 Hypothesis and objectives

Development of TVP requires a balance between optimization of extrusion parameters, desired TVP quality and functionality, as well as concidering contributions to health benefits. Since a TVP product's primary role is to replicate or replace animal meats protein content is a top priority, but only if good structural quality can be met. Secondly, inclusions can be made to improve structural quality like the addition of starch without compromising high protein content.

Lastly, inclusion of other components to improve health and functional quality can be added as long as structual quality can be met.

Therefore, it was hypothesized that faba bean protein could be an alternative source of protein for TVP based on structure-functionality similarities to pea protein. In addition, the inclusion of starch and dietary fiber was hypothesized to improve TVP expansion and functionalities. Meanwhile, the appropriate inclusion of starch could improve potential health benefits of TVP by increasing resistant starch without compromising protein content or TVP functionalities such as expansion, BD, WHC and OHC. The objectives of this thesis were two-fold:

i) to investigate potential structure-functionality relationships of faba bean and pea proteins at two moisture levels (50%, and 55%) with a focus on increasing protein content (60%-80%) of TVP (Chapter 2) and;

ii) to determine the impact of starch (5%-10% inclusion) and dietary fiber sources (insoluble 5%-10%, and soluble 5%-20% inclusion) on TVP structure, functionality, and the digestibility of starch (Chapter 3).

Achievement of the first objective will not only provide evidence that faba bean protein can be a viable alternative source of protein in TVP which can expand industry's protein options. It could also aid in the scientific understanding of physiochemical changes of faba bean and pea proteins during the extrusion process resulting in desired functionalities. Achievement of the second objective would provide academia with new insight into the starch and dietary fiber inclusion on TVP structure and functionality. In addition, the second objective would provide industry with a starting point for starch inclusion levels in TVP to improve functionalities of other

protein sources and maximize dietary fiber inclusion levels before negative effects on functionality occur, as well as any potential health benefits of starch and dietary fiber inclusion beyond protein content to the consumer.

Chapter 2: Effects of Moisture and Protein Content on Functional and Structural Properties of Faba bean and Pea Texturized Vegetable Protein

2.1 Introduction

Consumers, specifically flexitarians, are looking to adopt alternative sources of proteins into their diets to contribute to global sustainability efforts while still consuming healthy foods. Studies have shown that nutritional qualities can be met with the incorporation of texturized vegetable proteins into food products (Baune et al., 2021). TVP can be mixed with other plant-based ingredients, binders, and sensorial components to create reconstructed products typical of animal meats-like burger patties, meatballs, and sausage, which are familiar to and appeal to consumers. Therefore, the growing use of TVP from plant protein sources in food products is a stepping stone to increasing plant protein consumption in the diet. Not only could the incorporation of TVP into a healthier diet lower the risk of cardiovascular disease, and blood pressure, it could also contribute to a lower environmental impact and fewer green house gas emissions (Baune et al., 2021; Lee et al., 2008; Clifton, 2011; Xu et al., 2021) compared to traditional animal meat products. Studies on the sustainable life cycle of plant-based protein food products suggest prioritizing improving technologies and operational procedures (Allotey et al., 2023), so that formulating with plant-proteins is easier and more profitable for industry.

Among other techniques like electro spinning, wet spinning, freeze structuring and shear cell technology, extrusion is the main technique employed to mimic animal meats utilizing plant sources that is commercially available, scalable, and has low environmental impact (Dekkers et al., 2018a). TVP is considered a product of low moisture extrusion since it is produced with less moisture and at higher temperatures than a high moisture extrusion meat analogue (Zhang et al., 2022a). Changes in moisture content can affect the final TVP structure since water acts as a

plasticizer, lubricating the protein and contributes flow to the protein melt where proteins undergo conformational changes (Schmid et al., 2022). Upon mixing with water at high temperatures under shear force, protein chains denature and undergo conformational changes by unfolding and exposing hydrophobic amino acid groups. Once protein chains are exposed in the viscous melt, new protein-protein associations could occur along with potential aggregation, crosslinking, hydrophobic interactions, or hydrogen bonds, thus forming a protein network with possible fibrous structures (Zhang et al., 2019). LME also has a characteristic expansion caused by the release in steam from the decrease in high temperatures and pressures at the extruder die causing bubble formation that create open air pocket structures. LME has advantages over HME such that LME does not require an additional cooling die that would increase the number of parameters and processing steps, or refrigerated storage which both would increase production costs. In addition, low moisture TVP has an advantage over high moisture extrusion in that it can be dried and stored at room temperature, can come in a large range of sizes and textures, is currently being produced as an ingredient for product developers, and can be adapted into a wider variety of food products (Zhang et al., 2022a). LME can also produce TVP using high protein flours or concentrates so there may be no need for protein isolates. Soy and wheat are the most commonly used protein sources in TVP production currently on the market, though with the rise in allergenicity concerns associated with soy and wheat, other pulse-based proteins like pea are becoming more popular in TVP products and faba bean is starting to raise interest (Baune et al., 2022)

Increasing research interest in pulse proteins is occurring, with publications quadrupling in the past decade (Rajpurohit et al., 2023), and the use of pea protein in TVP is surpassing that of wheat and catching up to soy protein as a source of plant-based protein in food products (Baune et al., 2022). Faba bean (~27.6% protein) has higher protein content than pea (~23.4%) and has a

lower climate impact (2.45 vs. 3.06kg CO_2 equivalents of dried pulse/kg protein for faba bean and pea respectively), giving faba bean a competitive advantage over pea (Martineau-Cote et al., 2022; Svanes et al., 2022). Faba bean and pea are composed of mainly globulins (57-60%) and albumins (20%-26%). The globulins consist of 11S legumin hexamers (20%-30% in pea and 40%-45% in faba bean) containing acidic (40kDa) and basic (20kDa) units linked by a disulphide bond and 7S vicilin-like trimers (20%-40% of 150kDa in pea and 20%-25% of 158-163kDa in faba bean) including convicilin (Gueguen et al., 1994; Vatansever et.al., 2020). Faba bean and pea proteins also show similar functional characteristics such as water and oil holding capacities. This has led to the hypothesis that faba bean protein could be used in TVP just as pea protein is replacing soy in the market (Webb et al., 2023; Shi et al., 2022). In addition, high protein concentrates from air classified dry fractionation are less energy intensive to produce and less environmentally impactful processing method than protein isolates from wet fractionation. Therefore, protein concentrates may not be suitable for HME but are an excellent base formulation for LME.

There is currently more literature focusing on HME to prepare plant protein-based analogues than on LME analogues like TVP since HME is more recent and could mimic whole muscle fibers, though novel sources of plant protein use in TVP should still be studied more in depth. Current publications on LME focus on soy and pea and the relation of extrusion processing parameters to their TVP physiochemical properties. Literature on faba bean extrusion reported their nutritional use in livestock feed or as a supplementary ingredient in HME analogues, but little is known about use of faba bean as a major ingredient in TVP. Most literature on LME focuses on extrusion parameter optimization but does not uncover rheology or molecular interactions during black box extrusion processing, or the forementioned relationship to final TVP structure. Further investigation into the effect on protein structures needs to continue exploring in LME analogues

specifically (Twombly, 2020) as new protein sources enter existing markets. Moisture and protein content can alter rheological properties of protein melts within an extruder to affect their expansion and subsequently the protein structures and the physicochemical properties of TVP from pea and faba bean protein sources. The exploration of rheological properties and protein structural changes during low moisture extrusion relating to microstructure of extrudate are rarely discussed in depth but could provide scientific insight into the impact of protein and moisture content on TVP properties to improve product development, thereby expanding the use of pea and faba bean as TVP sources to provide developers with additional protein options.

Aim of this study is to investigate how changes in protein content and moisture content impact the rheological properties and microstructure of the melts and protein conformation during low moisture extrusion of faba bean and pea protein in relation to the TVP physiochemical properties. High protein concentrate fraction from air classification were used as the formulation base and were combined with protein isolates from a wet extraction process to adjust protein content of starting materials. Specifically, three protein levels (60%, 70%, 80%) and two total moisture levels (50%, 55%) were systematically studied to determine their effect on physiochemical properties of TVPs including expansion ratio, bulk density, water holding capacity and oil holding capacity. The rheology properties of pea and faba bean proteins were investigated under a 25°C-95°C-25°C temperature ramp, simulating initial temperature increase during extrusion. The TVP network microstructures were observed using confocal imaging and SEM imaging. The changes in protein secondary structure between starting material and TVP of faba bean and pea through FTIR and SDS-PAGE analysis were conducted. The correlation of protein structures, network microstructure, and rheological properties were discussed to provide insight on mechanism of protein network formation in relation to TVP quality such as expansion, density,

water holding capacity and oil holding capacity. To our best of knowledge, the effect of protein and moisture content on two similar globular protein sources, pea and faba bean, is not sufficiently studied together or side-by-side under the same extrusion conditions.

2.2 Materials and methods

2.2.1 Materials and chemicals

Commercial pea (55% protein concentrate) and faba bean (60% protein concentrate) were kindly provided by Ingredion (Westchester, Illinois, United States), whereas pea (85% protein isolate) and faba bean (90% protein isolate) were kindly provided by AGT Foods and ingredients (Regina, Saskatchewan, Canada). Compositional analysis of macro nutrients of starting materials and subsequent formulations were provided by suppliers (Table 2.2). SDS-PAGE 4-15% gels (Mini-PROTEAN®TGX™), SDS-PAGE broad-range molecular weight standards, sample buffer, and running buffer were purchased from Bio-Rad Laboratories Inc. (Hercules, California, United States). All other chemicals were purchased from Sigma-Aldrich Co. (Oakville, Ontario, Canada). Purified water used in this study was generated by Milli-Q Advantage A10 system (EMD Millipore Corporation, Massachusetts, United States). Canola oil was purchased from a supermarket locally.

2.2.2 TVP extrusion and sample preparation

Protein concentrates and isolates were mixed to achieve 60%, 70% and 80% final protein content for both pea and faba bean sources. The protein mixes were pre-hydrated to 15% moisture by even mixing with fine misted tap water prior to extrusion. TVP were extruded using a co-rotating twin screw extruder (Coperion ZSK 26, Coperion, Stuttgart, Germany) equipped with a 3mm die. All other extrusion parameters were optimized within the desired expansion range based on preliminary work to accommodate both faba bean and pea proteins and held constant throughout the experiment (Table 2.1). Water injection rate was adjusted to reach total moisture

contents of 50% and 55% in the melt. Once extruder conditions stabilized, TVP was pelletized and collected. Pelletized TVP were dried in a tray oven at 60°C for 30 minutes and stored in a sealed double plastic bag at 21°C. TVP samples were then ground with a conical mill equipped with a 12×12mm screen size at 31Hz motor speed. The ground TVP was passed through a 1.18mm screen and stored in double lined plastic bags at room temperature (21°C) until further analysis. Extrusion was performed in duplicate on separate dates for each replicate.

Table 2.1. Extrusion parameters held constant consisting of heating block temperature, feed rate, water pump pressure, screw speed, and pelletizer speed.

Heating Element Temperature (°C)										**Feed rate**	**Water Pump**	**Screw speed**	**Pelletizer speed**
Block	1	2	3	4	5	6	7	8	9	**Kg/hr**	**(psi)**	**(RPM)**	**(RPM)**
	35	50	100	150	170	170	170	170	150	15	20	450	250

2.2.3 Expansion ratio and bulk density

Expansion ratio (ER) was determined by using a vernier caliper to measure the diameter of three sections per extrudate on 10 extrudates per replicate. The expansion ratio is calculated by dividing the average extrudate diameter by the diameter of the die opening of the extruder (Equation 1). (Sahu et al., 2022).

$$\text{ER} = \frac{\text{Diameter of extrudate (mm)}}{\text{Diameter of extruder die (mm)}} \quad (1)$$

Bulk density (BD) was determined by using vernier calipers, to measure the diameter of three sections per extrudate on 10 extrudates per replicate, length of each extrudate, and weight of each extrudate. The bulk density was calculated by determining the ratio of mass to volume and expressed as g/cm^3 (Equation 2). (Sahu et al., 2022).

$$BD = \frac{(4 \times m)}{(\pi \times d^2 \times L)} \quad (2)$$

Where m is the mass in grams, d is diameter in centimeters, and L is the length in centimeters.

2.2.4 Water holding capacity

Water holding capacity was measured via AACC Approved Methods of Analysis 56-37.01 Water Holding Capacity of Pulse Flours and Protein Materials. Sample (1g) was weighed into a glass test tube and mix with a glass stir rod for 1 minute with an undetermined amount of Milli-Q water until saturated. The stir rod was cleaned with folded 2"x4" filter paper covering the tube and placed upside down in a syringe assembly consisting of a plastic syringe barrel in a 50ml plastic centrifuge tube. The assembly was centrifuged at 300xg for 10 minutes. WHC was calculated as g H_2O/g sample, dry matter (Equation 3).

$$\text{WHC (g } H_2O\text{/g sample, dry matter)} = \frac{(W3-W2)+(W1 \times Mc)}{(1-Mc)W1} \quad (3)$$

Where W1 is the sample weight in grams before water addition, W2 is the weight of syringe assembly (syringe, filter cloth, test tube, sample) before centrifugation, W3 is the weight of the syringe assembly after centrifugation, and Mc is the initial moisture content of the sample as a percentage.

2.2.5 Oil holding capacity

Oil holding capacity was determined according to the method by Wang et al. (2020) with modifications. Sample (1g) was mixed with 10g canola oil in pre-weighed 15ml centrifuge tubes. Tubes were inverted to shake for 10 seconds, and every 5 minutes for a total of 30 minutes. Tubes were centrifuged for 15 minutes at 2000×g, excess oil was decanted, and tubes placed upside down on paper towel for 30 minutes to drain. OHC was calculated as g oil/g sample.

2.2.6 SDS-Polyacrylamide gel electrophoresis

Sodium dodecyl-sulfate polyacrylamide gel electrophoresis was performed under reducing and non-reducing conditions. Faba bean and pea TVP samples (3mg protein equivalent) at 60%, 70% and 80% protein content (16.7mg, 14mg, and 12.5mg respectively) were weighed out, mixed with 2ml milli-Q water, and vortexed every 5 minutes for 30 minutes. Sample aliquots (0.1ml) were added to 0.1ml blue sample buffer for 30 minutes prior to boiling for 5 minutes and centrifuged at 4000rpm for 5 minutes. Samples (15µL) and standards (15µL) were loaded onto 4-20% 10 well comb Mini-PROTEAN® TGX™ precast gels in a tris/glycine/SDS buffer and run at 80mV. Samples were run against a protein standard ranging from 10-250kD. For reducing samples, 2% 2-mercaptoethanol (2-ME) was added to the blue sample buffer. Gels were stained with a solution of coomassie brilliant blue-R250 (1g)/ acetic acid/ methanol/ milli-Q water (1:4.5:4.5, v/v/v) for 30 minutes, drained, and rinsed with deionized water. Gels were de-stained with a solution of methanol/ acetic acid/ milli-Q water (1:1:8, v/v/v) for 30 minutes, drained, and de-stained again in fresh solution overnight.

2.2.7 Protein conformation in TVP by Fourier-transform infrared spectrum

Faba bean and pea protein structure in TVP was characterized by fourier-transform infrared spectrophotometry (Nicolet 6700, Thermo Fisher Scientific Inc, Pittsburgh, Pennsylvania, United States). Ground TVP and potassium bromide (KBr) were dried at 80°C for 30 hours in an oven and transferred to a desiccator. Each sample (1mg) was ground further with 99-101mg KBr with a mortor and pestle and pressed into a disk under 15000lb pressure for 5 minutes. The transparent disk was transferred to the FTIR spectrophotometer where the spectra read at a resolution of $4cm^{-1}$ and a wavenumber of $1111\text{-}4000cm^{-1}$ for 128 scans. Under the same conditions, the KBr background was subtracted from the spectra. Fourier self-deconvolution was performed by Omnic

8.1 software on the amide I band region (1700-1600cm^{-1}) with an enhancement factor of 2.5 and at a bandwidth of 24cm^{-1}. (Yang et al., 2021).

2.2.8 Rheological properties

Rheological behaviours of TVP starting materials were analyzed by a TA Discovery HR-3 rheometer (TA Instruments, Delaware, USA) equipped with a 40mm diameter parallel-plate with a gap of 1mm. Pea and faba bean protein starting material (60%, 70%, and 80% protein content) were hydrated to 50% and 55% total moisture content with milli-Q water to mimic moisture content in the extruder. A temperature sweep was performed to record storage (G') and loss (G'') modulus continuously. A temperature ramp was performed to mimic viscoelastic properties under semi-extrusion temperatures. Samples were heated from 25°C to 90°C at a rate of 2°C/ minute for 10 minutes and cooled to 25°C at a rate of 4°C/ minute. Samples were held for 20 minutes under 1% strain and at a frequency of 1Hz. Evaporation was prevented by using a trap cover and silicone oil.

2.2.9 TVP Morphology by confocal laser scanning microscope

Microstructures of proteins and starch in TVP were visualized by a confocal laser scanning microscope (LSM 510 META, Zeiss, Oberkochen Germany). Whole TVP samples were hydrated with room temperature (21°C) milli-Q water for 15 minutes in a ratio of 5:1 (H_20:TVP) and allowed to drain free of excess water on paper towel for 10 minutes. Drained TVP were frozen for 15 minutes and sliced thinner than 1mm with a razor blade. Sample proteins were stained red with Acid Fuchasin (0.1% w/v) for 2 hours and washed with milli-Q water twice. Samples starch were stained blue with Calcoflour white (0.01%w/v) for 2 minutes and washed twice with milli-Q water.

2.2.10 Scanning Electron Microscopy

Scanning electron micrographs of TVP were generated by using a Sigma SEM EDX (SEM EDX, Zeiss Sigma, Jena Germany) with an EHT voltage of 10kv. Micrographs were taken at magnifications of 50X, 500X, and 2.5kX. Samples were hydrated with room temperature (21°C) milli-Q water for 10 minutes, drained for 1 minute, and flash frozen with liquid nitrogen. Samples were then cut longitudinally with a scalpel to show the internal air pocket structures formed running parallel with the extruder barrel. Samples were then air dried and mounted onto platforms and sputter coated with a thin layer of gold for 120 seconds for conduction.

2.2.11 Statistical analysis

All quantitative analysis were performed at least in triplicate on two independent extrusion repetitions. Origin version 2022b (OriginLab Corporation, Northampton, MA, USA) software was used for statistical analysis and results presented as the mean ± standard deviation. Statistical analysis was conducted by one-way analysis of variance (ANOVA) at a confidence interval of 95% utilizing Tukey's test at $p>0.05$. Two-way ANOVA was conducted to determine the interactions and impact of moisture and protein content treatments on TVP functional characteristics.

2.3 Results and discussion

2.3.1 Functional property characterizations of TVP

Expansion ratio and bulk density are characteristics measured to quantify the degree of puffing which is a main physical characteristic in TVP structure quality, whereas water and oil holding capacity are the main physical attributes for use of TVP in meat analogues (Altan et al., 2023; Vatansever et al., 2020). Water and oil holding capacity of TVP are important functionalities if

Table 2.2. Proximate composition (%dry basis) of faba bean (F) and pea (P) protein concentrates/isolates and treatment starting materials.

Treatment	Protein (%)	Starch (%)	Fiber (%)	Fat (%)	Ash (%)
Faba bean concentrate	60.0	11.5	13.6	3.8	11.1
Faba bean isolate	89.0	2.0	2.0	6.5	0.5
Pea concentrate	55.0	18.2	15.9	4.2	6.7
Pea isolate	85.0	2.0	4.0	8.5	0.5
Protein inclusion					
F60	60.0	11.5	13.6	3.8	11.1
F70	69.7	8.3	9.7	4.7	7.6
F80	79.5	5.1	5.8	5.6	4.0
P60	60.0	15.5	13.9	4.9	5.7
P70	70.0	10.1	10.0	6.4	3.6
P80	80.0	4.7	6.0	7.8	1.5

being used in meat analogues to mimic the mouthfeel and texture of animal meat products, which impact not only tenderness and juiciness but also cook loss (Baune et al., 2022; Webb et al., 2023). Expansion of TVP creates a porous structure providing a sponge-like quality and enables the uptake of water or oil needed to improve meat analogue texture. Oil is an important characteristic in meat analogues to improve texture and mouthfeel but to also enhance or amplify meat-like flavours. Both oil and water holding capacity of TVP impact meat analogue texture and product properties like moisture retention, shrinkage and cook loss which should be minimized by enhancing the oil and water holding properties of TVP to a certain extent (Baune et al., 2022). Under high pressure, shear and temperature within the extruder, the proteins, starch, and other components mix together with water and form a protein melt in the extruder. This protein melt conveys down the extruder barrel as conformational changes in protein occur by unfolding to open up the protein chains, allowing for new bond formations to occur further down the extruder barrel and during cooling after extrusion (Kristiawan et al., 2020; Beck et al., 2017a*).* Air pockets are formed from other components like fiber, aggregated proteins, residual starch granules, or from

the initial presence or air in the protein melt (Kristiawan et al., 2020). As the melt exits the die at ambient temperature and atmospheric pressure, water flashed off into steam, which in turn causes the melt to expand followed by solidifying void structure (fixation of structure) as the extrudate cools. This process under set conditions creates expanded TVP containing air pockets filled with water vapor, which may have been previously retained in the melt (Fig 2.1).

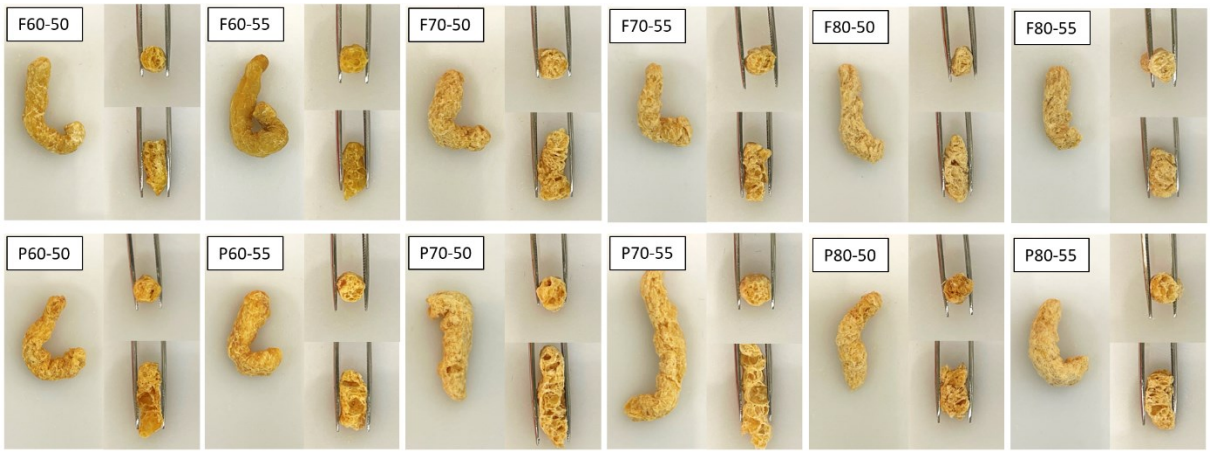

Figure 2.1. Whole (left), cross section (top right), and longitudinal (bottom right) cuts respectively of faba bean (F) and pea (P) TVP at 60%, 70%, and 80% protein levels and moisture content of 50% and 55%.

2.3.2 Effect of moisture and protein inclusion rates on faba bean and pea TVP functional properties

Preliminary work from moisture level examination (45%-60%) indicated that appropriate TVP expansion of both faba bean and pea were at 50% and 55% final moisture of melt within the extruder. Lower moisture levels led to dry crumbly unexpanded whereas higher moisture levels led to wet gel-like under expanded products. Moisture content had an effect on faba bean TVP expansion ratio which was higher at 50% moisture (1.64-1.79 ER) than 55% moisture (1.58-1.7 ER) (Fig. 2.2). Similar results were reported separately in pea and mungbean protein isolate TVPs

such that when moisture content decreased there was an increase in expansion and lowering of bulk density attributed by an increase in specific mechanical energy (Beck et al., 2017a; Brishti et al., 2021b). Often a lower moisture content can contribute to the expansion of extruded products (Twombly, 2020). An increase in expansion (larger or more pores) based on bubble formation within the protein melt can be explained by two theories that both result in an larger pressure drop at the die: (i) lower moisture causes an increase in viscosity; and (ii) lower moisture causes an increase in specific mechanical energy (Beck et al., 2017a; Twombly, 2020). Low moisture content will allow formation of a protein-based melt with higher viscosity, thus creating more shear force (Beck et al., 2017a) and higher SME. An increase in SME then leads to enhanced protein texturization through restructuring of protein bonds (Lee et al., 2022). Decreased melt viscosity can also result in a stronger melt flow at the extruder die, promoting expansion of TVP (Lyu et al., 2023; Lee et al., 2022). The directional change in faba bean TVP expansion correlates to the change in bulk density where more expansion creates a less dense extrudate with more or larger air pocket pores (Fig. 2.1). For example, as moisture content decreases from 55% to 50% there is a corresponding increase in expansion (Fig. 2.2) and a decrease in bulk density (Fig. 2.3). When fixing moisture at 50% and 55%, an increase in faba bean protein content led to slightly better TVP expansion but a stronger increase in bulk density.

For pea TVP the expansion was not significantly impacted by moisture content, but 80% protein had better expansion (1.95-2.14 ER) than pea at 60% (1.78-1.82 ER) and 70% (1.82-1.87 ER) protein content. An increase in moisture causes an increase in bulk density with a corresponding decrease in expansion ratio attributed to decreased bubble formation and stability from a less viscous protein melt causing lack of dough elasticity and starch gelatinization (Sahu et al., 2022; Xie et al., 2006). Most research on protein content and expansion or bulk density focus

on protein content of expanded snack products (10%-50% protein) rather than high protein content (50%-80% protein) of expanded TVP products (Phillip et al., 2017; Hong et al., 2022). Protein will compete with starch and absorb more water than starch at a higher starch-protein starting material ratio, therefore limiting the amount of water available for starch during extrusion (Buhler et al., 2022b). Thus, in a high starch LME product, the addition of protein will cause decreased extrudate expansion. Because TVP is a high protein LME product, the conventional understanding of higher protein content causing less expansion and higher bulk density (Phillip et al., 2017) can not be extrapolated to TVP products. Bulk density can be impacted more by intrinsic properties of components other than protein in the raw material such as starch or fiber, and by extrusion

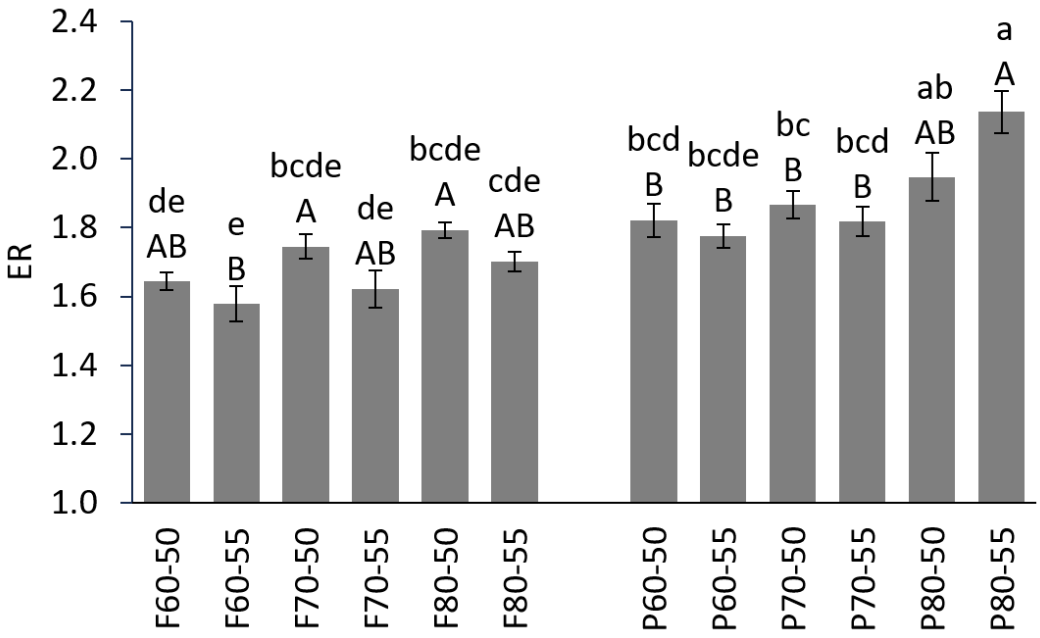

Figure 2.2. Expansion ratio of faba bean and pea TVP where uppercase letters show significance ($p>0.05$) within protein sources pea and faba bean, and lowercase letters show significance ($p>0.05$) between all samples.

parameters like temperature, moisture, shear force, and die profile (Hong et al., 2022; Kristiawan et al., 2020). Research on the impact of protein content on TVP products is limited and should be further explored.

Faba bean TVP bulk density ranged from 0.43-0.60g/cm^3, and pea TVP from 0.26-0.45g/cm^3 (Fig 2.3). The pea TVPs showed a lower bulk density than those based on faba bean when prepared each moisture and protein level. Bulk density has been attributed to changes in TVP cell wall structure and pore size distribution (Beck et al., 2017a). Generally lower bulk density values of pea extrudates suggest that either larger air pockets (increased pore size) or more air pockets (increased frequency of pore distribution) are formed from the pea protein structure leading to a decrease in bulk density but not a corresponding increase in expansion ratio. This indicates that the pea TVP overall may be lighter and airier (higher expansion, lower density) compared to the faba bean extrudates. Although faba bean and pea have similar 7S and 11S globular structures, differences in emulsion and foaming capabilities, protein solubility (Kimura et al., 2008) and their tendency to aggregate (Yang et al., 2018) may contribute to their differences in expansion and bulk density among pea and faba bean extrudates. For example, pea foams formed under pressure and heat from extrusion can lead to greater expansion and foam stability contributed by flexible proteins with higher surface interactions at the air-water interface (Hall et al., 2021). Higher solubility of pea protein (Kimura et al., 2008) could allow it to better diffuse and unfold to adsorb at the air-water interface, forming viscoelastic films around air bubble surfaces during extrusion, which could partially explain an increase in expansion and lower TVP density, thus promoting extrudate air pockets. Whereas faba bean protein has lower solubility and higher tendency to aggregate (Yang et al., 2018). Therefore, increasing protein molecular size could interfere with their ability to move (slower) and unfold (bound as aggregates) to adsorb on

air-water interface for bubble stabilization, resulting in a less expanded, denser extrudate (Tsoukala et al., 2006).

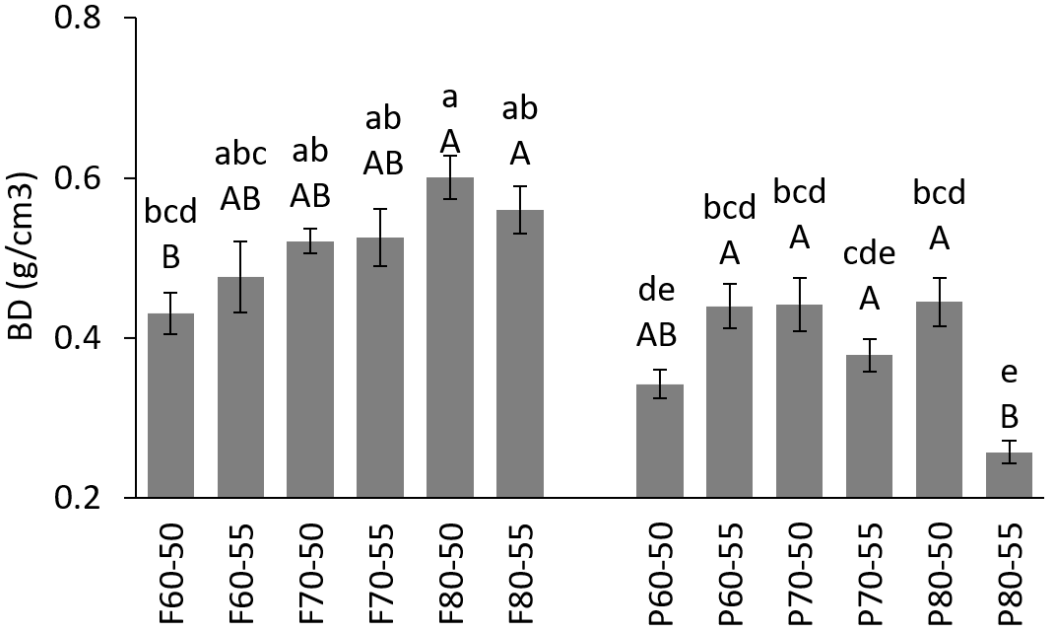

Figure 2.3. Bulk density of faba bean and pea TVP where uppercase letters show significance ($p>0.05$) within protein sources pea and faba bean, and lowercase letters show significance ($p>0.05$) between all samples.

Extrudate microstructure and the presence of exposed hydrophilic and hydrophobic amino acid groups can have an impact on a protein's ability to hold water or oil after extrusion (Webb et al., 2023). Therefore, water and oil holding capacity of faba bean and pea TVP along with their starting materials were evaluated. The water holding capacity of the starting materials increased as protein content increased, though this degree of increase was not the same for faba bean or pea TVP. Compared to the corresponding starting materials (1.14-2.96g/g), extrusion increased WHC of faba bean TVP at 60% protein (2.57-2.65g/g) and 70% protein (2.30-2.80g/g) at 50% and 55% moisture respectively, which is most likely due to the uptake of free water filling the pores

characteristic of TVP and binding to exposed hydrophilic protein groups (Fig. 2.4) (Beck et al., 2017b; Webb et al., 2020). Conversely, an increase in protein content to 80% decreased WHC of faba bean TVP (1.39-1.51g/g) for both 50% and 55% moisture levels respectively. WHC of pea TVP was higher than the starting material (1.57g/g) at 60% protein (2.85-3.13g/g) but much like faba bean at 80% protein, the WHC was lower than the corresponding starting materials (2.21-3.12g/g) at 70% protein (1.41-1.42g/g) and 80% protein (1.39-1.29g/g) at both 50% and 55% moisture levels respectively. The reduced water holding for TVPs made from 80% faba bean protein and from 70%-80% pea protein may be due to excess protein denaturation and aggregation from exposure to heat and shear force and therefore fewer exposed hydrophilic amino acid side chains to bind water. In addition, at a higher protein content there are more available hydrophobic amino acid residues exposed from unfolding denatured protein chains, causing a decrease in WHC. Chan et al. (2023) found similar results with pea protein TVP at 70%, 76% and 82% protein content where there was an increase of WHC at below 82% protein. Whereas WHC of the TVP was not improved through extrusion when increasing the protein content to 82% (Chan et al., 2023). The authors hypothesized it was mainly from decreased starch content at 82% protein content, and the increase of hydrophobic amino acid exposure that caused the decrease in WHC at high protein levels. Under conditions involving moisture and heat, starch present in the protein melt can swell and bind water through the process of gelatinization, therefore less starch present could prevent additional water holding capabilities (Webb et al., 2020). Moisture at 50% or 55% had no effect on WHC for either faba bean or pea TVP.

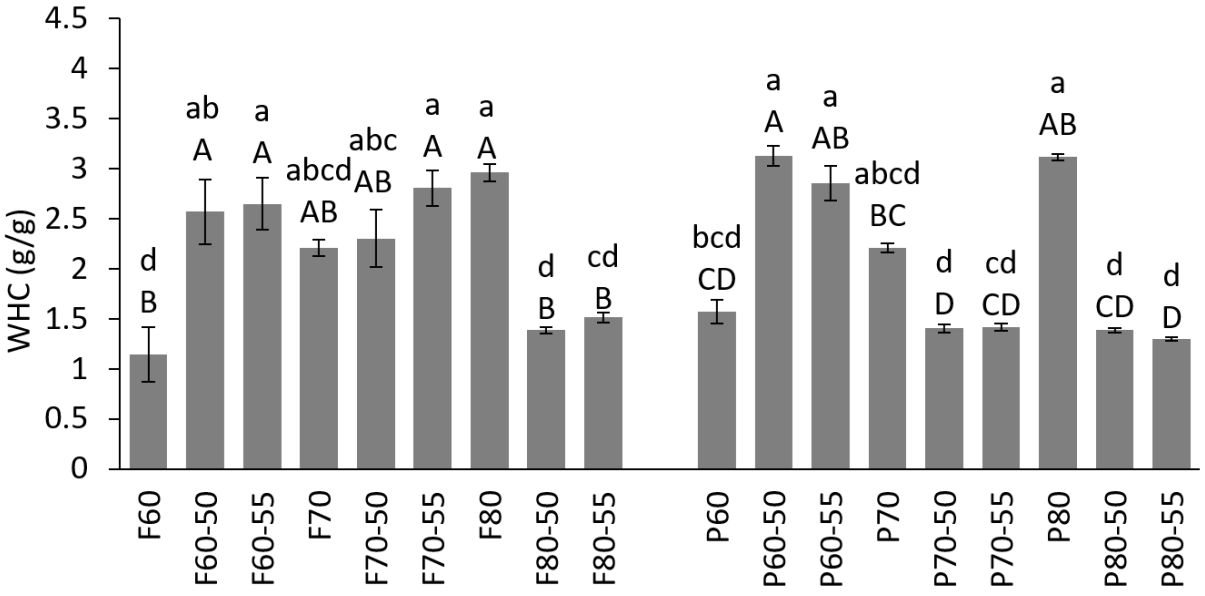

Figure 2.4. Water holding capacity of faba bean and pea TVP where uppercase letters show significance ($p>0.05$) within protein sources pea and faba bean, and lowercase letters show significance ($p>0.05$) between all samples.

Faba bean and pea TVP had similar values of oil holding capacity (2.25-2.44g/g and 2.19-2.57g/g for faba bean and pea TVP respectively) (Fig. 2.5). Therefore, all faba bean and pea TVP were comparable and can offer additional oil holding capabilities as an ingredient in meat analogue food products. Extrusion improved oil holding capacities in all TVP compared to the starting materials (Webb et al., 2023; Chan et al., 2023). This increase in oil holding could be attributed to denaturation of the proteins while under extrusion heat and shear conditions, causing unfolding and opening up of protein structures, thus exposing more hydrophobic groups (Osen et al., 2014). The increase in OHC in the TVP can also be attributed to the formation of pore structures during the expansion of TVP at the extruder die. Although increase in moisture could be related to an increase in OHC (trend in pea TVP 50% to 55% moisture content at all protein levels), it is more

likely that an increase in OHC is attributed to TVP protein melt expansion and porosity through oil uptake via capillary action (Saldanha et al., 2023).

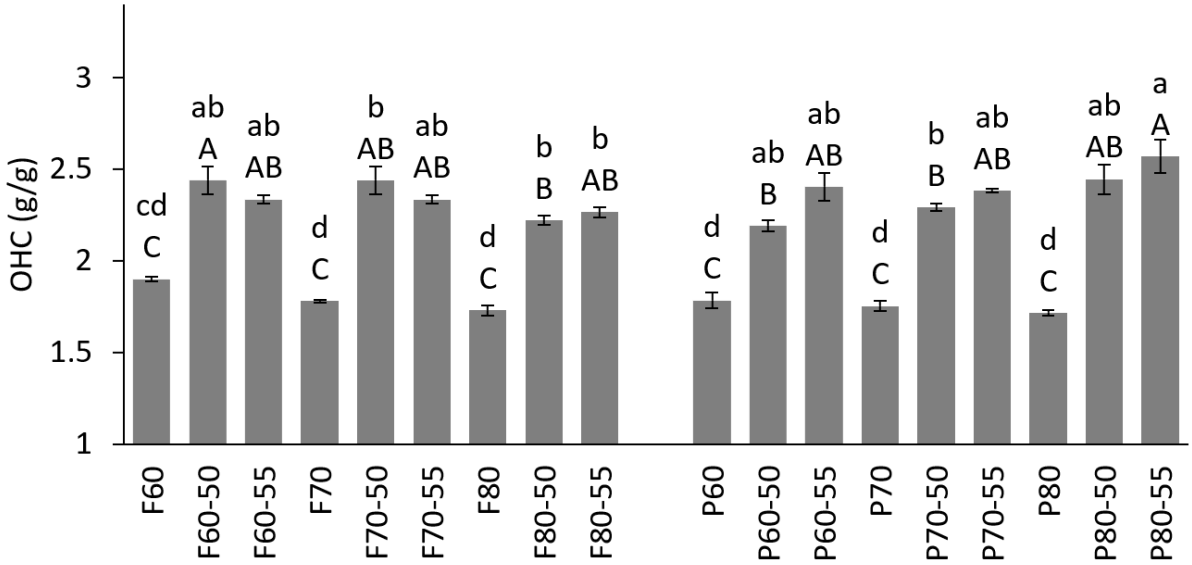

Figure 2.5. Oil holding capacity of faba bean and pea TVP where uppercase letters show significance ($p>0.05$) within protein sources pea and faba bean, and lowercase letters show significance ($p>0.05$) between all samples.

Although expansion and density rely heavily on extrusion parameters, expansion of faba bean (1.56-1.75 ER) and pea (1.78-2.14 ER) tended to be slightly lower than other soy TVP ER (1.25-3) and similar in density (0.06-0.7g/cm^3) (Lyu et al., 2023), but denser than wheat TVP (0.16-0.29g/cm^3) (Maningat et al., 1999). Faba bean and pea proteins are similar to soy proteins and are all quite different from wheat protein which consists of albumins and globulins, though majority of wheat proteins (70%-80%) consist of gliadins and glutenins (Gueguen et al., 1994; Vatansever et.al., 2020). Although WHC of both faba bean and pea starting materials increased as protein content increased, the WHC of TVP only increased compared to their corresponding starting materials in faba bean up to 70% protein and in pea at 60% protein. Moisture did not have much influence on WHC of extrudates. WHC of starting materials were comparable to other pea

and faba bean isolates (1.8g/g) and higher than soy (1.3g/g), but lower than wheat (3g/g) (Webb et al., 2023). The WHC of extrudates vary drastically among literature due to extrudate size, porous structure, and WHC method. Pea, soy and wheat TVP WHC at 60% protein content range between 1.5-4g/g (Esbroeck et al., 2023; Lyu et al., 2023) with wheat having the larger WHC between 2.5-4g/g (Maningat et al., 1999). The WHC of TVP at 60% protein content and 70% faba bean content were comparable to those reported in literature. Though the 80% TVP and pea at 70% were lower in WHC but higher in protein content than reported (Esbroeck et al., 2023; Lyu et al., 2023; Maningat et al., 1999).

All extrudates improved OHC compared to their corresponding starting material and were all within similar range of 2.19-2.57g/g. Faba bean and pea starting materials were generally higher in OHC compared to other isolates (faba bean 1.6g/g, pea 1.2g/g, soy 1.1g/g), but lower than wheat gluten (3.5g/g) (Webb et al., 2023). Comparison of exact TVP functionalities may be difficult due to variation in equipment, extrusion parameters, and non-standardized methods. TVP OHC of faba bean (2.22-2.44g/g) and pea (2.19-2.57g/g) were higher compared to other TVP sourced from pea (0.93g/g), soy (0.74g/g), and wheat (0.79g/g) (Hong et al., 2022). However, from this study it can be concluded that faba bean protein can compete with pea TVP based on WHC and OHC functionalities even though they lack the degree of expansion or bulk density of soy protein or wheat gluten based TVPs, though a dense structure may actually be desired in certain products that faba bean and pea TVP could provide. For example, when Hong et al., (2022) measured textural properties of soy, wheat and pea TVP based patties, the pea TVP patties were not significantly different from the wheat TVP patties for hardness, resilience, springiness, shear force or compressed juice, and was actually more resilient and springier than soy TVP patties. Expansion ratio generally increased with protein content, at lower moisture, was higher in pea than faba bean

TVP, and was congruent with lower bulk density from either larger or more frequent air pockets in the TVP.

2.3.3 Gel electrophoresis characterization of TVP

The SDS-PAGE gels run under reducing conditions for both starting materials, faba bean and pea TVP at 60%, 70% and 80% proteins content at 50% and 55% moisture contents are shown in Fig. 2.6 and Fig. 2.7. Moisture content did not have a visual effect on faba bean or pea SDS-PAGE gels. Bands characteristic of faba bean protein subunits under non-reducing conditions in the starting material (SM) were visible as legumin minor subunits (MS) (~75-80kDa), convicilin (CV) (~70kDa), legumin A (L-A) (~60 kDa), legumin B (L-B) (~60kDa), vicilin (V) (~50kDa), α-legumin (L-α) (~40kDa), β-legumin (L-β) (~20kDa), and small protein aggregates below 20kDa (Fig. 2.6A). All major bands present in faba bean starting material became faint in TVP, indicating extrusion caused protein denaturation and aggregation. The bands at 20kDa (β-legumin), 40kDa (α-legumin), 50kDa (vicilin) and 60kDa (legumin A and B) appeared in TVP under reducing conditions (Fig. 2.6B) once the disulfide bonds were cleaved by sodium dodecyl sulfate and 2-mercaptoethanol. This result indicates that disulfide bonds played an important role to contribute faba bean protein aggregation after unfolding by extrusion. Faba beans have a higher content of sulfur containing amino acids (0.19%-0.34% dry basis) than pea (0.23%-0.15% dry basis) of methionine and cysteine respectively, which may be contributing to increased aggregation of faba bean proteins (Martineau-Côté et al., 2022).

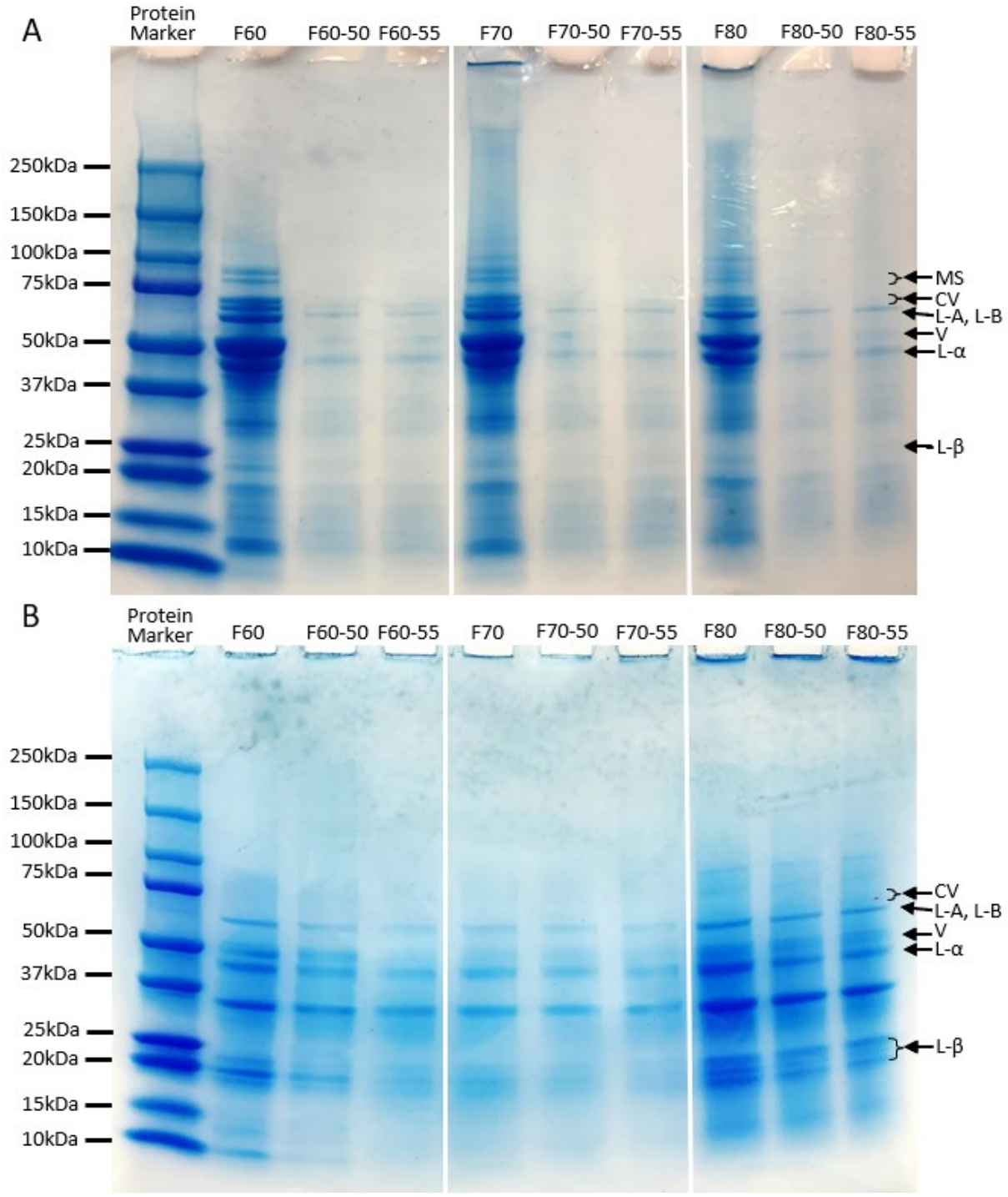

Figure 2.6. Non-reducing (A) and reducing (B) SDS-PAGE gels of faba bean starting materials and TVP at 60%, 70%, and 80%, protein levels and 50% and 55% moisture content. Minor subunits (MS), convicilin (CV), legumin (L), Legumin A (L-A), Legumin B (L-B), vicilin (V), α-legumin (L-α), and β-legumin (L-β).

Bands characteristic of pea protein subunits under non-reducing conditions (Fig. 2.7A) were visible as convicilin (CV) (~70kDa), legumin (~60kDa), vicilin (V) (~44kDa), α-legumin (L-α) (~40kDa), vicilin fragments (~30-35kDa), β-legumin (L-β) (~20kDa), and small protein aggregates below 20kDa. Pea protein also underwent unfolding and aggregation by extrusion as the major bands became faint in TVP. On the other hand, the bands are stronger in pea protein TVPs that those of faba bean protein, supporting more protein aggregation in faba bean protein TVPs when compared to pea protein. The bands at 60kDa are almost invisible in TVP under non-reducing conditions indicating legumin was more susceptible to break down into α and β subunits and/or aggregation by extrusion. Under reducing conditions (Fig. 2.7B) disulphide bonds in TVPs were interrupted, accompanied by increased band density of the acidic and basic subunits of legumin (Tzitzikas et al., 2006) as expected.

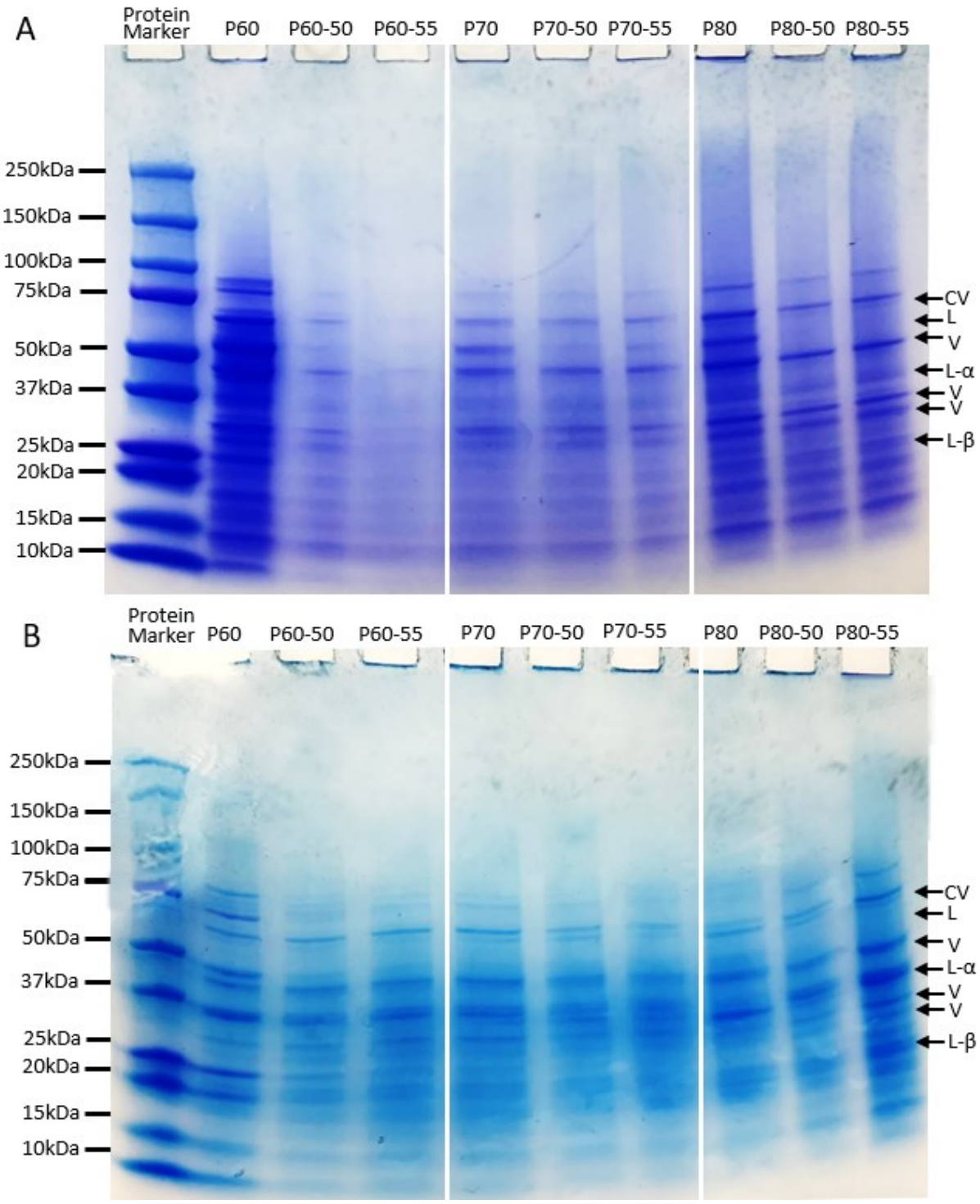

Figure. 2.7. Non-reducing (A) and reducing (B) SDS-PAGE gels of pea starting materials and TVP at 60%, 70%, and 80%, protein levels and 50% and 55% moisture content. Convicilin (CV), legumin (L), vicilin (V), α-legumin (L-α), and β-legumin (L-β).

2.3.4 FTIR secondary structures of TVP

Fourier-transform infrared spectra of TVP are displayed in Figure 2.8. The protein mix contained 7 dominant bands at 1628cm^{-1} (β-sheets), 1643cm^{-1} (random coil), 1660cm^{-1} (α-helix), 1670cm^{-1} (β-turn), 1680-1693cm^{-1} (β-sheets/turns) and 1608cm^{-1} (amino acid residues). The band at 1618cm^{-1} corresponds to protein aggregates of intermolecular β-sheets formed by hydrogen bonds (Zhang et al., 2022c; Yang et al., 2021). FTIR spectra of the protein mix showed

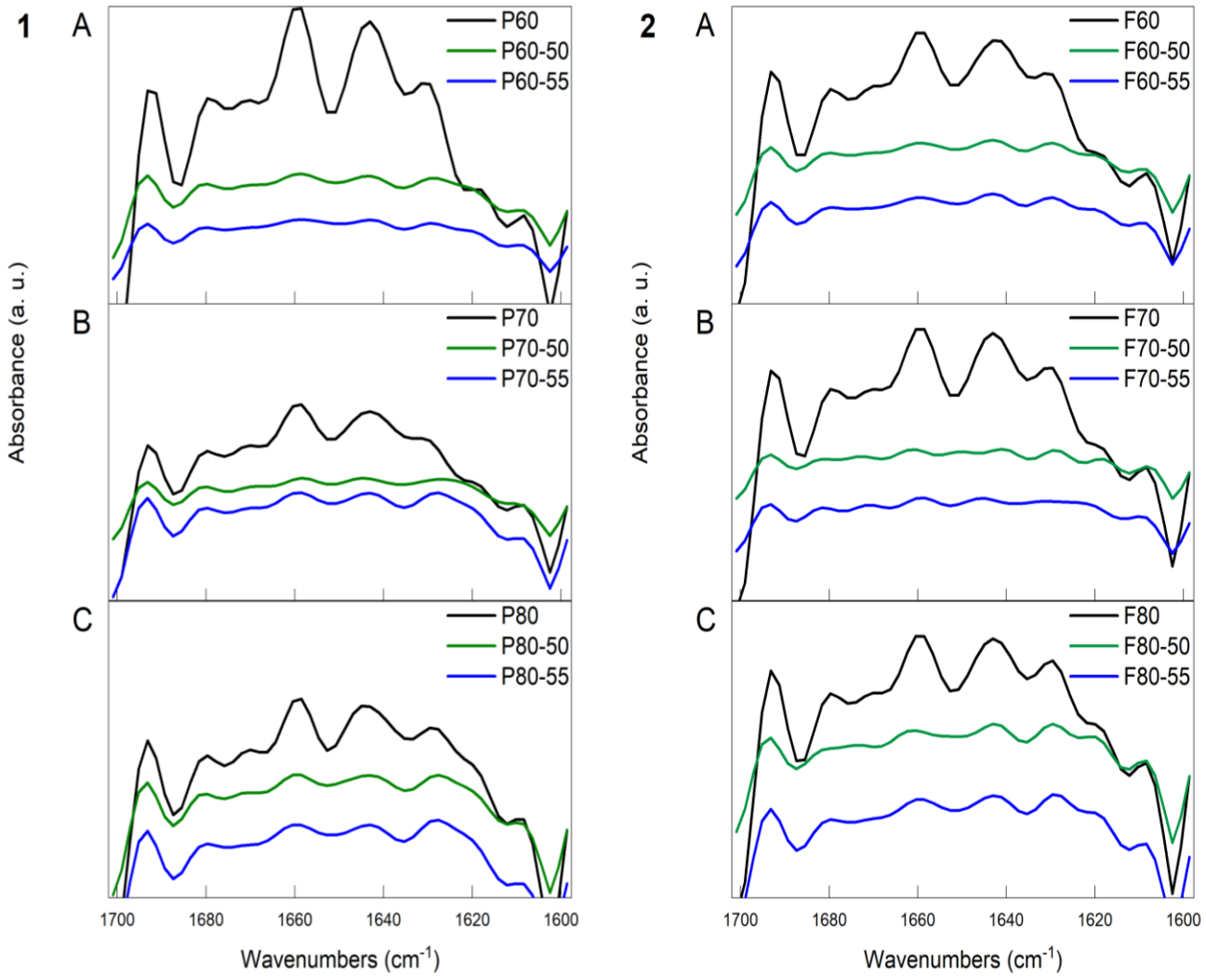

Figure 2.8. FTIR spectra of pea (1) and faba bean (2) raw protein and extruded TVP at 60% (A), 70% (B) and 80% (C) protein contents.

denaturation of proteins from extrusion processing at all protein levels and moisture contents for both pea and faba bean TVP as the intensity of the bands associated with major secondary structures were decreased significantly (Fig. 2.8) as expected. Interestingly, the starting material β-sheet structure at 1618cm^{-1} had a small amount of aggregation already prior to extrusion, indicating small level of protein aggregates had formed during the protein fractionation or extraction process (Yang et al., 2021). Changes in moisture content (50% and 55%) or protein content (60%, 70%, and 80%) of TVP did not affect protein secondary structure in either faba bean or pea TVP. The bands at 1618cm^{-1} increased obviously in TVP at 80% protein content of faba bean, further supporting more aggregation in faba bean protein during extrusion. An increase in protein aggregates has been suggested to be beneficial to expansion and stabilization of TVP extrudates because of increased intermolecular protein interactions in the network (Beck et al., 2017b).

2.3.5 Rheological properties of faba bean and pea melts

A temperature sweep over time was used under heating conditions to understand the rheological property changes during extrusion by analyzing the storage modulus dynamics of faba bean and pea proteins (60%, 70%, and 80%) at both 50% and 55% moisture levels (Fig. 2.10). The storage modulus (G') was always higher than the loss modulus (G") indicating the protein based melts were in a solid-state with gel-like rheological properties when heated to 95°C and cooled back to 25°C (Wittek et al., 2021a), therefore this discussion will focus on the storage modulus. Protein concentrates and isolates with varying starch and protein contents display different typical curves (Fig 2.9) under heating based on both starch and protein behaviour (Rodriguez et al., 2023). During heating, thickening is caused by starches starting to swell and gelatinize and proteins start

to unfold and reform hydrophobic interactions and disulfide bonds. Whereas during cooling, thickening is caused by starches gelatinizing and proteins forming cross-links between other proteins (Kornet et al., 2020).

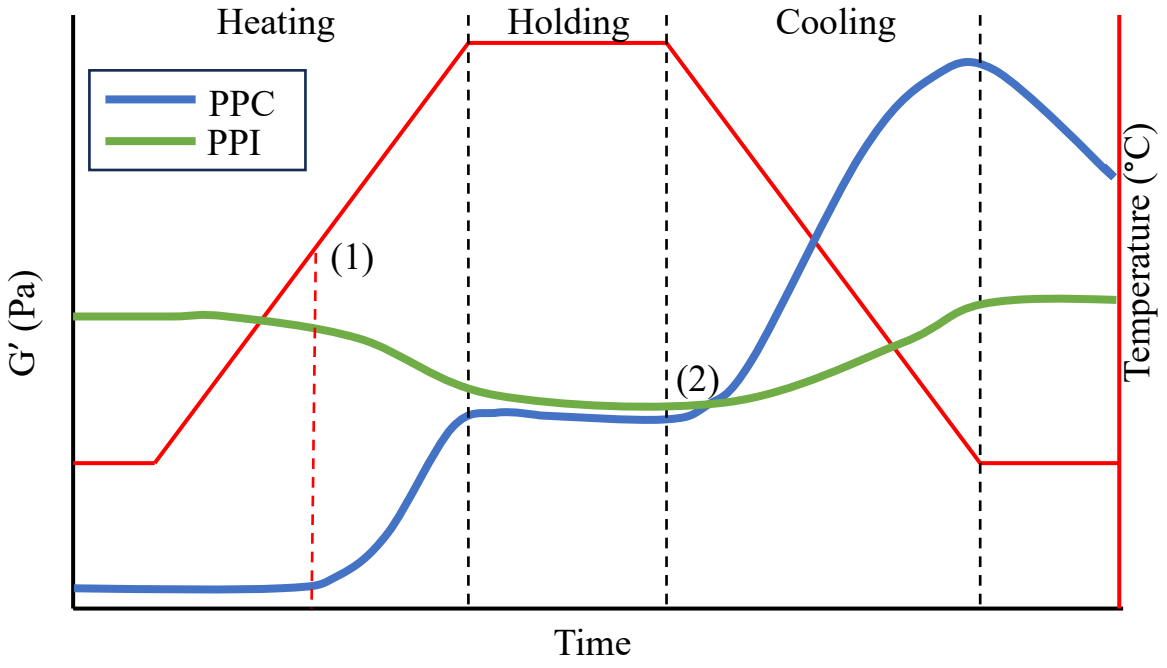

Figure 2.9. Typical temperature sweep curve of pea protein isolate (PPI=green) and concentrate (PPC=blue) under heating conditions from 20°C-95°C-20°C. Thickening of protein melt takes place at (1) and (2) and is caused by both starch and proteins. (1) is the point at which starches start to swell and gelatinize, proteins start to unfold and reform hydrophobic interactions and disulfide bonds between proteins. (2) is the point where starches start to gelatinize and proteins form cross-links between other proteins. Adapted from Rodriguez et al., 2023.

As expected, with an increase in protein content there was a subsequent increase in G' of protein curves, since the starting material water absorption also increased with an increase in protein content and thus contributed to a less viscous flow (Dekkers et al., 2018b). The higher protein isolate inclusion of formulations (60%<70%<80% protein isolate inclusion) may also have

contributed to an increase in overall curve viscosity since an increase in both particle size and protein aggregation is characteristic of alkali extracted isoelectric precipitation method used to obtain high protein content of isolates and has been shown to increase the viscosity of protein solutions (Kornet et al., 2020; Rodriguez et al., 2023). As the mixture heated there was an increase in G' until 95°C was reached, which may be caused by: (i) starches swell as they overcome their glass transition temperature to form a rubbery state (Damodaran, 2008b) (ii) proteins unfold and

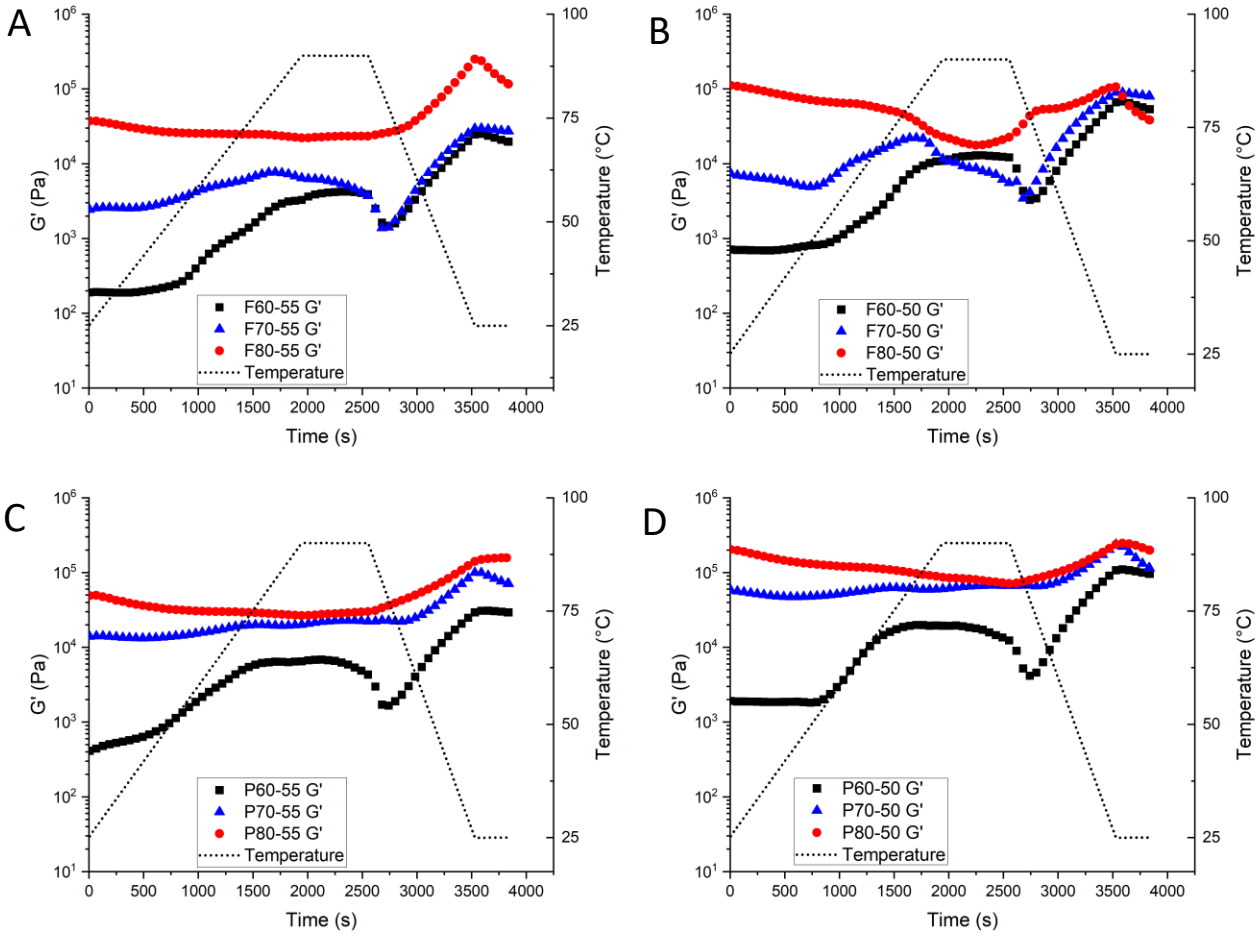

Figure 2.10. Storage modulus (G') development while heating and cooling of 60%, 70%, and 80% faba bean (A, B) and pea (C, D) proteins at moisture levels of 55% (A, C) and 50% (B, D). Dashed line indicates temperature change over time.

start to form new disulfide bonds and hydrophobic interactions, both resulting in an increase in viscosity (Rodriguez et al., 2023). Once 95°C was met and held, the storage modulus held mostly constant as proteins and starches equilibrated (Rodriguez et al., 2023). As the mixture cooled there was a rapid increase in G' until 25°C was reached. The increase in G' as the melt starts to cool could be due to starches gelatinizing and starting to recrystallize into a firm matrix (Damodaran, 2008b), and from the unfolded proteins forming new protein-protein interactions like hydrogen bonds (Zhang et al., 2022c) and protein network crosslinks (Rodriguez et al., 2023), ultimately strengthening the melt. However, at faba bean and pea 80% protein, G' decreased slightly as the temperature reached 95°C, causing the protein melt to thin until cooling started. Initial denatured state of proteins in the starting material (from protein extraction process) may be the cause of thinning since denatured proteins have already formed protein-protein interactions prior to rheological testing, which was previously stated as a reason for thickening upon heating (Beliciu et al., 2011; Rodriguez et al., 2023). The 80% protein G' demonstrated a pseudoplastic thinning behaviour upon heating, and then follow the same pattern as the 60% and 70% protein content when cooled. It can be hypothesized that this pseudoplastic behaviour may in part be due to over dispersion of proteins and starch phases, resulting in a weakening of bond formations or unfolding and breaking of protein bonds when heated (Wittek et al., 2021b). More likely, the lack of starch (F80 5.1%, P80 4.7% starch content) indicates the available starch present was not sufficient to provide enough substantial thickening upon gelatinization to counterbalance any effect of thinning from protein bond structure breaking down until cooling started. Although these proteins were able to realign upon cooling and increase in bonding structure as shown by a similar increase in G' when cooled and gelatinization of starches could increase the viscosity. At 70% pea protein (Fig.

2.10 C, D), the storage modulus continued to increase until 95°C was reached then rapidly increased at the melt cooled and did not start to decrease until melt was held at 25°C.

Melts with higher protein content (80%) tend to decrease in viscosity upon heating due to the proteins of raw materials unfolding and the interruption of original bonds causing dissociation of proteins unto protein subunits (Wittek et al., 2021b). In addition, the available starch present was low, thus not sufficient to provide enough substantial thickening upon gelatinization to counterbalance any effect of thinning from protein. During cooling the viscosity increased significantly due to reforming of protein intermolecular interactions to form crosslinked networks. Whereas starch behavior dominated in samples with lower protein content (60%) with an increase in viscosity upon heating caused by starches starting to swell and gelatinize. During cooling, such samples experienced a decrease in viscosity (shear-thinning) initially owing to the breakdown of swollen starch granules and lack of protein encircling the starch granules, which would help to withstand starch breakdown (Kesarwani et al., 2016). The breakdown of starches was followed by viscosity increase upon further cooling due to both starch gelatinization forming new networks, as well as protein crosslinking and new hydrogen bond formations. Interestingly, the faba bean curve of the 80% melt displayed more shear thinning at 50% moisture than at 55% moisture. This may be due to the increased apparent protein content decreasing the number of available starches to swell within the melt, as well as less water available for starch swelling (Xie et al., 2008). In addition, melts with higher protein content showed higher initial viscosity because globular proteins exhibit higher molecular weights than starches (Kornet et al., 2020). Moreover, higher storage modulus resulted from a lower moisture content since an increase in moisture caused a lower viscosity and possibly increases the distance between protein-protein interactions.

Expansion may be more related to overall curve viscosity and not correlated to either the peak or final viscosity since the differences in peak and final viscosities (setback) remain similar among each 60%, 70%, and 80% protein level samples at different moisture levels (Kesarwani et al., 2016). Curve viscosity of storage modulus was generally higher at 50% moisture levels than 55% for both faba bean and pea at 60% and 70% protein levels. This increase in viscoelasticity at 50% moisture may partially explain why there was a slight increase in ER values, since more elastic protein melts allow for stretching and therefore more expansion. At 80% protein content, the viscosity of storage modulus was higher in pea than with faba bean, indicating pea proteins may form strong interactions in the protein networks at a higher protein concentration than faba bean proteins. This assumption can be supported by the fact that 80% pea had higher expansion values and lower bulk density (holding more and/or larger air pockets). In addition, increased aggregation of faba bean proteins presented from FTIR and SDS-PAGE data may conformationally hinder the formation of new crosslinks or protein-protein interactions.

2.3.6 Confocal imaging of protein-starch phase structures

Protein (red) and starch (blue) distribution within faba bean and pea TVP were analyzed by confocal imaging as shown in figure 2.11 and figure 2.12 displaying a starch-in-protein network with both a starch phase and protein phase. The suggested degree of phase separation to be discussed will be defined as; the degree to which starches and proteins are associated with themselves while holding the physical structure of the TVP together. The protein content had an obvious impact on the starch-in-protein matrix for all faba bean and pea TVP samples. The pea TVP displays three very distinct structures based on protein levels. Dispersion of starch (Fig. 2.11A, D) at the 60% protein level in pea TVP were homogenously spread within the pockets of the protein matrix, starch and oblong shaped pores elongated in the same orientated direction. This

elongation of the protein matrix is orientated with the length of the extruder barrel within the melting zone after expansion at the extruder die. Starches were distributed evenly and seemed to allow for protein structure to form oblong pores around the regularly occurring starch bodies, rather than starches migrating to available spaces between irregular shaped pores in the protein matrix. Tolstoguzov (1993) suggests that this elongation of pores is caused by the starch dispersed phase solidifying before or at the same time as the protein continuous phase is elongated and solidified when exiting the extruder die at the time of expansion. Grabowska et al. (2016) found similar structures when increasing soy protein levels using shear cell technology where starches were homogenously dispersed within the protein matrix at 35% protein and displayed aligned anisotropic structure at a higher 45% protein level. They suggested that an increase in shear force resulting from increased protein concentration was necessary for phase alignment and texturization (Grabowska et al., 2016). This was also demonstrated in this study as reflected by increased visual elongated structure (Fig. 2.11B, E) when protein concentration was increased to 70% with corresponding higher G' values found. Pea protein TVP (Fig. 2.11) tended to have more and larger air pockets than the faba bean TVP (Fig. 2.12), which matches work performed by Duque-Estrada et al. (2023) who used confocal imaging to compare microstructure of TVP made with different ratios of pea, faba bean, and fiber sources (quinoa and hemp). All TVP's contained rigid fibers in a protein matrix in which the pea dominant TVP displayed a greater number of air cells contributing to a low density, sponge like protein matrix. The authors did not speculate why pea TVP formed these open structures, but it could be due to the 7S to 11S globular protein ratio of pea and the ability of each protein to spread at the air-water interface of formed air pockets and hold the structure after expansion when TVP is cooled. 7S proteins in soy have been known to spread more efficiently to air-water interfaces than 11S globulins which aggregate in the bulk

phase and do not move efficiently to the air-water interface (Carrera Sanchez et al., 2004). Since pea has a lower 11S to 7S ratio than faba bean (Gueguen et al., 1994; Vatansever et.al., 2020), this may partially explain why the pea TVP generally had more and larger air pockets seen in both confocal (Fig. 2.11) and photographic imaging (Fig. 2.1) as well as in observed expansion ratio and bulk density. In addition, the formation of more aggregation in faba bean protein during extrusion makes the protein molecule larger and less flexible, thus may move slower to the air-water interface, and less efficient to adsorb at the interface, leading to formation of less air pockets in the protein melt (Tsoukala et al., 2006).

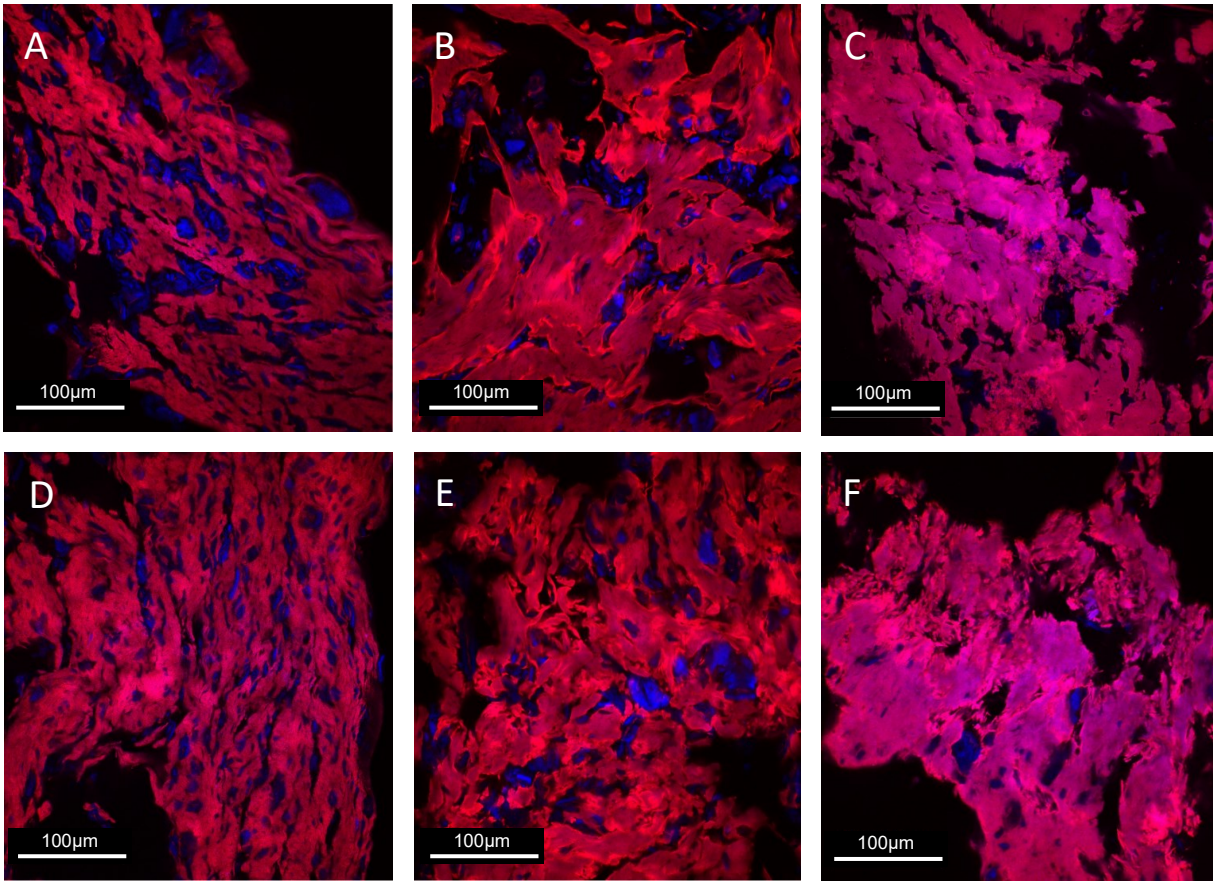

Figure 2.11. Confocal micrographs of pea protein TVP extruded at protein levels 60% (A, D), 70% (B, E), and 80% (C, F) and moisture levels of 50% (A, B, C) and 55% (D, E, F).

A further degree of phase separation may have occurred in the 70% pea protein TVP (Fig. 2.11B, E) between the starch and the protein matrix which is displayed as elongated protein structures consisting of gelatinized starch particles gathering in the larger pores of the protein matrix. The 80% pea protein TVP (Fig. 2.11C, F) had a distinctively dense protein matrix with less homogenous distribution of starch located sporadically deep in the protein matrix. Larger air pockets (shown as black in the confocal imaging) tended to break up the dense protein matrix, causing TVP to crumble. Starch distribution within the protein matrix of the faba bean TVP was similar to the pea TVP at 60% (Fig. 2.12A, D) and 70% (Fig. 2.12B, E) protein levels. Generally, the faba bean TVP had smaller air pockets and the protein matrix was more dense due to high level of protein aggregation, and had noticeable differences in the 80% faba bean protein TVP (Fig. 2.12C, F) compared to the pea TVP. This dense structure was confirmed by lower expansion ratio and higher bulk density values in faba bean TVP compared to pea. This result suggests that a certain amount of starch (higher than 5%) is required for even distribution and expansion and structuring of faba bean protein based TVP.

Gelatinized starch granules in both faba bean and pea TVP were more evenly distributed at 55% moisture. The increase of moisture in the protein melt could allow for more flow (less viscous) and movement of starch in the extruder, which was indeed more evident at the 60% protein levels (Fig. 2.11A, D and Fig. 2.12A, D). The even distribution of starch within the protein matrix at 55% moisture reflected lower final G', lower expansion ratios, and higher bulk density. This possibly suggests that starch placement and size may interfere with protein-protein interactions during the formation of air-pockets, resulting in less air pockets and a denser structure. Gelatinized Starch granule size was consistent between 50% and 55% moisture content within each protein levels.

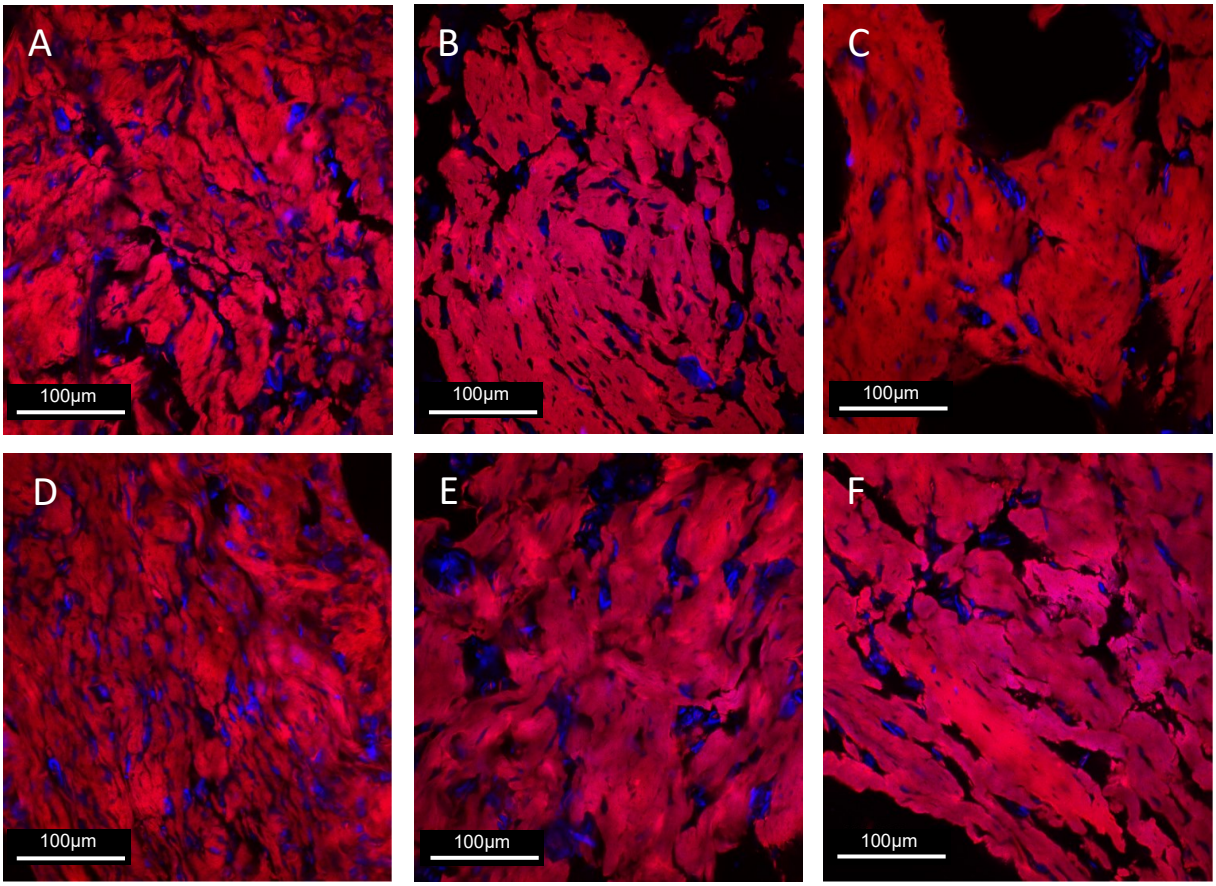

Figure 2.12. Confocal micrographs of faba bean protein TVP extruded at protein levels 60% (A, D), 70% (B, E), and 80% (C, F) and moisture levels of 50% (A, B, C) and 55% (D, E, F).

Confocal imaging suggests that 70% protein in both faba bean and pea has a higher degree of phase separation between protein and starch which can be a favourable structure to form continuous protein matrix with starch distribution in the pockets and the air pockets (shown as black) formation indicates the protein matrix in TVP structure was strong to hold together tightly during air expansion. In addition, the elongated protein matrix allowed some fibrous structure formation in TVP to better simulate meat fibers.

2.3.7 *Scanning electron microscope images of TVP surface structures*

.The TVP matrix microstructure was observed using scanning electron microscope. Overall similarities between faba bean and pea SEM micrographs (Fig. 2.13 and 2.14) were observed. Any starch granules were only visible at the higher magnification (Fig 2.13D, E, Fig. 2.14C, E) and tended to be located mainly around the surface of the air pockets as small, round, protruding lumps. The lack of visible starch granules and rheology of starting material following typical heating curves reaching gelatinization temperatures during extrusion (Fig. 2.9) indicates the starch was

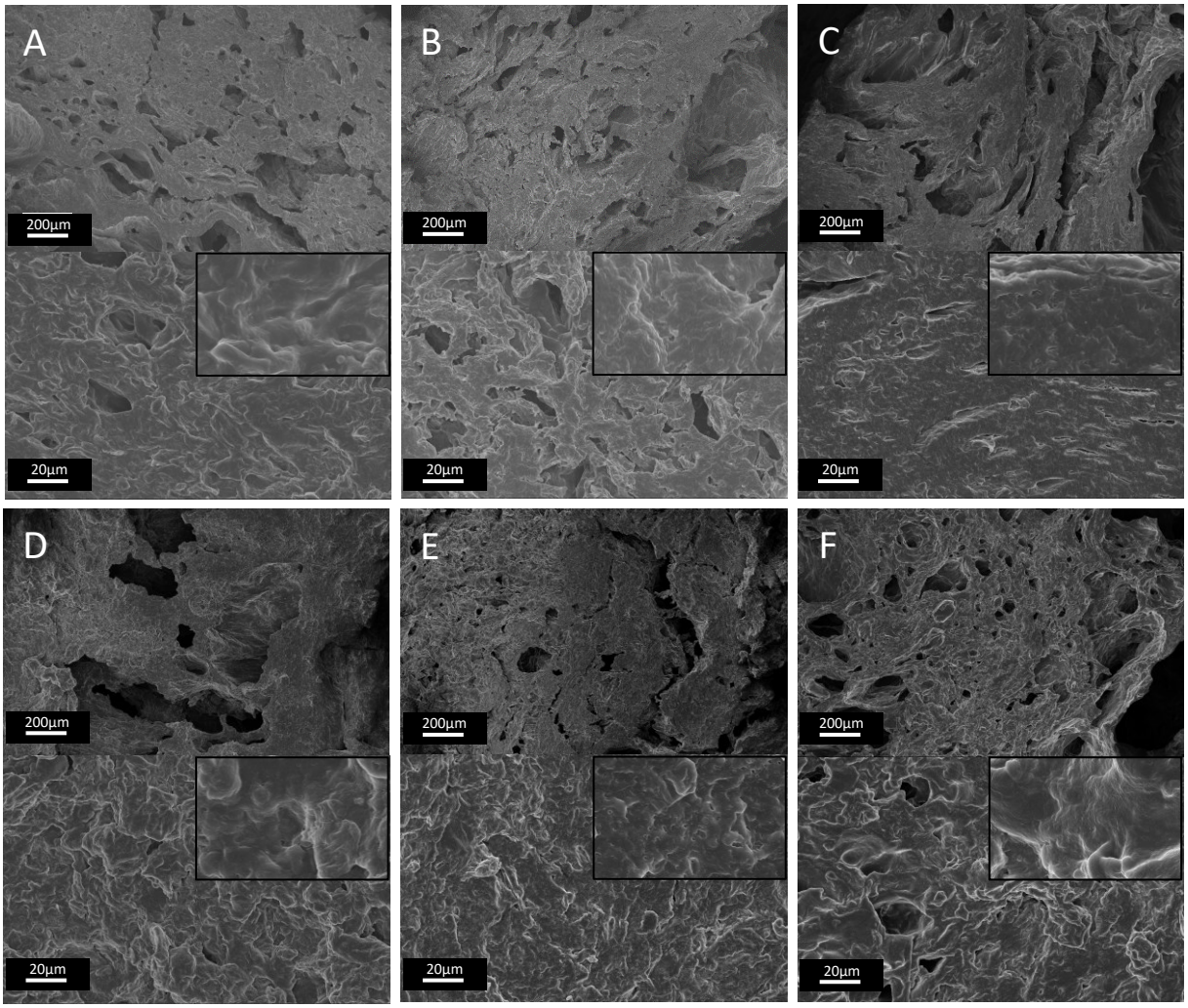

Figure 2.13. SEM micrographs of faba bean protein TVP extruded at protein levels 60% (A, D), 70% (B, E), 80% (C, F) and moisture levels of 50% (A, B, C) and 55% (D, E, F).

gelatinized in the TVP and created a smooth surface (Ferawati et al., 2021; Nilsson et al., 2022; Rodriguez et al., 2023). Although extrusion temperature and internal conditions are different than conditions performed under rheological testing in this study, an increase in G' between 55°C-60°C observed is close to the initial point of starch gelatinization (Ferawati et al., 2021; Nilsson et al., 2022), suggesting that gelatinization could indeed be occurring. In addition, rheological results showed thickening of melt when cooled, which is typical of rheological starch pasting curves of gelatinized starches (Fig 2.10). A rough crater-like surface would form as the consequence of air bubble rupture and collapse during extrusion, whereas a homogeneous surface indicates there is good compatibility between protein and starch without obvious macroscopic phase separation in the TVP which demonstrates good expansion (Beck et al., 2018). Micronucleation (greater frequency of small pockets) at 55% moisture, as well as uniform starch distribution based on confocal imaging at higher moisture (55%), resulted in more nucleation points visible through SEM imaging. Although there were more nucleation points visible, ER at 55% moisture displayed a decrease in expansion in both faba bean and pea. This decreased expansion may be influenced by the differences in pressure between the bubble walls and the protein melt in which the thinner protein melt at 55% moisture weakened protein or starch interactions, causing the bubbles to coalesce and collapse, preventing large bubble formation (Twombly, 2020). A greater degree of starch-protein phase separation is needed for starch to diffuse within the protein melt and gather in greater volumes in the protein matrix, which subsequently cause greater expansion based on bubble growth or nucleation points that have coalesced and become larger (Twombly, 2020). This result further suggests that starch distribution in the protein matrix can impact the degree of micronucleation and bubble growth in the protein melts, and subsequently their expansion to form strong desirable TVP structures.

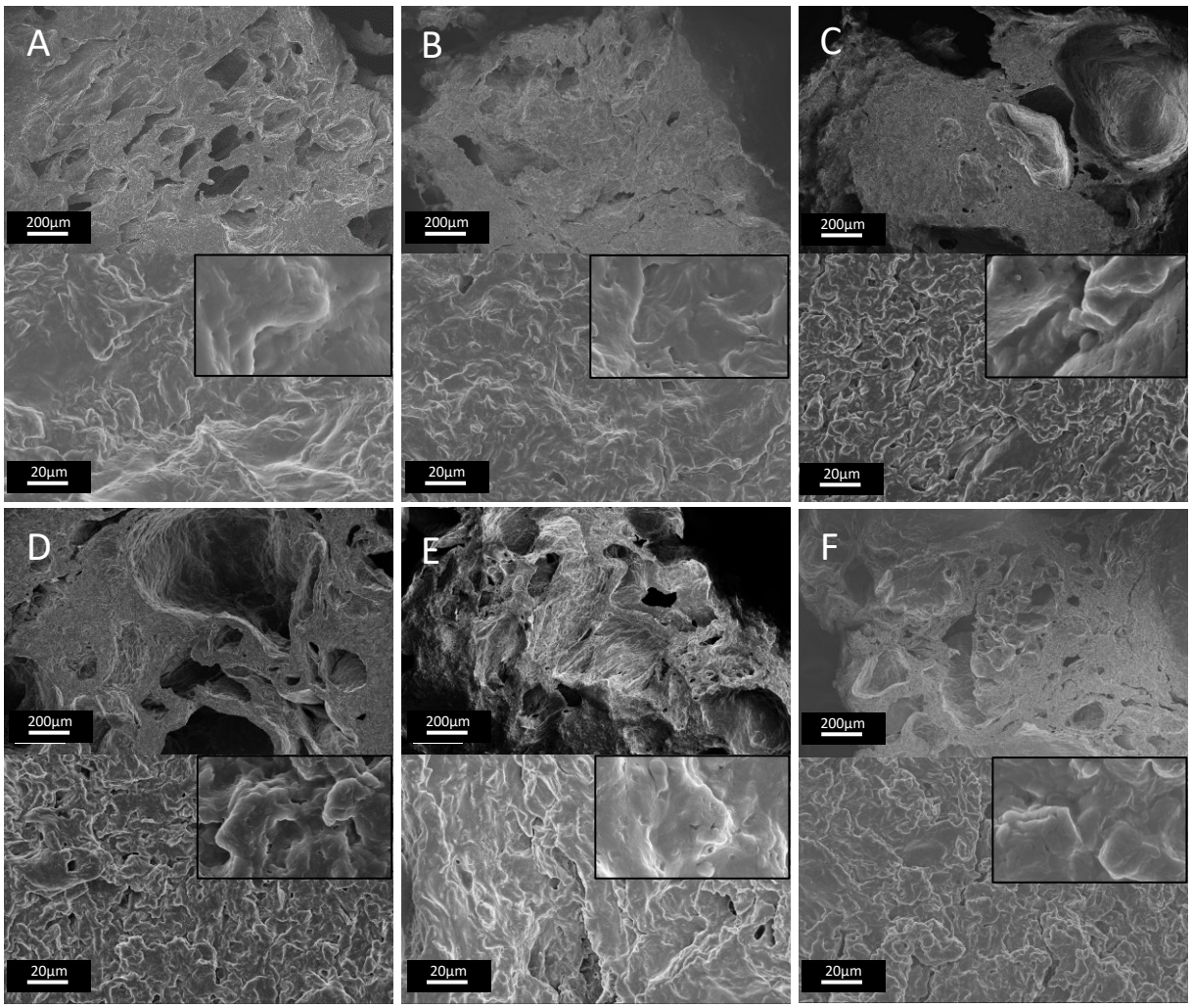

Figure 2.14. SEM micrographs of pea protein TVP extruded at protein levels 60% (A, D), 70% (B, E), 80% (C, F) and moisture levels of 50% (A, B, C) and 55% (D, E, F).

Faba bean TVP at 80% protein (Fig. 2.13C, F) had a layered structure which was observed in both SEM image and photographic imaging (Fig. 2.1), both of which were cut longitudinal to display formation and elongation of air pockets. The ability for faba bean proteins to form layered structure would be desired in high moisture meat analogues but the ability for proteins to form around air pockets and hold their structure during expansion is desired in TVP. This lack of continuous structural integrity could also be an indication of air pocket collapse at the point of

expansion when protein melt is exiting the extruder die since large air pockets at the 80% protein level were much further apart, creating dense structures loosely held together. As faba bean protein content increased, air pockets increased in number and decreased in size, which is confirmed by increased bulk density at the 80% protein level.

Pea TVP (Fig. 2.14) tended to have larger air pocket overall compared to faba bean TVP, which coincides with the increased expansion ratio and lower bulk density of pea TVP. In addition, larger air pockets of pea TVP and specifically at 70% protein in pea TVP was more evident in traditional photographic imaging when TVP was cut longitudinally to show the extend of air pocket size and frequency (Fig. 2.1). As discussed above, pea protein may have better expansion due to lower legumin/vicilin ratio than faba bean and less protein aggregation during extrusion, which could allow formation of viscoelastic protein film at the air-water interface of the bubble nucleation sites to promote expansion. Legumin is larger than vicilin causing slower movement to the air pocket air-water interface, and the rigid protein conformation from disulfide bonds can interfere with unfolding and thus prevent the protein flexibility needed to form around air pockets (Shi et al., 2002). Higher formation of rigid protein aggregates in faba bean TVP could also have interfered with the proteins ability to form a film at the air-water interface for the same reasons. Small legumin subunits may be faster to move to the air-water interface and could provide the required flexibility to form around the air pockets since the disulfide bonds between subunits are broken, reducing protein rigidity, which would allow for protein flexibility around those air pockets (Shi et al., 2002).

2.4 Conclusion

This study was able to expand beyond previous work that that is limited to investigating input and output extrusion parameters of a black box technology on TVP functionalities. By

correlating microstructures modulated by protein content and moisture to expansion and subsequently TVP quality, industry ingredient and product developers can better understand the inter-molecular phase structures of TVP to adopt new protein sources. In this study, microstructure shifted at 60% protein from a homogenously dispersed and gelatinized starch-in-protein phase with evenly dispersed oblong pockets to larger sporadic air pockets within a denser protein matrix at 80% protein, implying a degree of starch phase separation is required at 70% protein to improve TVP expansion and quality. Lower moisture (50%) provided better expansion as influenced from increased rheological G' and smooth SEM imaging to improve TVP quality. Faba bean TVP had greater protein aggregation lessening expansion, though microstructure and functionality was similar to that of pea and can become a viable high protein source to expand the TVP market options and value. With a wide range in protein content from 60%-80% and a lower range in moisture from 50% to 55%, results suggest protein content had more impact than moisture content on WHC, rheological properties and microstructure phase separation from confocal imaging. Moisture between 50%-55% during TVP production contributed mostly to differences in expansion and BD. Whereas protein source was more important to protein flexibility, aggregation and air pockets shown in SEM imaging.

In addition, this study has also shown that high protein concentrates from air classification (dry fractionation) can be used as a more sustainable base formulation supplemented with protein isolates to improve high protein TVP content and microstructure quality. Protein concentrates are less expensive to produce and could contain more native proteins and fewer aggregated proteins that have not been subjected to harsh extraction conditions like protein isolates produced from wet fractionation processing. Therefore, the use of concentrates can lower costs while maintaining high protein TVP with favorable functionality and structure.

Chapter 3: Effects of Starch and Dietary Fiber Content on Functional and Structural Properties of Faba Bean and Pea Texturized Vegetable Protein

3.1 Introduction

Extrusion is highly suitable for development of value-added products and can provide a method to incorporate by-product streams from other processes with potentially improved functional properties to increase nutritional value and structural properties of extruded products like TVP. Development of TVP stems primarily from the 1960's to early1980's with the use of soy and wheat as the protein source, though there has been a lag of continued research, renewed interest in meat analogue development has been brought on by a segment of the population that has been termed flexitarians who eat meat but follow a plant forward diet (Von Kaufmann et al., 2023; Baune et al., 2022; Grasso et al., 2023). However, a new generation of TVP is emerging by the investigation of other macronutrient effects on TVP protein matrix structure in relation to functionality such as starch and dietary fiber. Specifically, low moisture TVP has high potential for inclusion in hybrid meat products and can provide both improved functionality, texture, and potentially improve nutritional components like increasing dietary fiber intake and catering to starch digestion needs (Grasso et al., 2023).

Legume starches provide excellent stability against shear force and heat form extrusion while providing high gel strength and resisting disintegration during the cooking process (Tas et al., 2021), making them ideal for use in extruded products. Pea starch has been found to exhibit good expansion and physiochemical characteristics in extruded products (Rangira et al., 2020) and can be utilized as a by-product from pea protein extraction, assisting in less waste products, creating a more circular economy, and adding value to a waste stream. Under extrusion conditions of high heat, shear, and pressure, starch undergoes physiochemical changes by modifications of

the crystalline and amorphous regions, and phase changes from a glassy state to rubbery viscoelastic state during the extrusion process (EK et al., 2020b). High temperature and shear melt the crystalline region by uncoiling starch double helices, breaking hydrogen bonds between amylopectin and amylose, therefore increasing mobility of starch granules within the melt (EK et al., 2020b). Starches can generally be divided into four different classifications based on ease of digestibility, resulting in fluctuating effects on short-term health and long-term health (individuals with diabetes). They are readily digestible starch, slowly digestible starch, total digestible starch and resistant starch which are deemed as indigestible (Bello-Perez et al., 2020). Pea starch is high in amylose which is more likely to form starch-lipid complexes, a type of resistant starch that has been known to form through extrusion, providing beneficial regulation of blood glucose levels (Gulati et al., 2020; McCready et al., 1950). In addition, legume starches including yellow pea has been shown to have high levels of retrogradation in extrudates which can increase resistance of digestive enzymes, promoting a lower release of sugars into the blood stream and lowering glycemic response (Tas et al., 2021). Specifically, high amylose starch like in pea can form resistant starch and resist enzymatic attack based not on crystallinity of resistant starch but rather the dense molecular packing (Ye et al., 2018). Changes in starch formation can be measured by various methods. FTIR can be used to determine the short range ordered structure of starches whereas x-ray diffraction can be used to determine the long-range ordered structure of starches and packing of double helices along with the type of crystallinity, both based on starch double helices (Pozo et al., 2018).

Fibers tend to undergo less or no phase transitions at all under high heat, shear, and pressure conditions during extrusion, although soluble fibers could change phases owing to their increased solubility and higher affinity with water (EK et al., 2020b). The addition of β-glucan has been

shown to retain functional properties and improve nutritional quality of faba TVP by increasing soluble dietary fiber content of TVP (Sayanjali et al., 2017; Saldanha et al., 2023). A Government of Canada's source of fiber health claim could be applicable in the final meat analogue product if it contained was a minimum of 2g β-glucan or pea hull fiber per 75g serving size (Food and Drug Regulations, 2024). Fiber inclusion in extruded snack products has been shown to provide beneficial health responses by extending postprandial glucose release, possibly affecting satiety responses (Brennan et al., 2012). Contradicting reports on insoluble fiber either increasing or decreasing expansion based on particle size mostly involve starch based extrudates and not protein based TVP (Wang et al., 2017; Robin et al., 2012). Small insoluble particle sizes have been shown to increase expansion by increasing the number of nucleation sites so that air pockets can form while at the same time acting as a filler distributed uniformly in cell walls without causing cell rupture (Wang et al., 2017). Studies have also shown a decrease in expansion from insoluble fibers rupturing cell structure, specifically at higher inclusion rates which over saturate the melt and from larger particle sizes physically causing cell rupture preventing bubble growth, and decreasing cell size (Wang et al., 2017; Robin et al., 2012). To determine effects of insoluble fiber on low moisture TVP we could apply combined concepts both from starch expanded products previously mentioned and from high moisture extrusion. Insoluble fiber in HME had been shown to prevent protein aggregation up to 15% inclusion in soy based TVP but at 20% inclusion the insoluble fiber disrupted the continuous protein network and prevented cross-linking between proteins (Deng et al., 2023). There is limited knowledge on how insoluble and soluble fibers interact with the structural matrix of low moisture extruded products, especially in TVP (Xiao et al., 2023), therefore further investigation in this area is warranted for improved extrudate nutrition.

The aim of this study is to investigate how the addition of starch to faba and pea TVP can impact the protein matrix structure and product quality of the extrudates. The protein conformation and rheology were studied while determining the effect of extrusion on changes in starch type. Starch inclusion TVP were produced from faba bean and pea protein concentrates and isolates which were supplemented with 5%, 7.5%, 10% and 20% pea starch. The most promising pea TVP was then supplemented with 5% and 10%, insoluble pea fiber with 100µm or 150µm particle size, or with soluble β-glucan fiber at 5%, 10% and 20%. The TVP supplemented with insoluble and soluble dietary fiber in pea extrudates were also investigated to determine the effects on extrudate product characteristics and protein matrix structure in addition to inclusion of starch. Functional properties including expansion ratio, bulk density, water holding capacity and oil holding capacity were analyzed along with rheological properties under a 25°C-95°C-25°C temperature ramp to simulate the initial temperature increase during extrusion. Changes to protein confirmation in TVP was analyzed with FTIR and changes to dietary starch were investigated through starch digestion, FTIR and x-ray diffraction, whereas protein matrix microstructure was observed by confocal and SEM imaging techniques. The supplementation of starch and dietary fiber in TVP were discussed to provide insight on structural and functional impact to TVP by connecting the influence of starch and dietary fiber on protein matrix structure. To the best of our knowledge, the study of the effects of starch on protein based TVP with pea or faba and dietary fiber on low moisture extrusion is scarce, especially on the impact to protein matrix microstructure in relation to the extrudate product functional characteristics.

3.2 Materials and methods

3.2.1 Materials and chemicals

Commercial pea (55% protein) and faba bean (60% protein) starting material were kindly provided by Ingredion (Westchester, Illinois, United States), whereas pea (85% protein) and faba bean (90%) isolates were kindly provided by AGT Foods and Ingredients (Regina, Saskatchewan, Canada). Oat protein and β-glucan (containing of 34% soluble fiber) was purchased from Lantmannen (Stockholm, Sweden). Pea hull fiber 125 and 200 were purchased from Avena Foods Ltd (Regina Saskatchewan, Canada) composed of 79.6% insoluble fiber. Compositional analysis of macro nutrients of starting materials and subsequent formulations were provided by suppliers. SDS-PAGE 4-15% gels (Mini-PROTEAN®TGX™), SDS-PAGE broad-range molecular weight standards, sample buffer, and running buffer were purchased from Bio-Rad Laboratories Inc. (Hercules, California, United States). Digestible and resistant starch assay kit (K-DSTRS) was obtained from Megazyme (Bray Wicklow, Ireland). All other chemicals were purchased from Sigma-Aldrich Co. (Oakville, Ontario, Canada). Purified water used in this study was generated by Milli-Q Advantage A10 system (EMD Millipore Corporation, Massachusetts, United States). Canola oil was purchased from a supermarket locally.

3.2.2 TVP extrusion and sample preparation

Protein concentrates and isolates were mixed to achieve 70% starting protein content for both faba bean (F) and pea (P) sources, then starch was added in the formulation with 5%-20% inclusion levels. Fiber inclusion was based on the favourable results of the starch inclusion treatments. Specifically, the formulations contained 70% protein, then 10% starch and then 5%-10% insoluble fiber or 5%-20% soluble fiber. Macronutrient composition is displayed in Table 3.1. Insoluble pea hull fiber specification passed though US mesh sizes of 100 and 150 resulting

in particle sizes of 150.11µm (150µm) and 97.63µm (100µm), respectively, based on polynomial trend line equation ($y=19880x^{-1.061}$) from the American National Standard for Industrial wire cloth (ASTEM E11-01) conversion table and will be referred to as 150µm and 100µm in this chapter. The starting materials were pre-hydrated to 15% moisture content by even mixing with fine misted tap water prior to extrusion. TVP were manufactured with a co-rotating twin screw extruder (Coperion ZSK 26, Coperion, Stuttgart, Germany) equipped with a 3mm die. All other extrusion parameters were optimized within the desired expansion range based on preliminary work in order to accommodate both faba bean and pea proteins and held constant throughout the experiment. Treatments with added starch were extruded at 170°C and a screw speed of 450rpm whereas treatments with added dietary fiber were extruded at 150°C and a screw speed of 550rpm based on initial optimization. Water injection rate was adjusted to reach total moisture contents of 50% in the melt. Once extruder conditions stabilized, TVP was pelletized and collected. Pelletized TVP were dried in a tray oven at 60°C for 30 minutes and sealed in a double plastic lined bags stored at room temperature (21°C). TVP samples were then ground with a conical mill equipped with a 12×12mm screen size at 31Hz motor speed. The ground TVP was passed through a 1.18mm screen and stored in double lined plastic bags at room temperature (21°C) for further analysis. Extrusion was performed in duplicate on separate dates for each replicate.

3.2.3 Expansion ratio and bulk density

Expansion ratio was determined by using vernier calipers, to measure the diameter of three sections per extrudate on 10 extrudates per replicate. The expansion ratio is calculated by dividing the average extrudate diameter by the diameter of the die opening of the extruder (Equation 1). (Sahu et al., 2022).

$$ER = \frac{\text{Diameter of extrudate (mm)}}{\text{Diameter of extruder die (mm)}} \quad (1)$$

Bulk density was determined by using vernier calipers, to measure the diameter of three sections per extrudate on 10 extrudates per replicate, length of each extrudate, and weight of each extrudate. The bulk density was calculated by determining the ratio of mass to volume and expressed as g/cm^3 (Equation 2). (Sahu et al., 2022).

$$BD = \frac{(4 \text{ x } m)}{(\pi \text{ x } d^2 \text{ x } L)} \quad (2)$$

Where m is the mass in grams, d is diameter in centimeters, and L is the length in centimeters.

3.2.4 Water holding capacity

Water holding capacity was measured via AACC Approved Methods of Analysis 56-37.01 Water Holding Capacity of Pulse Flours and Protein Materials. Sample (1g) was weighed into a glass test tube and mix with a glass stir rod for 1 minute with an undetermined amount of Milli-Q water until saturated. The stir rod was cleaned with folded 2"x4" filter cloth covering the tube and placed upside down in a syringe assembly consisting of a plastic syringe barrel in a 50ml plastic centrifuge tube. The assembly was centrifuged at 300xg for 10 minutes. WHC was calculated as g H_2O/g sample, dry matter (Equation 3).

$$\text{WHC (g } H_2O\text{/g sample, dry matter)} = \frac{(W3-W2)+(W1 \text{x } Mc)}{(1-Mc)W1} \quad (3)$$

Where W1 is the sample weight in grams before water addition, W2 is the weight of syringe assembly (syringe, filter cloth, test tube, sample) before centrifugation, W3 is the weight of the syringe assembly after centrifugation, and Mc is the initial moisture content of the sample as a percentage.

3.2.5 Oil holding capacity

Oil holding capacity was determined according to the method by Wang et al., (2020) with modifications. Sample (1g) was mixed with 10g canola oil in pre-weighed 15ml centrifuge tubes. Tubes were Inverted to shake for 10 seconds, and every 5 minutes for a total of 30 minutes. Tubes were centrifuged for 15 minutes at 1000×g, excess oil was decanted, and tubes placed upside down on paper towel for 30 minutes to drain. OHC was calculated as g oil/ g sample.

3.2.6 Protein conformation in TVP by Fourier-transform infrared spectrum

Pea and faba bean protein structure in TVP was characterized by fourier transform infrared spectrophotometry (Nicolet 6700, Thermo Fisher Scientific Inc, Pittsburgh, Pennsylvania, United States). Ground TVP and potassium bromide (KBr) were dried at 80°C for 30 hours in an oven and transferred to a desiccator. Each sample (1mg) was ground further with 99-101mg KBr with a mortor and pestle and pressed into a disk under 15000lb pressure for 5 minutes. The transparent disk was transferred to the FTIR spectrophotometer where the spectra read at a resolution of 4cm^{-1} and a wavenumber of 1111-4000cm^{-1} for 128 scans. Under the same conditions, the KBr background was subtracted from the spectra. Fourier self-deconvolution was performed by Omnic 8.1 software on the amide I band region (1700-1600cm^{-1}) with an enhancement factor of 2.5 and at a bandwidth of 24cm^{-1} (Yang et al., 2021) and the starch region (1070-960cm^{-1}) with an enhancement factor of 3.4 and at a bandwidth of 46.5cm^{-1}.

3.2.7 Rheological properties

Rheological behaviours of TVP starting materials were analyzed by a TA Discovery HR-3 rheometer (TA Instruments, Delaware, USA) equipped with a 40mm diameter parallel-plate with a gap of 1mm. Pea and faba bean protein starting material with starch and fiber inclusions were hydrated to 50% total moisture content with milli-Q water to mimic moisture content in the

extruder. A temperature sweep was performed to record storage and loss modulus continuously. A temperature ramp was performed to mimic viscoelastic properties under semi-extrusion temperatures. Samples were heated from 25°C to 90°C at a rate of 2°C/minute for 10 minutes and cooled to 25°C at a rate of 4°C/minute. Samples were held for 20 minutes under 1% strain and at a frequency of 1Hz. Evaporation was prevented by using a trap cover and silicone oil.

3.2.8 TVP Morphology by confocal laser scanning microscope

Microstructures of proteins and starch in TVP were visualized by a confocal laser scanning microscope (LSM 510 META, Zeiss, Oberkochen Germany). Whole TVP samples were hydrated with room temperature (21°C) milli-Q water for 15 minutes in a ratio of 5:1 (H_20:TVP) and allowed to drain free of excess water on paper towel for 10 minutes. Drained TVP were frozen for 15 minutes and sliced thinner than 1mm with a razer blade. Sample proteins were stained red with Acid Fuchasin (0.1% w/v) for 2 hours and washed with milli-Q water twice. Samples starch were stained blue with Calcoflour white (0.01%w/v) for 2 minutes and washed twice with milli-Q water.

3.2.9 Scanning Electron Microscopy (SEM)

Scanning electron micrographs of TVP were generated by using a Sigma SEM EDX (SEM EDX, Zeiss Sigma, Jena Germany) with an EHT voltage of 10kv. Micrographs were taken at magnifications of 50X, 500X, and 1KX. Samples were hydrated with room temperature (21°C) milli-Q water for 10 minutes, drained for 1 minute, and flash frozen with liquid nitrogen. Samples were then cut longitudinally with a scalpel to show the internal air pocket structures formed running parallel with the extruder barrel. Samples were then airdried and mounted onto platforms and sputter coated with a thin layer of gold for 120 seconds for conduction.

3.2.10 X-ray diffraction

X-ray diffraction of starting materials and TVP was measured by a Bruker D8 Advance (D8 Advance, Bruker, Massachusetts, US) diffractometer with Co Kα radiation at 35kV and 40mA. Continuous scan mode was used with 2θ diffraction angle and scanning regions of 3-80° range at steps of 0.0100° and a scan speed of 1.00s/step.

3.2.11 Dietary fiber and resistant starch

Readily digestible starch, slowly digestible starch, total digestible starch and resistant starch were measured according to procedures from Megazyme Digestible and resistant starch assay protocol with slight modifications (Fig. 3.1). Briefly, TVP were ground by mortar and pestle and passed through a 100μm screen prior to analysis. Samples (0.5g) were wetted with 95% EtOH (1ml) for 10 minutes, vortexed with sodium maleate buffer (17.5ml) and incubated at 37°C for 5 minutes. An additional 1.5ml sodium maleate buffer was added with 1ml $(NH_4)_2SO4$ pancreatic α-amylase/amyloglucosidase (PAA/AMG) enzyme suspension and incubated in a shaking water bath until determining digestible starch, stirring occasionally. At 20 minutes (RDS), 2 hours (SDS) and 4 hours (TDS) 1ml of digested sample was mixed with 20ml acetic acid to stop the reaction. 2ml was centrifuged at 13,000rpm for 5 minutes of which 0.1ml was vortexed with 0.1ml of dilute AMG to hydrolyze remaining polymers to glucose and incubated at 50°C for 30 minutes. The standard (0.2ml acetic acid buffer), blank (0.1ml acetic acid buffer, 0.1ml D-glucose), and sample were each vortexed with 3ml GOPOD (glucose oxidase and peroxidase) reagent and incubated at 50°C for 20 minutes. Absorbance was measured at 510nm against the blank. Resistant starch was measured after 4 hour digestion by vortexing 4ml digested sample with 4ml 95% EtOH and centrifuged at 4,000rpm for 10 minutes, supernatant decanted, and washed twice with 50% EtOH following the same procedure. Samples were analyzed for RS by resuspending the pellet in 2ml

cold NaOH and stirring over ice water for 20 minutes. The sample was then vortexed with 7.5ml sodium acetate buffer, 0.5ml HCl, and 0.1ml AMG and incubated at 50°C for 30 minutes. After centrifuging at 13,000rpm for 5 minutes, 0.1ml was vortexed with 0.1ml sodium acetate buffer and 3ml GOPOD reagent then incubated at 50°C for 20 minutes before measuring absorbance at 510nm against the blank.

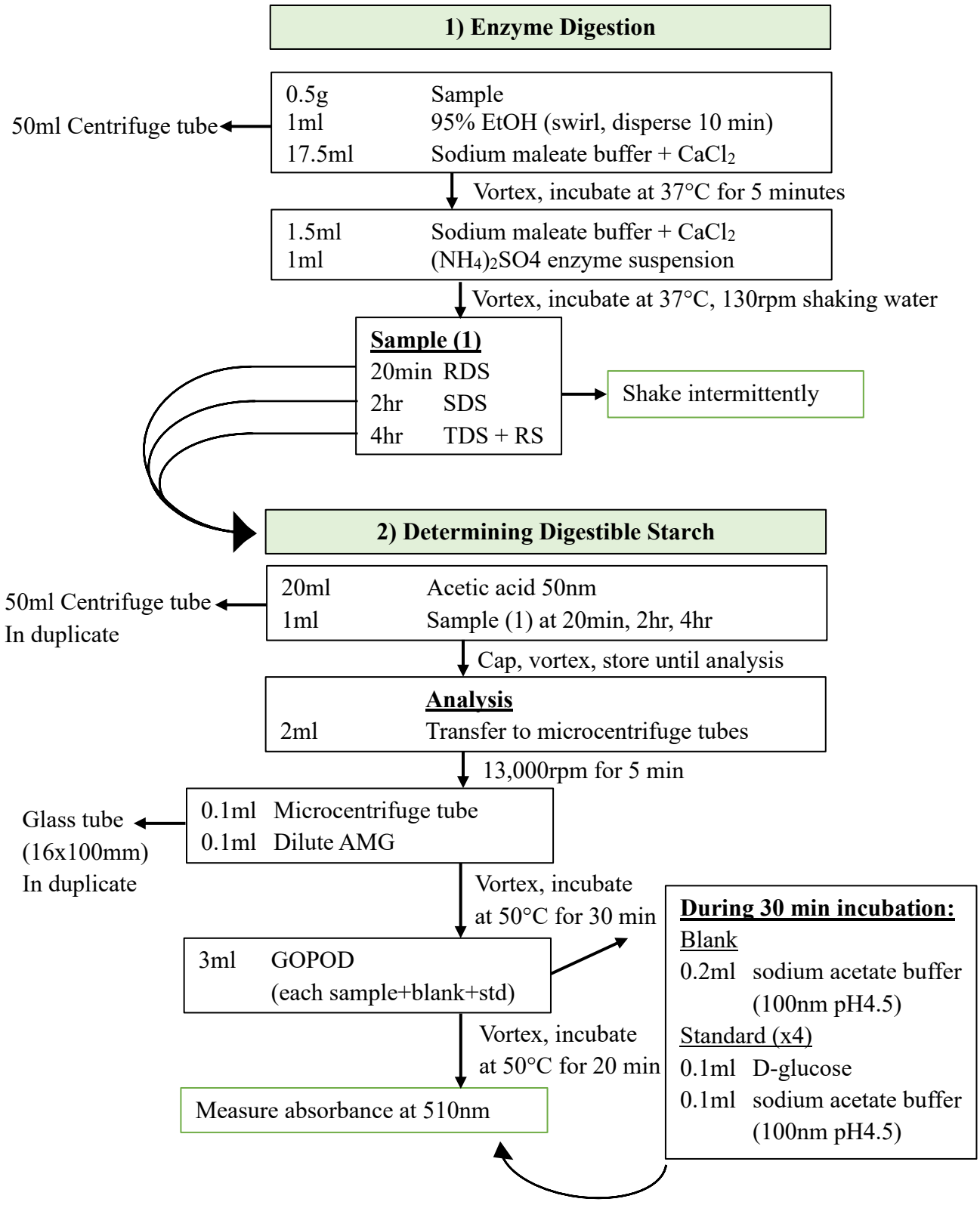
1) Enzyme Digestion
0.5g Sample
1ml 95% EtOH (swirl, disperse 10 min)
17.5ml Sodium maleate buffer + CaCl2
50ml Centrifuge tube
Vortex, incubate at 37°C for 5 minutes
1.5ml Sodium maleate buffer + CaCl2
1ml (NH4)2SO4 enzyme suspension
Vortex, incubate at 37°C, 130rpm shaking water
Sample (1)
20min RDS
2hr SDS
4hr TDS + RS
Shake intermittently
2) Determining Digestible Starch
20ml Acetic acid 50nm
1ml Sample (1) at 20min, 2hr, 4hr
50ml Centrifuge tube
In duplicate
Cap, vortex, store until analysis
Analysis
2ml Transfer to microcentrifuge tubes
13,000rpm for 5 min
0.1ml Microcentrifuge tube
0.1ml Dilute AMG
Glass tube
(16x100mm)
In duplicate
Vortex, incubate
at 50°C for 30 min
3ml GOPOD
(each sample+blank+std)
Vortex, incubate
at 50°C for 20 min
Measure absorbance at 510nm
During 30 min incubation:
Blank
0.2ml sodium acetate buffer
(100nm pH4.5)
Standard (x4)
0.1ml D-glucose
0.1ml sodium acetate buffer
(100nm pH4.5)

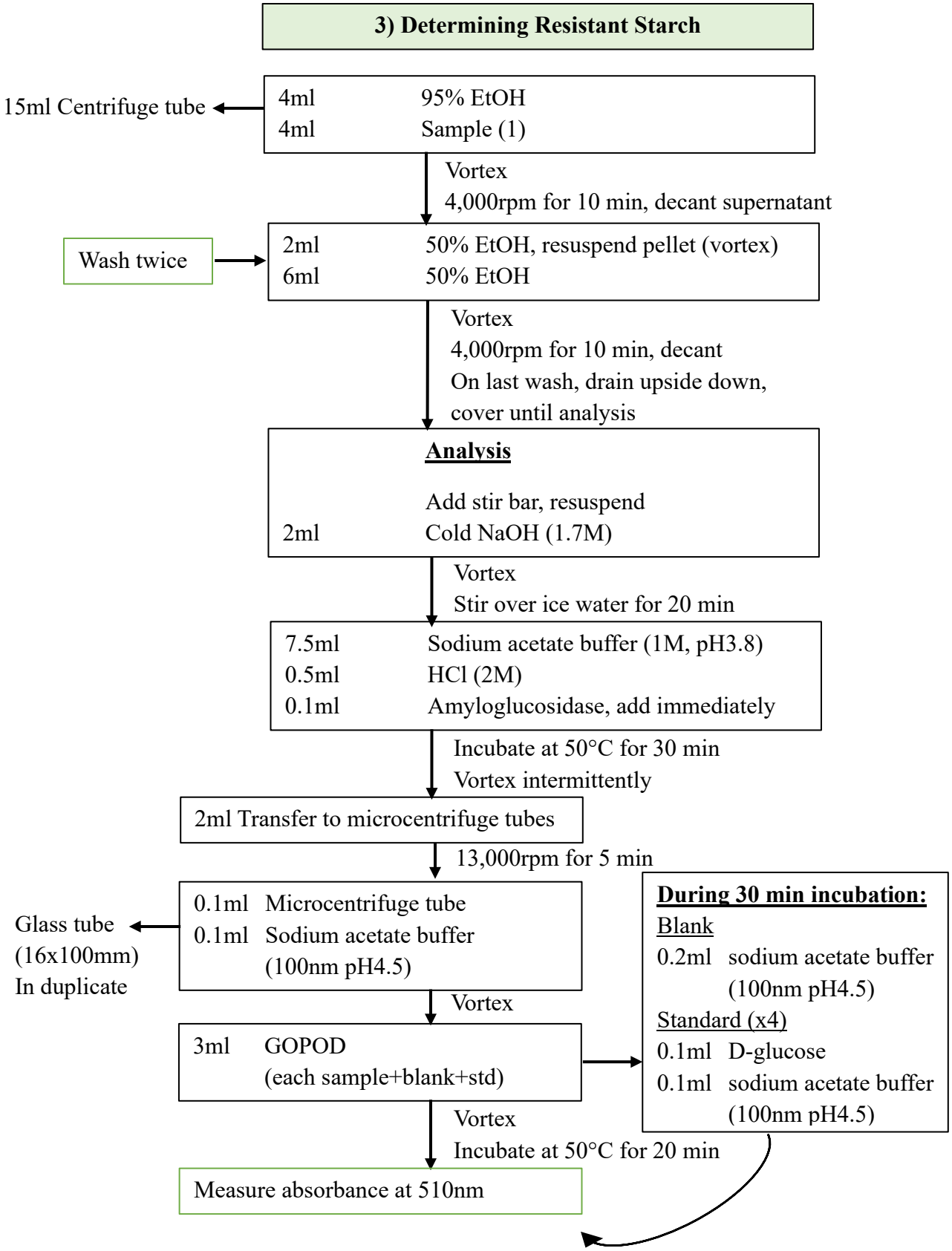

Figure 3.1 Adapted Megazyme digestible starch and resistant starch determinization method.

3.2.12 Statistical analysis

All quantitative analysis were performed at least in triplicate on two independent extrusion repetitions. Starch digestion was performed in duplicate. Origin version 2022b (OriginLab Corporation, Northampton, MA, USA) software was used for statistical analysis and results presented as the mean ± standard deviation. Statistical analysis was conducted by one-way analysis of variance (ANOVA) at a confidence interval of 95% utilizing Tukey's test at $p>0.05$.

3.3 Results and discussion

3.3.1 Effect of starch inclusion rates on faba bean and pea TVP functional properties

Inclusion of starch can increase desirable expansion of TVP and improve texture of extrudates (Ek et al., 2020b). TVP had dense internal structures at low starch levels more evident in the faba bean TVP. As starch inclusion levels increased, TVP expanded and internal structures changed in bubble nucleation amount and bubble size (Fig. 3.2). Starch caused an increase in expansion of faba bean TVP up to the 7.5% inclusion rate (1.92 ER) and then with further increase of starch content up to 10% (1.93 ER) and 20% (1.89 ER), the ER remained almost unchanged (Fig. 3.3A). For pea protein, 10% and 20% starch inclusion significantly increased the TVP expansion rate from 5% starch inclusion (1.82 ER) and 7.5% starch inclusion (1.78 ER) to an ER of 1.99 and 2.02 respectively. The addition of starch can cause increased expansion of extrudates from several mechanisms based on; starch swelling, flow behavior, nucleation, gelatinization, and stabilization of expanded network. With the addition of water and onset of swelling, the water acts as a plasticizer, allowing more space between starch granules and creating a more even distribution within the melt and access to water to aid in swelling (Kristiawan et al., 2020). When the starch is mixed with water, the high swelling of starches promotes uniform heating and internal mixing within the extruder (Wang et al., 2014). The hydration and swelling of starch then affects viscous

flow behavior by decreasing viscosity upon heating due to the swelling of starch granules, allowing for nucleation and bubble growth (Parmar et al., 2021; Hong et al., 2022). As starches swell, gelatinization starts to occur which results in a stable expanded structure (Wang et al., 2014).

Table 3.1 Macronutrient composition (dry basis) of faba bean (F) and pea (P) protein concentrates/isolates, pea starch, pea hull fiber (150µm and 100µm), β-glucan (BG), and starting material inclusion rates.

Treatment	Protein (%)	Starch (%)	Fibre (%)	Fat (%)	Ash (%)
Faba bean concentrate	60.0	11.5	13.6	3.8	11.1
Faba bean isolate	89.0	2.0	2.0	6.5	0.5
Pea concentrate	55.0	18.2	15.9	4.2	6.7
Pea isolate	85.0	2.0	4.0	8.5	0.5
Pea starch	7.9	82.4	6.0	0.7	2.5
Pea hull fiber 150µm	5.0	2.9	89.0	0.3	2.8
Pea hull fiber 100µm	5.0	2.9	89.0	0.3	2.8
β-glucan	3.5	48.0	40.0	6.5	2.0
Pea starch inclusion					
F0%	69.7	8.3	9.7	4.7	7.6
F5%	66.6	12.0	9.6	4.5	7.3
F7.5%	65.0	13.9	9.5	4.4	7.2
F10%	63.5	15.7	9.4	4.3	7.1
F20%	57.3	23.1	9.0	3.9	6.6
P0%	70.0	10.1	10.0	6.4	3.6
P5%	66.9	13.7	9.8	6.1	3.5
P7.5%	65.3	15.5	9.7	5.9	3.5
P10%	63.8	17.3	9.6	5.8	3.5
P20%	57.6	24.6	9.2	5.2	3.4
Dietary fiber inclusion					
150 5%	60.9	16.6	13.5	5.5	3.5
150 10%	57.9	15.9	17.5	5.2	3.4
100 5%	60.9	16.6	13.5	5.5	3.5
100 10%	57.9	15.9	17.5	5.2	3.4
BG 5%	60.8	18.9	11.1	5.8	3.4
BG 10%	57.8	20.4	12.6	5.9	3.3
BG 20%	51.7	23.5	15.6	5.9	3.2

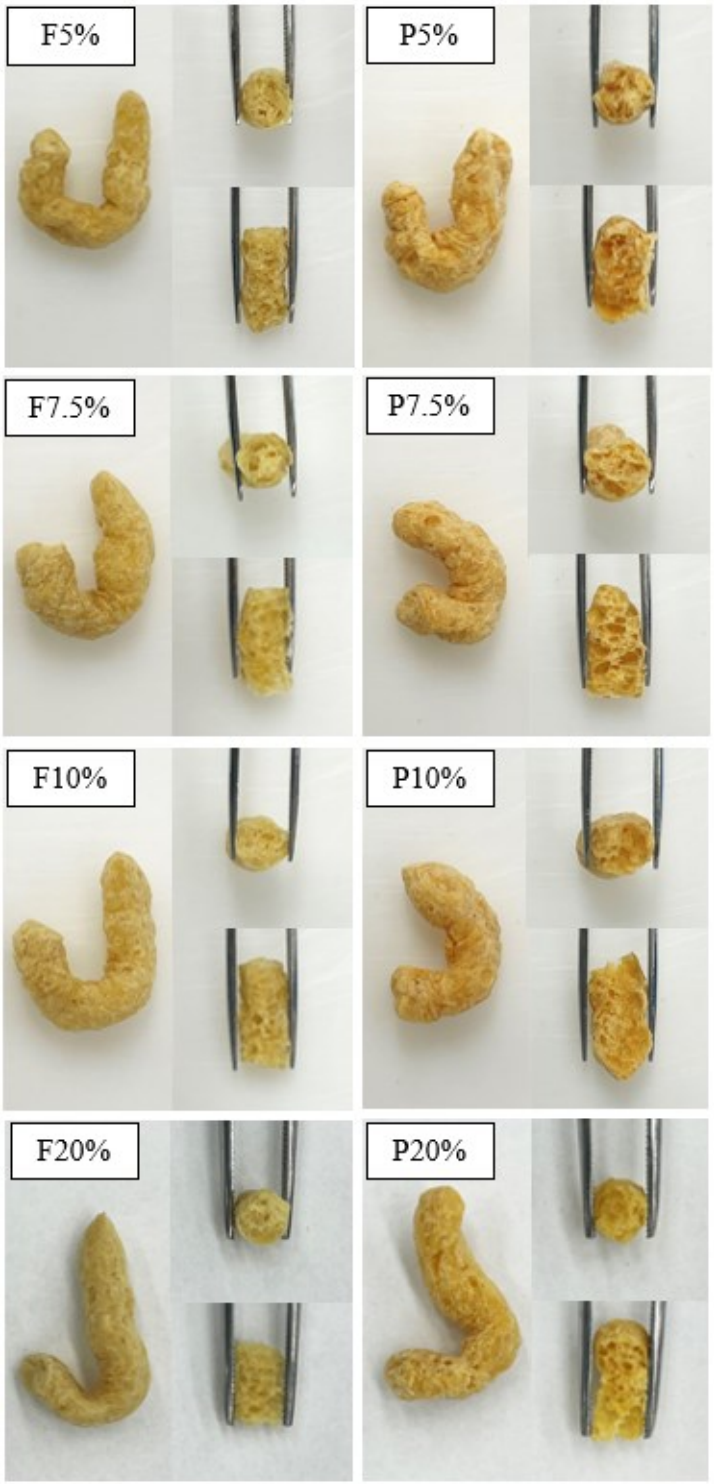

Figure 3.2 Whole (left), cross section (top right), and longitudinal (bottom right) cuts respectively of faba bean and pea TVP with 5%, 7.5%, 10%, and 20% starch inclusion levels.

In the work of Parmer et al. (2021), protein was added to starch based extrudates, which then competed with the water distribution in the melt, therefore reducing the expansion and the extrudate porosity. In this work, starch was added to the protein based extrudate. Therefore, the opposite effect was observed and additional starch increased expansion. Though it may be possible that a maximum starch level can be reached in relation to protein content to achieve expansion, but in excess no longer contributes to expansion. Crowding of excess starch and increased shear from decreased viscosity from swelling of starch may cause starch degradation into shorter chains which can no longer participate in expansion (Wang et al., 2014). Decrease in viscosity can increase residence time (time the melt spends in the extruder) and thus increase time starches are exposed to high temperatures of the extruder barrel (Yacu, 2020). The lack of continual expansion above faba bean 7.5% starch inclusion and pea 10% starch inclusion may be due to starch crowding, decreased viscosity, and from starch molecules reaching temperatures high above gelatinization, causing molecular degradation (towards dextrinization) and thus poor expansion since only gelatinized starches participate in contributing to the stable expanded structure (Wang et al., 2014; Allen et al., 1007). Beyond gelatinization, starches may further degrade into small molecular dextrins which have not been shown to increase expansion ratio, therefore medium sized amylose-protein complexes may be forming and stabilizing the elastic recoil of the extrudate at the die and holding the TVP structure (Allen et al., 2007). Pulse proteins contribute to the network by providing strength through covalent bonds and complex non-bonding formations (Parmar et al., 2021; Hong et al., 2022). Briefly, unlike proteins alone, the addition of starch to TVP promotes expansion through the swelling and gelatinization of starches that assist in melt flow, nucleation, and in holding the protein matrix structure. All samples in this study fell within the expansion range of TVP made from soy protein isolate, wheat gluten, and 20% starch of about 1.43-2.40 ER

between temperatures of 180°C-190°C and screw speeds of 350-450rpm (Lyu et al., 2023), more specifically the faba bean TVP at 7.5%-20% starch inclusion and pea TVP at 10%-20% starch inclusion fell right in the middle of this estimated range.

As previously shown in chapter 2, extrudates with more expansion also had lower bulk density, producing a more light and airy extrudate (Fig. 3.3B). All starch included faba bean TVP had similar bulk density (0.32-0.39g/cm^3), which were less dense than the TVP with no starch inclusion (0.54g/cm^3). In starch expanded extrudates where starch is the dominant phase, fiber and proteins act as the dispersed phase and fill the gaps that a starch films can form around until a limit is reached when the starch film is not elastic enough to hold bubble expansion or the cell walls upon exiting the die, causing decrease in expansion and increase in BD (Kristiawan et al., 2020; Guy, 2001). To our best knowledge, very little literature investigates the system where protein is the dominant phase and starch becomes the dispersed phase which can effect product characteristics, therefore extrapolated assumptions be made within reason. For example, if protein decreases expansion in a protein-in-starch matrix which had high expansion, then similar concepts could be applied where starch can increase expansion in a starch-in-protein matrix where there is less expansion, though further research is required in this area to verify if extrapolation of concepts is applicable to different starch or protein dominant matrices. The inclusion of starch had more impact on faba bean TVP than pea TVP and created a less dense extrudate with more or larger air pockets. This may be because faba bean protein has a higher tendency to aggregate (Yang et al., 2018) than pea protein so the addition of starch was able to interrupt faba bean protein aggregation to a certain extent, and add enough elasticity to support air bubble formation while the proteins were able to unfold and interact with the starch to hold the cell walls in place (Zhang et al., 2019; Verbeek et al., 2010). It was noticed that the pea TVP with starch included (0.32-0.45g/cm^3) had

similar bulk density as the extrudate with no starch inclusion (0.38g/cm^3), though the pea TVP with 10%-20% starch inclusion (0.34g/cm^3 and 0.32g/cm^3) were significantly less dense than the 5% starch inclusion (0.45g/cm^3) extrudate. It could be that the addition of pea starch to pea TVP did not increase the number of nucleation points or bubble size until 10% starch, at which the number of nucleation points or bubble size increased which not only increased expansion but also decreased BD since more bubbles or larger bubbles would make the TVP lighter and less dense. Varying extrusion parameters can produce a density of 0.12-0.35g/cm^3 from extruded pea starch alone (Rangira et al., 2020) due to the much better expansion capacity of starch than protein. Extruded starch inclusion TVP BD was again within range of other TVP (approximately 0.15-0.45g/cm^3) made from soy protein isolate, wheat gluten, at a 20% starch inclusion (Lyu et al., 2023). The inclusion of pea starch overall improved expansion ratio and bulk density of extrudates.

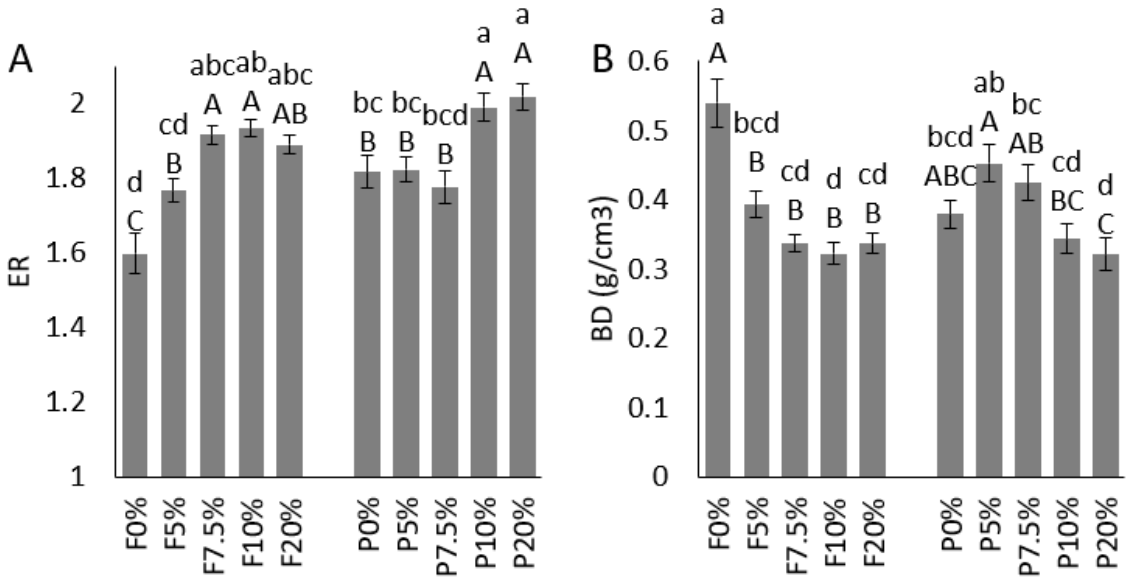

Figure 3.3 Expansion ratio (A) and bulk density (B) of faba bean and pea TVP at 0%, 5%, 7.5%, 10%, and 20% starch inclusion levels. Uppercase letters indicate significant differences within protein sources and lowercase letters indicate significant differences among all TVP samples.

Differences in WHC of TVP (Fig. 3.4A) could be attributed to pore structure and size, or exposed binding sites from the presence of starches, fibers, protein type which all influence the water absorption of TVP (Esbroeck et al., 2024). As in previous chapters, one of the major reasons for extrusion to improve WHC (2.43-3.65g/g) is due to water uptake via capillary forces of the TVP porous structure (Esbroeck et al., 2024). An increase in starch caused a subsequent increase in WHC of extrudates, more so in the faba bean TVP. WHC of faba bean TVP ranged from 2.73-3.65g/g. It was noticed in faba bean TVP that WHC was lowest at the highest starch inclusion of 20% (2.73g/g), which may be because too much starch in the TVP formulation could interfere with the protein unfolding and formation of network, and thus decreasing the TVP water holding capacity (Zhang et al., 2019; Verbeek et al., 2010). Though this would need additional investigation and analysis. Contrary to faba bean TVP, only when 20% starch was included in pea TVP was there a significant increase in WHC (3.31g/g) compared to the other pea samples (2.43-2.77g/g). SEM images in section 3.3.5 show an increase in number of pores at 20% starch inclusion for pea TVP which could mean there is more surface area available in the protein network to hold more water. WHC from extruded pea starch alone under different extrusion parameters can range from 10.98-12.10g/g indicating that starch based extrudates should be able to hold more water than protein based extrudates (Rangira et al., 2020) which was anticipated. The starch included TVP in this work falls within the higher range and above of previous reports on WHC (approximately 1.25-3.2g/g) of TVP from soy protein isolate which also included 20% starch (Lyu et al., 2023).

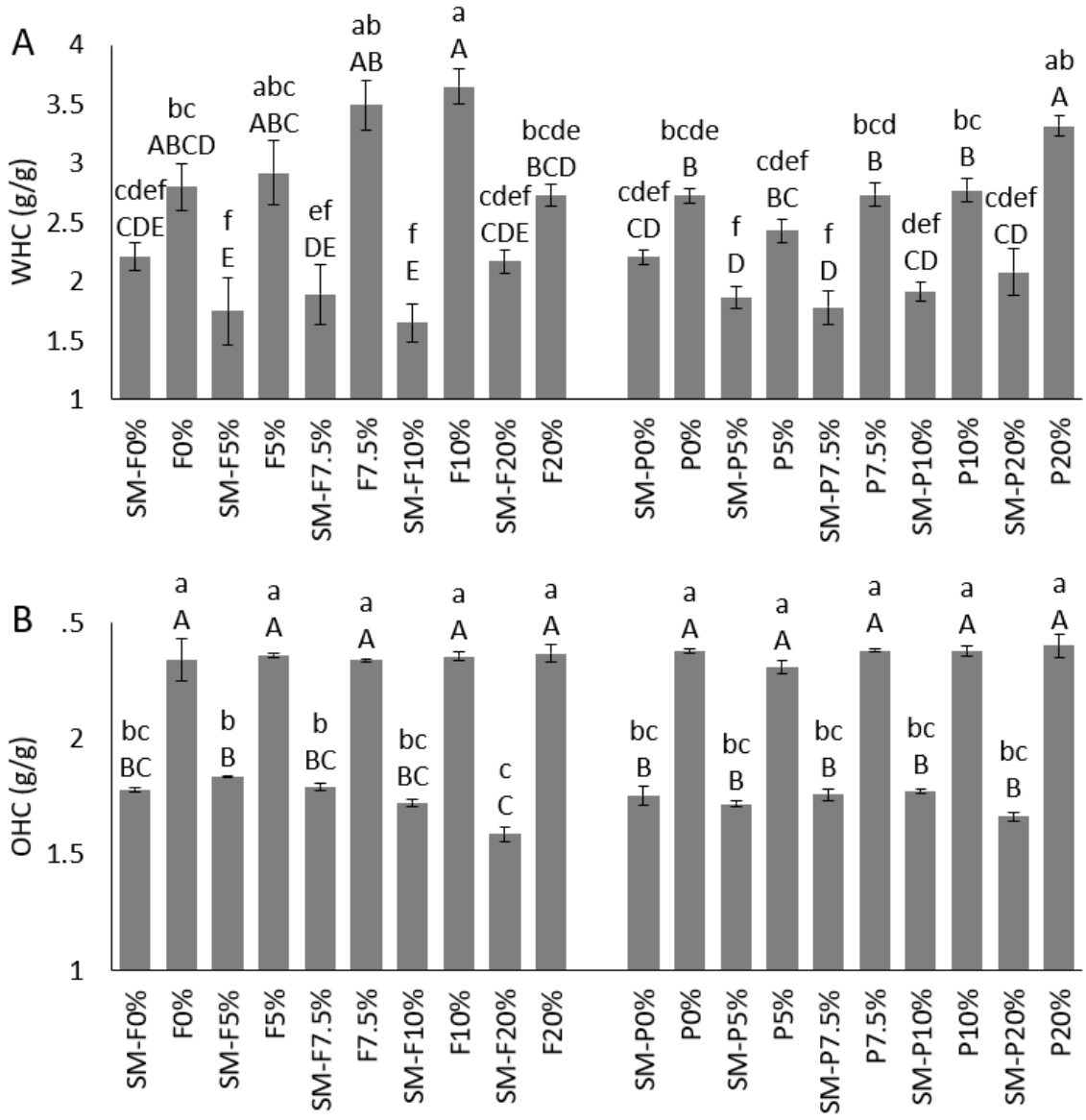

Figure 3.4 Water holding (A) and oil holding (B) content of faba bean and pea TVP at 0%, 5%, 7.5%, 10%, and 20% starch inclusion levels. Uppercase letters indicate significant differences within protein sources and lowercase letters indicate significant differences among all TVP samples.

OHC of faba bean (1.59-1.84g/g) and pea (1.66-1.77g/g) starting materials were again lower than the OHC of faba bean (2.34-2.37g/g) and pea (2.31-2.40g/g) extrudates (Fig. 3.4B). OHC was improved through extrusion though starch levels or protein source had no impact on

oil holding capacity. Oil may be held within the air pockets through capillary action or within hydrophobic regions formed by the unfolding of proteins during extrusion processing to expose more hydrophobic groups which were hidden in the starting material (Xiao et al., 2023). OHC of typical pea TVP range from 0.75-0.90g/g (Chan et al., 2023). The addition of starch to faba bean and pea TVP did not have a negative impact on OHC. Even though the addition of starch may have decreased the overall protein content slightly and thus lowered the possible exposed hydrophobic groups available for oil binding, the expansion of the extrudates kept the OHC constant so there was no decrease in OHC of extrudates.

The inclusion of a small amount of pea starch at 7.5% for faba bean TVP and 10% for pea TVP can significantly improve expansion ratio and bulk density of extrudates which is favorable as the extrudates still contained 63.8%-65% protein, keeping the nutritional protein value of TVP extrudates. The increase in expansion may be linked to the starch-in-protein matrix to be discussed alongside confocal microstructure results in more detail (section 3.3.4). Starch inclusion improved WHC for faba bean TVP at 10% inclusion whereas pea TVP required a higher starch inclusion level of 20% to improve WHC. The inclusion of starch in TVP kept OHC constant for both faba bean and pea TVP.

3.3.2 FTIR protein secondary structure of faba bean and pea starch inclusion extrudates

Eight dominant absorption peaks were present in Fourier Transfer Infrared spectra of the raw materials at 1618cm^{-1} (protein aggregates), 1628cm^{-1} (β-sheets), 1643cm^{-1} (random coil), 1660cm^{-1} (α-helix), 1670cm^{-1} (β-turn), 1680-1693cm^{-1} (β-sheets/turns) and 1608cm^{-1} (amino acid residues). All absorption peaks flattened, specifically the amount of ordered α-helix at 1660cm^{-1}, while unordered structures like random coils (1643cm^{-1}) and β-sheets/turns (1680-1693cm^{-1}) remained (Sadat et al., 2020), both indicating the unfolding and denaturation of proteins occurred.

The absorptions for the secondary protein structures became much weaker in faba bean and pea TVP with starch included (Fig. 3.5), indicating protein denaturation in all extrudates.

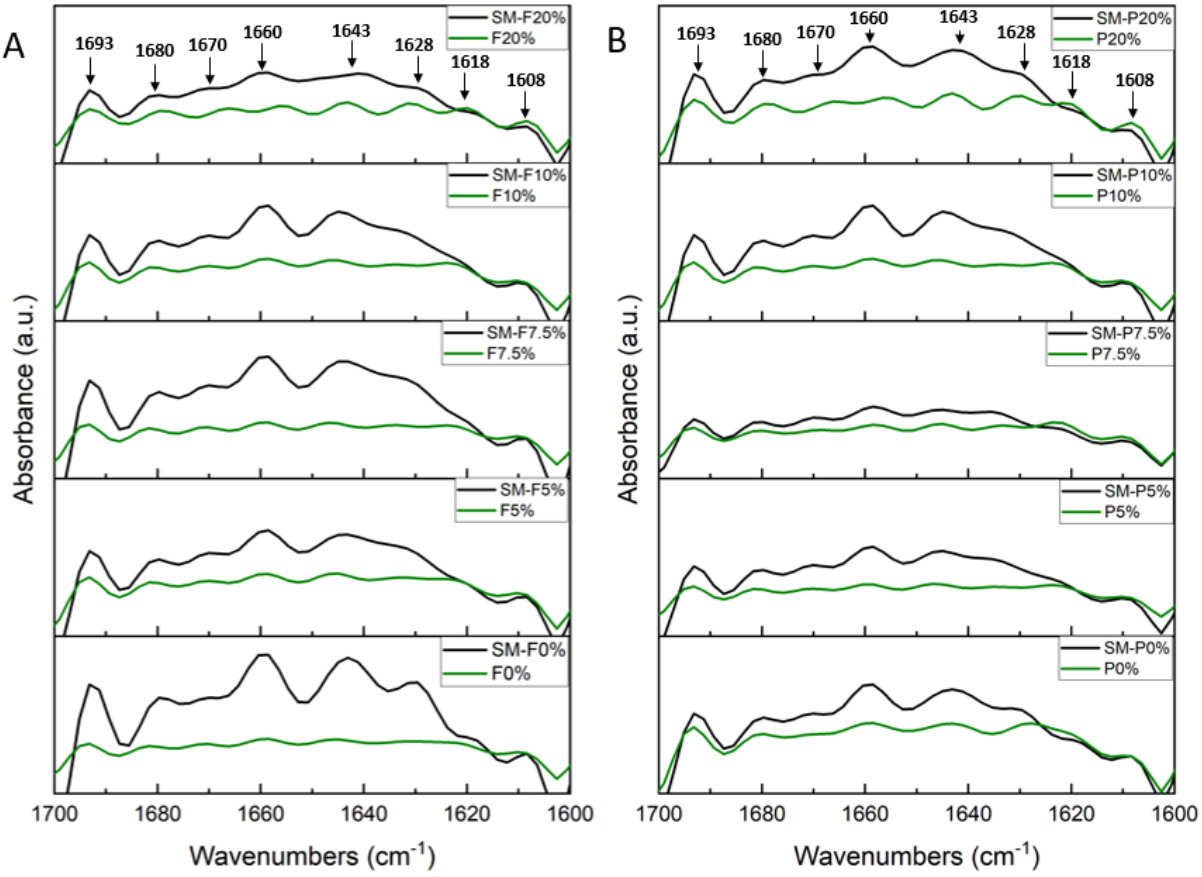

Figure 3.5 FTIR spectra of faba bean (a) and pea (b) TVP with corresponding starting materials at 0%, 5%, 7.5%, 10%, and 20% starch inclusion levels in the protein region (1700-1600cm^{-1}).

3.3.3 Rheological properties of faba bean and pea starch inclusion extrudates

Rheological properties of TVP starting materials with starch included were all in a solid state since the storage modulus was higher than the loss modulus. In general, the G' curves for faba bean starting material (Fig. 3.6A) and pea starting material (Fig. 3.6B) were different. Overall, the faba bean G' were generally lower than the pea G', indicating pea proteins formed stronger interactions in the extrudate networks than faba bean proteins. Starch had an impact on faba bean G' during the initial heating step up to about 50°C which may be due to the swelling and initial

gelatinization temperature of the starches, but pea starch had more impact on faba bean G' when cooling. The addition of pea starch to faba bean starting material resulted in a slight decrease in slope and increased stabilization of the G' curve when the melt started to cool, most likely from the gelatinization of starch. Pea starch has been known to have resistance to shear thinning and high gel elasticity, from the higher amylose content found in pea starch (Rangira et al., 2020). High gel elasticity from pea starch may have helped the faba bean proteins to form a more cohesive network and stabilize the structure while cooling since faba bean proteins tend to aggregate more than pea proteins which form weaker structures if unfolded linear protein chains aggregate and tighten. In addition, a higher degree of gelatinization from the pea starch can cause further stretching of molecules resulting in a higher ER (Rangira et al., 2020) once cooled. The elasticity provided by the pea starch improved the faba bean network structure when cooled, promoting an increase in ER for all included starch faba bean TVP. Pea starch also had more impact on pea G' during the cooling stage, implying that indeed the gelatinization of starch was stabilizing the network structure of the pea starting material as well. Contrary to the faba bean starting materials, the pea starch had less effect on G' during initial heating of the starting material which may be due to the compatibility of the pea starch present in the starting material and the pea starch that was added. Interestingly it is not until starch is included at 20% when the G' of faba bean and pea results in a more viscous curve more characteristic to starch rheological properties than protein rheological properties explained in more detail in chapter 2. Both faba bean and pea at 20% starch inclusion had an increase in final G' compared to other starch inclusion (5%-10%), indicating a stronger network brought on by more starch gelatinizing.

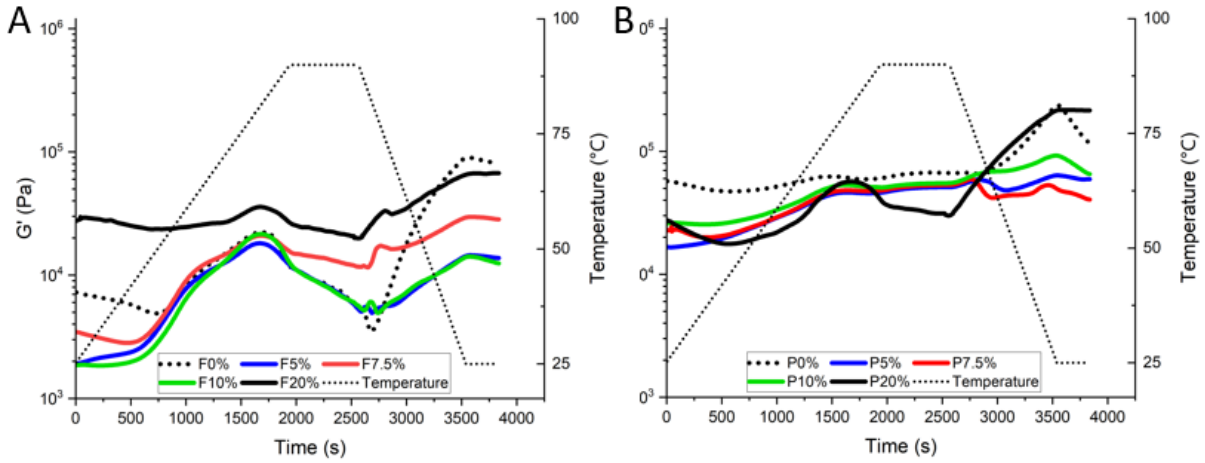

Figure 3.6 Rheological properties of storage modulus (G') for faba bean (A) and pea (B) extrudates at 0%, 5%, 7.5%, 10%, and 20% starch inclusion level over a temperature ramp 25°C-90°C-25°C.

3.3.4 Effects of starch distribution on protein matrix phase for faba bean and pea extrudates

Confocal imaging of faba bean and pea TVP depicts the interactions between protein (red) and starch (blue) at each starch inclusion level (Fig. 3.7). At higher starch levels (10% and 20% inclusion levels), the starch and protein are observed as two phases, in addition to some starch distributed within the protein network (shown as purple). Below 10% starch inclusion, the amount of gelatinized starch granules (blue) does not increase proportionally with the increase of starch in the raw material. Beyond 10% inclusion, a homogenous phase emerges where the excess starch blends with the protein and becomes part of the protein phase. While there is a distinction of two separate phases in the TVP structure, the amount of protein (red) is still larger than the amount of starch (blue), indicating that it is still a starch-in-protein matrix. This change of protein phase is supported by expansion ratio results such that expansion increased in both faba bean and pea TVP until 10% starch inclusion in which additional starch did not contribute to expansion. A bi-continuous phase between protein and another component could start to develop when levels of 20%-30% inclusion of another component is included, which may decrease the desired protein

matrix structure (Deng et al., 2023). A bi-continuous phase between the protein and starch had not yet developed in this work since there are two defined protein and starch shapes, though at 10% and 20% starch inclusion, a change in phases to a protein-in-starch matrix may be starting to occur but is not fully developed. This shift in starch is seen in both faba bean and pea TVP. In addition, expansion ratio was maximized at 7.5%-20% for faba bean and 10-20% for pea, suggesting that expansion of TVP will increase with an increase in starch inclusion until a change in the starch and protein phase starts to occur where starches blend within the protein matrix and no longer promotes expansion. Buhler et al. (2022a) suggests that in a meat analogue where protein exceeds 30% and starch is greater than 2% of the formulation, a multiphase blend occurs and various protein-starch morphologies can occur based on protein state, size, and continuity of protein aggregates. Depending on the level of cooked starch in the extruder that causes expansion and the level of proteins and starches, the protein matrix could either surround starches or the starch could form a continuous matrix around protein aggregates (Buhler et al., 2022a). It is possible that the starch content is not quite high enough to induce a bi-continuous network or phase flip from starch-in-protein to protein-in-starch, but rather the dominant protein phase surrounds the starches which are just starting to form a continuous phase with the protein. Additional starch would need to be included above 20% to determine at what point a bi-continuous phase could occur before flipping to a protein-in-starch matrix.

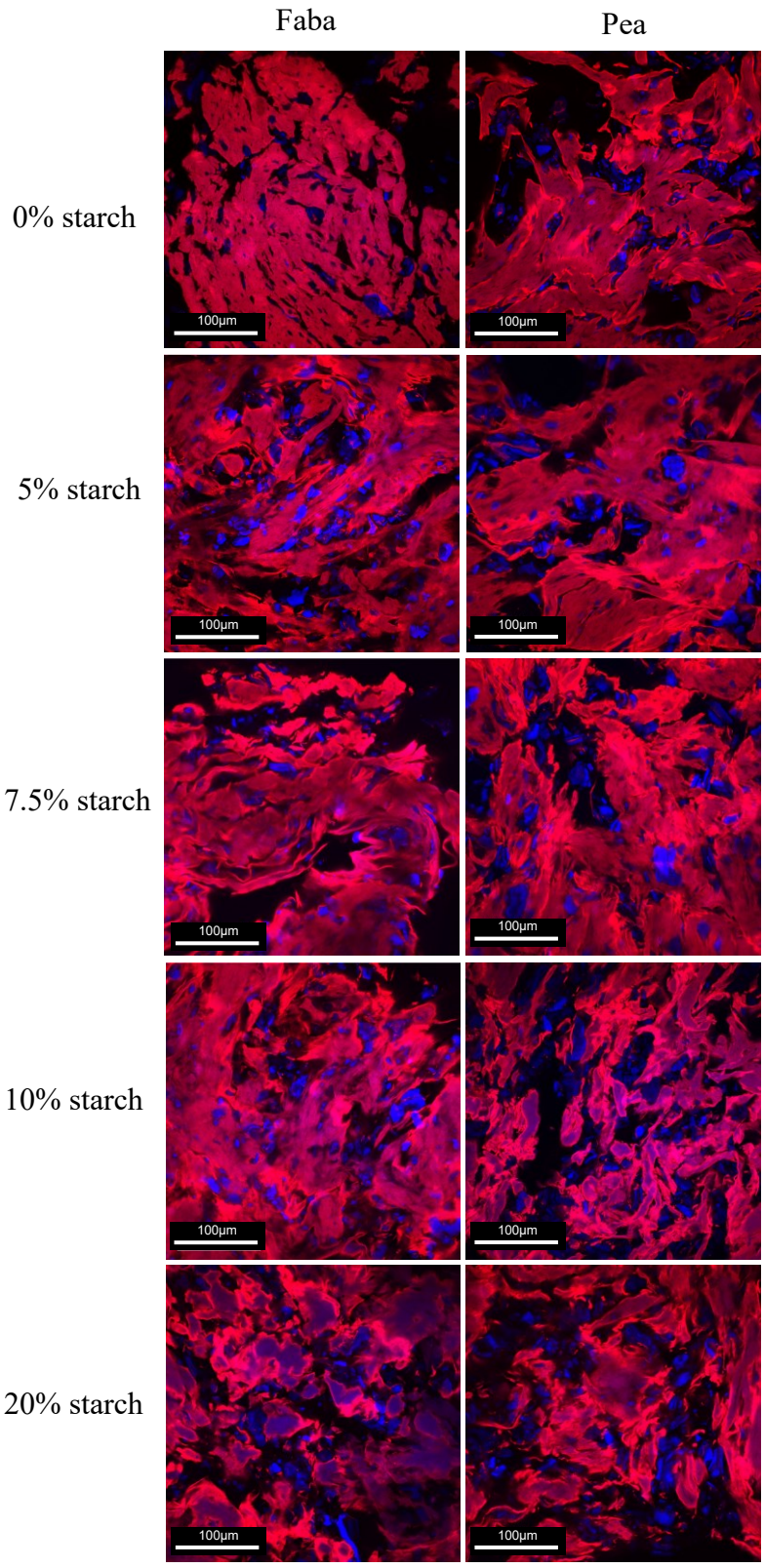

Figure 3.7 Confocal imaging of faba bean and pea TVP with pea starch inclusion at 0%, 5%, 7.5%, 10%, and 20% where the protein is dyed red, and starch is dyed blue.

Differences in material strength of the starch dispersed phase can contribute to elongation and the directional structure of the TVP structure which is related to the shear rate of the protein melt within the extruder. As shear rate increases, the elongation of the dispersed starch phase increases until shear rate is too high and the larger elongated pockets break (Twombly et al., 2020). At 20% starch inclusion in faba bean TVP, the protein matrix becomes more globular in structure rather than elongated and fibrous, as well as more purple in colour, meaning starch could be migrating from the starch-in-protein phase to possibly interact with the proteins more closely (Fig. 3.7). WHC increased in faba bean TVP until 20% starch inclusion where there was a drop in WHC, suggesting that the decrease in WHC may be caused in part to starch interacting with the proteins rather than absorbing more water, or the globular structured protein matrix is less effective in holding water than the elongated protein matrix. SEM images (Section 3.3.5) of faba bean TVP also show a more open structure with fewer and larger pores which may hold less water.

3.3.5 *Effects of starch on microstructure of faba bean and pea extrudates*

SEM micrographs of faba bean TVP (Fig. 3.8) and pea (Fig. 3.9) were taken to observe the structure of the TVP, the surface of air pockets, as well as the structure within the protein matrix. There are no visible starch granules either at the surfaces of air pocket walls or the internal protein matrix. Rheological results of the starting material G' when heated provides supporting evidence that even up to 20% starch inclusion on both faba bean and pea extrudates had gelatinized and created a smooth air-water interface of the air pocket walls which has been shown to display better expansion than a rough surface (Rodrigues et al., 2023; Hussain et al., 2013).

The micrograph of air pockets in the faba bean TVP (Fig. 3.8) at a lower starch inclusion (5% and 7.5%) tended to have a smooth striated surface and the faba bean at 5% inclusion had a

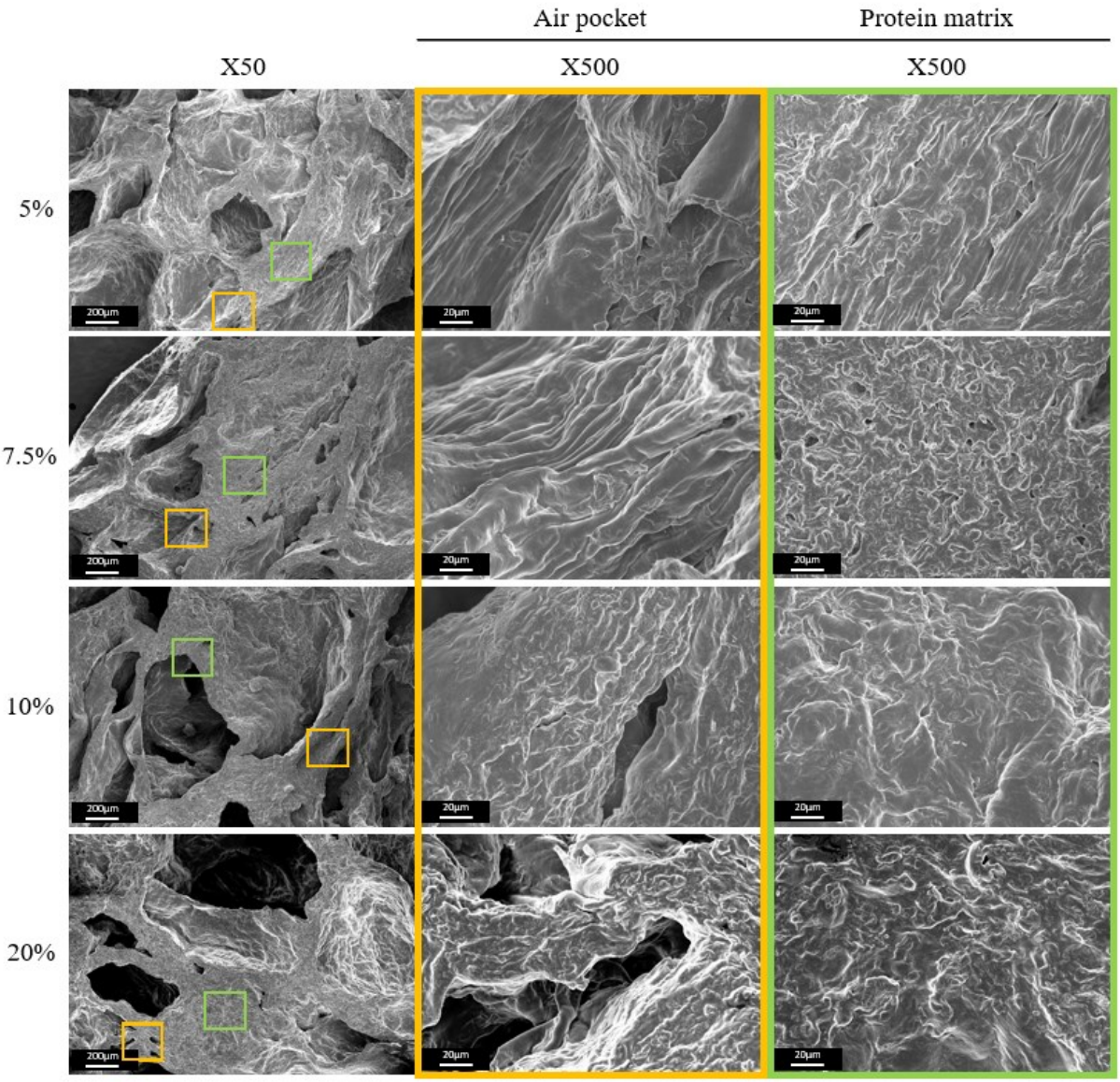

Figure 3.8 SEM micrographs of faba bean TVP at 5%, 7.5%, 10%, and 20% starch inclusion.

similar smooth long fibril texture within the internal protein matrix. These fibers may have developed from the available proteins unfolding and aligning along the length of the barrel which were covered with smooth gelatinized starch (Cabrera-Ramirez et al., 2021). As starch inclusion increased, air pockets became larger and cell walls thickened (Rangira et al., 2020). In addition to the hydrophilic nature of the starch that allowed more water absorption, thickening of cell walls in SEM imaging may further contribute to the increase in WHC of extrudates since thick cell walls hold large volumes of water, even though extrudates with many small pores could hold even more

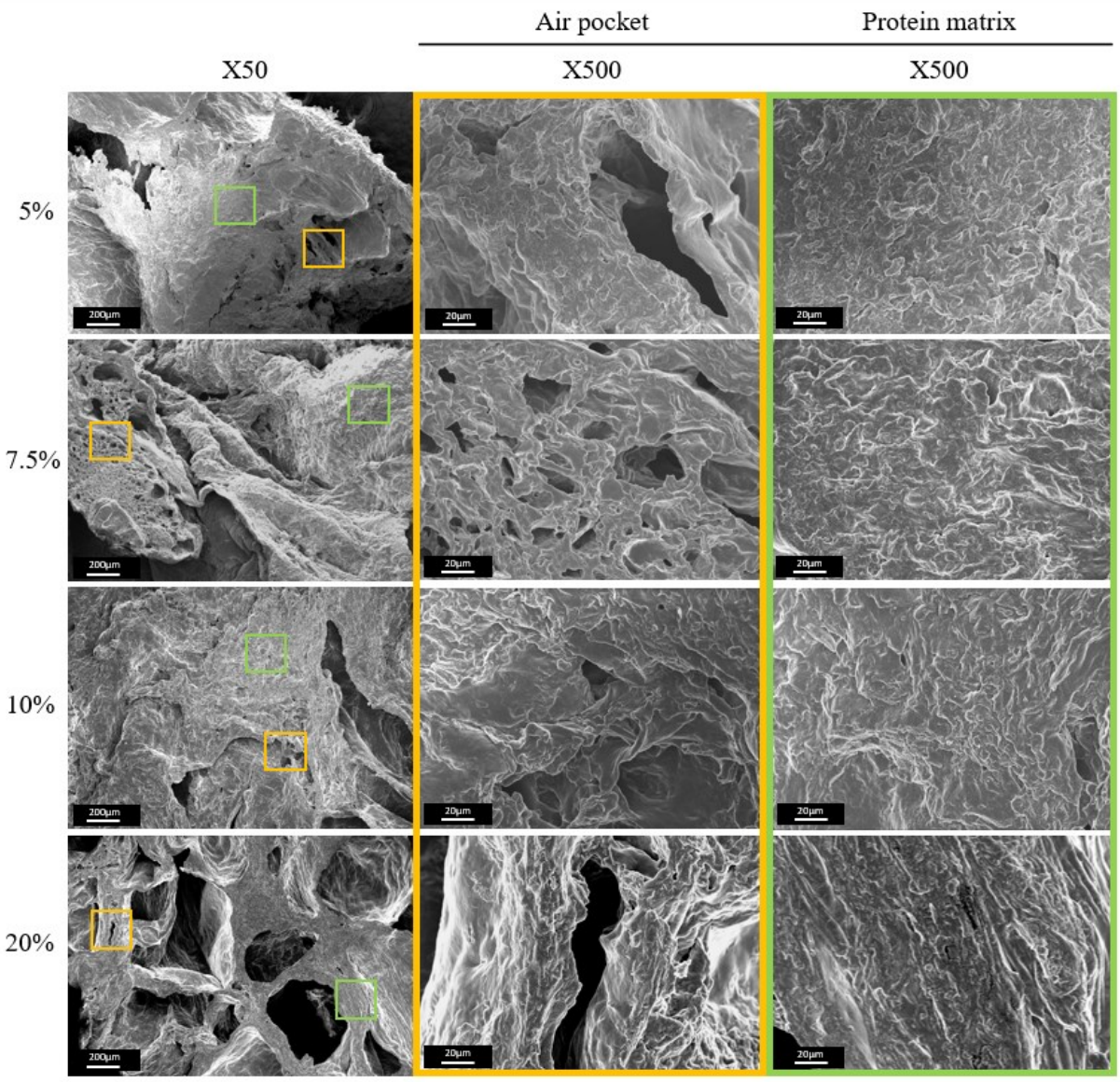

Figure 3.9 SEM micrographs of pea TVP at 5%, 7.5%, 10%, and 20% starch inclusion.

water based on lowered capillary forces required to hold the water. As the walls thicken, more water is held although has a slower uptake than an extrudate with thin walls or smaller pores. The WHC of faba bean TVP with 20% starch inclusion may be lower because pore size may have increased to the point there were larger pores and fewer thick walls to hold more water (Esbroeck et al., 2023). Therefore, fewer number of pores but larger pore size can increase the expansion and WHC of faba bean TVP but at 20% starch inclusion WHC decreased because the pore size became

too large to effectively hold more water. Higher frequency and larger pores were also found in pea TVP (Fig 3.9) with an increased inclusion of starch. The pea TVP at 20% inclusion of starch had smaller pores than faba bean TVP at 20% inclusion of starch, which may indicate why WHC of pea increased at 20% inclusion of starch since the pores were still able to hold more water and were not too large.

Extrusion of pea starch alone has shown to produce highly expanded extrudates with thick, elongated pores (Rangira et al., 2020). The benefit of adding starch to protein dominant TVP is that starch can help increase TVP expansion and structure. Pea starch extruded alone has high water solubility and dissolves when rehydrated, which is undesired in a meat analogue product (Rangira et al., 2020). Whereas the protein matrix is able to hold the expanded structure of TVP when rehydrated in water for meat analogue development. Therefore, starch can be used to assist in TVP expansion while the protein matrix can hold that structure when rehydrated, creating a higher quality TVP.

3.3.6 Long-range crystalline order of faba bean and pea extrudates with x-ray diffraction

X-ray diffraction was used to determine the long-range ordering state of starch crystalline structure of the pea starch starting material and within the TVP extrudates (Fig. 3.10). Typical A-type and B-type crystallinity peaks were present, indicating the pea starch had C-type crystallinity prior to extrusion due to the defining shoulder peak at 18°. Although it could be hypothesized that the pea starch measured showed more prominence towards A-type pattern than B-type pattern since stronger peaks were present correlated to A-type than B-type, for example no clear peaks at 2θ of 5.6°, 22°, 24° (B-type) were defined though a well-defined shoulder peak at 18° was present when it should be separated and equal to the peak at 17° (A-type).

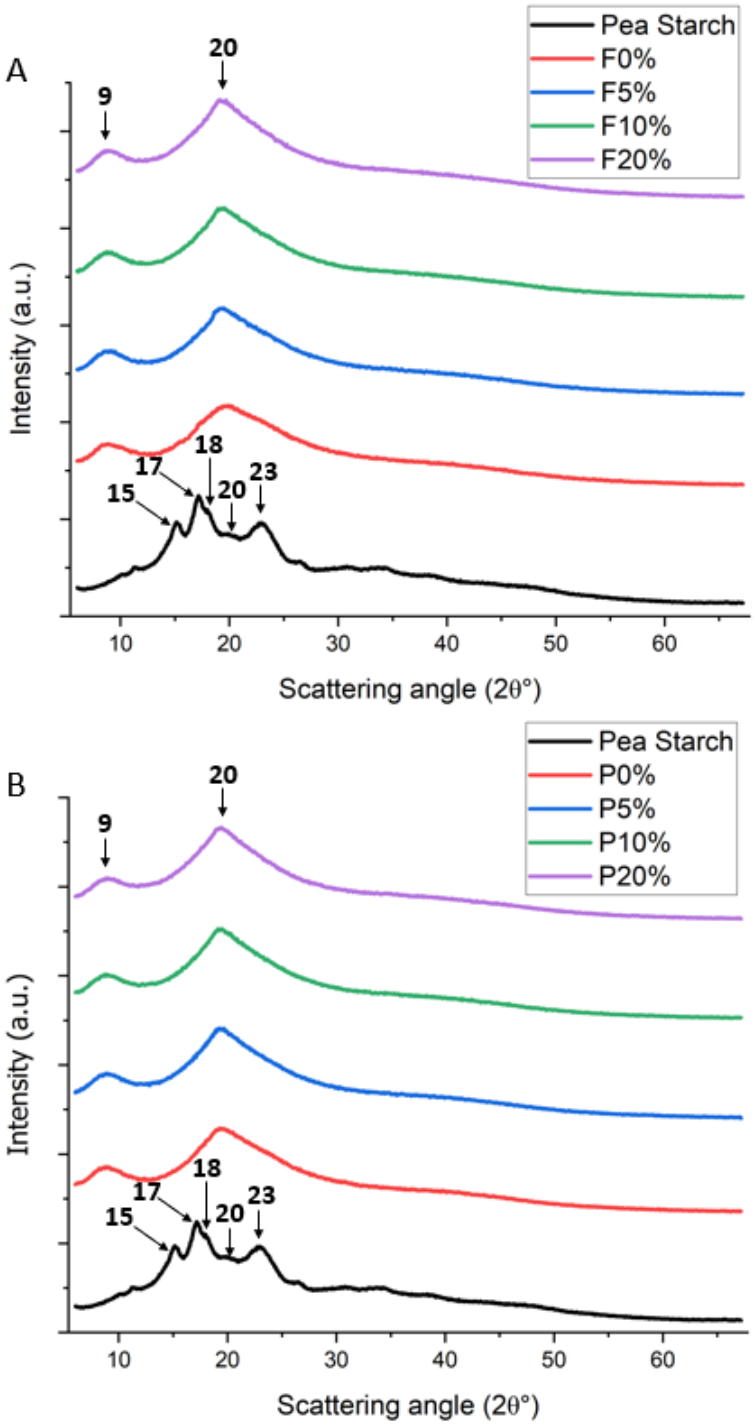

Figure 3.10 X-ray diffraction light scattering of pea starch, faba bean (A), and pea (B) TVP at 0%, 5%, 10%, and 20% inclusion levels.

V-type starch complexes are indicated by peaks at 7.4°, 13° and a well-defined peak at 20° 2θ related to V-type amylose-lipid complexes (He et al., 2024; Xu et al., 2023; Chen et al., 2015). The strong peak at 2θ of 9° and 20° is characteristic of amylose-lipid V-type pattern of acylated starch (Chi et al., 2008; Arijaje et al., 2015). Both faba bean (Fig. 3.10A) and pea (Fig. 3.10B) TVP showed a clear shift from C-type starch crystallinity to V-type starch crystallinity based on the strong peak at 2θ of 20°. This indicates that any lipids that were present may have complexed with available starches under high heat, pressure, and shear from the extrusion process to shift from C-type to V-type crystallinity. Amylose-lipid V-type complexes have been formed previously through low moisture extrusion in corn and cereals determined by the characteristic peak at 20° 2θ while retaining some crystallinity patterns of native starch (Wang et al., 2022). Though in this study all native C-type crystallinity from pea starch was either fully gelatinized (showing no crystalline peaks in x-ray diffraction) or converted to amylose-lipid complex V-type crystallinity which was not present in the native pea starch. Literature specific to formation of V-type crystallinity of pea starch in high protein TVP is scarce, though findings from this study show clear evidence of V-type crystallinity formation to further stimulate and encourage future investigation on this topic which is outside the scope of this study.

3.3.7 Short-range crystalline order of faba bean and pea extrudates with FTIR

FTIR spectra of the starch region (960-1060cm^{-1}) reveal short-range ordering of starch granules in crystalline and amorphous forms (Fig. 3.11). Peaks were present in all starting material and extrudate samples at 1045cm^{-1} and 995cm^{-1} which are assigned to crystalline starch (Lu et al., 2019). Absorption at 1045cm^{-1} were assigned to bending of C-OH groups whereas absorption at 995cm^{-1} was attributed to the stretching of C-O in C-O-C groups (Altan et al., 2023). Peaks in the starting materials at 1014cm^{-1} and 1030cm^{-1}were attributed to C-O stretching (Altan et al., 2023;

Basiak et al., 2018). Only the extruded samples contained peaks at 1022cm^{-1} which are typically assigned to amorphous starch since this peak intensity increases as starch is gelatinized and were attributed to the stretching of C-O (Basiak et al., 2018; Ponzo et al., 2018).

Starches present in the starting material in the crystalline form are melting under extrusion temperatures, after which those starches are then gelatinized (Lu et al., 2019, Vatansever et al., 2021) during the extrusion process. The melting of crystalline starch of the starting material may be indicated by the absence of peaks at 1030cm^{-1} and 1014cm^{-1} in faba bean extrudates (Fig. 3.11A) with the emergence of an amorphous peak at 1022cm^{-1}. Both the peak intensities at 1022cm^{-1} and 995cm^{-1} increase as the addition of pea starch increases in the extrudates but not in the starting materials, indicating conformational changes are occurring in the starch due to the extrusion process (Vatansever et al., 2021). An increase in intensity of the peak at 1022cm^{-1}, should result in a decrease in intensity of crystalline peaks at 1045cm^{-1} and 995cm^{-1}, which is not seen in Figure 3.11A. A decrease in these crystalline peaks could be occurring but may not be visible in the FTIR spectra because even though the starch was increasing, it was gradually being converted into the amorphous peak at 1022cm^{-1}.

In pea extrudates (Fig. 3.11B), the melting of the crystalline starch is indicated by a shift in peaks at 1030cm^{-1} and 1014cm^{-1} which merge into the amorphous peak at 1022cm^{-1}. The extrusion process has previously reported to cleave glycosidic bonds of starch chains, causing a decrease of peak intensity at 1030cm-^{1} (Torres et al., 2019). In addition, a decrease in crystallinity indicates untwisting of starch structure and better digestion which was found during section 3.3.7 on starch digestibility (Li et al., 2020). Interestingly, the amorphous starch peak (1022cm^{-1}) within the pea extrudates (Fig. 3.11B) does not fully emerge until 7.5% of starch inclusion is met, (Fig. 3.11A). It is possible that the pea starches present in the starting material may be bound to proteins

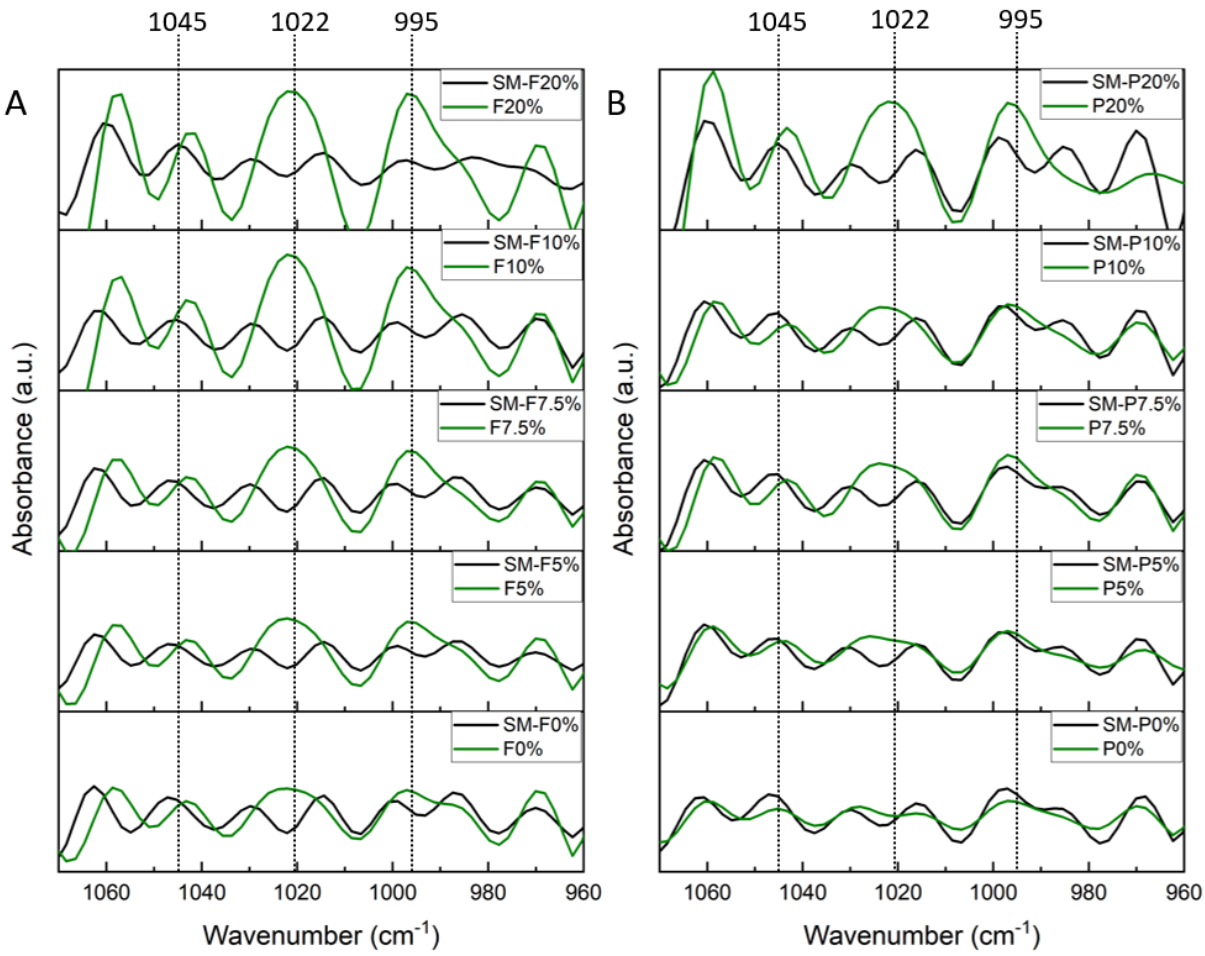

Figure 3.11 FTIR spectra of faba bean (A) and pea (B) starting materials and TVP within the starch region (1060-960 cm^{-1}).

and are more resistant to phase changes from crystalline to amorphous states. The high protein content of TVP could form a matrix creating a physical barrier between starches and water needed for swelling, or protein could outcompete starch for available water, thus increasing the gelatinization temperature and ultimately delaying starch gelatinization (Li et al., 2022). Lipids in the starting materials (3.9%-4.7% in faba bean and 5.2%-6.4% in pea) were higher in the pea extrudates than the faba bean and could form amylose-lipid complexes preventing these starches

from swelling (Li et al., 2022). In addition, only the amorphous peak at 1022cm^{-1} increases intensity as pea starch inclusion increases.

3.3.8 Degree of order (DO) and degree of double helix (DD) of faba bean and pea extrudates

The ratio of crystalline to amorphous regions can be defined as the degree of order (1045cm^{-1}/1022cm^{-1} ratio) and changes in double helical structure can be defines as the degree of double helix (995cm^{-1}/1022cm^{-1} ratio) (Xu et al., 2023; Vatansever et al., 2021). The DO in the faba bean and pea extrudates remained unchanged and unaffected by the increase in pea starch (Table 3.2). With increasing pea starch in TVP all values of DD were higher than DO, indicating the conformational changes of crystalline starch into amorphous starch (Vatansever et al., 2021). In addition, pea extrudates displayed a decrease in DD as starch inclusion increased, indicating a reduction in double helices, even though pea generally had higher DD than faba bean. Because this decrease in DD was not seen in the faba bean extrudates, the conformational change can be attributed to the pea starch originally in the starting material. Possibly, strong hydrogen bonds in pea starch between double helices may have helped hold the double helical conformation in place through extrusion, though the decrease in DD may be because the added starch diluted the intensity of double helices originally present in the pea starting material.

Table 3.2 FTIR peak intensity determination of starch degree of order (DO) and degree of double helix (DD) of faba bean and pea starch inclusion extrudates.

Treatment	DO 1045/1022cm^{-1}	DD 995/1022cm^{-1}
F0%	0.569 ± 0.014	0.979 ± 0.033bc
F5%	0.436 ± 0.016	0.910 ± 0.003c
F7.5%	0.407 ± 0.008	0.942 ± 0.028bc
F10%	0.581 ± 0.134	0.873 ± 0.026c
F20%	0.570 ± 0.068	0.943 ± 0.027bc
P0%	0.760 ± 0.067	1.618 ± 0.098a
P5%	0.565 ± 0.206	1.179 ± 0.075ab
P7.5%	0.523 ± 0.001	1.266 ± 0.009b
P10%	0.439 ± 0.009	0.958 ± 0.139bc
P20%	0.640 ± 0.009	0.971 ± 0.014bc

3.3.9 Digestible starch analysis of starch included faba bean and pea extrudates

Ye et al. (2018) reviewed that extrusion of high-amylose starch can form resistant starch in which the dense amorphous molecular packing (rather than crystallinity) can either slow down enzymatic attack or can prevent and limit binding, keeping the dense amorphous starches intact. Digestible starch analysis of the starting materials and TVP were evaluated to determine changes in starch digestibility with increasing starch inclusion in faba bean and pea extrudates (Table 3.3). Digestible starch analysis of the starting materials revealed resistant starch in faba bean (3.5%-7.7% dwb) and pea (0.48%-7.9% dwb) samples were more abundant than slowly digestible starch in faba bean (0.95%-3.17% dwb) and pea (0.80%-3.06% dwb) samples, followed closely by readily digestible starches in faba bean (0.86%-1.79% dwb) and pea (0.73%-1.88% dwb) samples. The drastic decrease in resistant starch in all extrudates from their respective starting materials (Fig. 3.12) is most likely due to high extrusion temperature (170°C) reaching or even surpassing the melting temperature of available starches in which the crystalline regions of starches melt (EK et al., 2020b) and starches become more prominent in the amorphous state. Previous studies have

Table 3.3 Starch content in g/100g dry basis for faba bean and pea starting material and extrudates digestibility at 0%, 5%, 10%, and 20% starch inclusion.

Treatment	RDS (%)	SDS (%)	TDS (%)	RS (%)	Total Starch (%)
SM-F0%	0.86f	0.95cdef	2.71ij	3.51abcd	6.21cde
SM-F5%	1.42ef	1.28cd	4.17gh	5.72ab	9.89bc
SM-F10%	1.50ef	2.53b	6.25f	7.72a	13.97ab
SM-F20%	1.79ef	3.17a	7.86cde	6.92ab	14.78a
SM-P0%	0.73f	0.80defg	2.00j	0.48cd	2.48e
SM-P5%	1.08ef	1.17cde	3.40hi	2.71bcd	6.10cde
SM-P10%	1.49ef	1.55c	4.94g	4.64abc	9.58bc
SM-P20%	1.88ef	3.05ab	7.64cde	7.91a	15.55a
F0%	6.84d	0.14gh	7.09ef	0.02d	7.14cd
F5%	8.20cd	ND	8.02cde	0.01d	8.21c
F10%	8.79c	0.46efgh	8.75c	0.01d	8.99c
F20%	17.25a	0.30fgh	17.06a	0.05d	17.36a
P0%	2.43e	ND	2.29	0.20cd	2.63de
P5%	7.37cd	0.11h	7.23def	0.02d	7.64c
P10%	8.13cd	ND	8.33cd	0.04d	8.38c
P20%	15.39b	ND	15.62b	0.04d	15.66a

found that extrusion above 180°C or excessive shearing cause starch to degrade into short chained molecules which do not retrograde efficiently, preventing the formation of amylose double helical RS. In addition, degradation of amylopectin has shown to increase the retrogradation rate of amylopectin into amylopectin double helices which contribute mainly to the formation of SDS and not RS (Huang et al., 2022). The shift or absence of FTIR peaks in the crystalline region and the emergence of a peak at 1022cm-^{1} in the amorphous region suggests some but minimal crystallinity in the extrudates. Starch-lipid complexes could have formed which are an example of RS that show v-type crystallinity (Cabrera-Ramirez et al., 2021). Therefore, the small amount of RS in the TVP could be the v-type crystallinity seen from the x-ray diffraction results, though additional research should be performed to verify this conclusion. Mostly all RS and SDS in the starting material was converted to RDS starch by the extrusion process. Extrusion may have caused the breakdown of

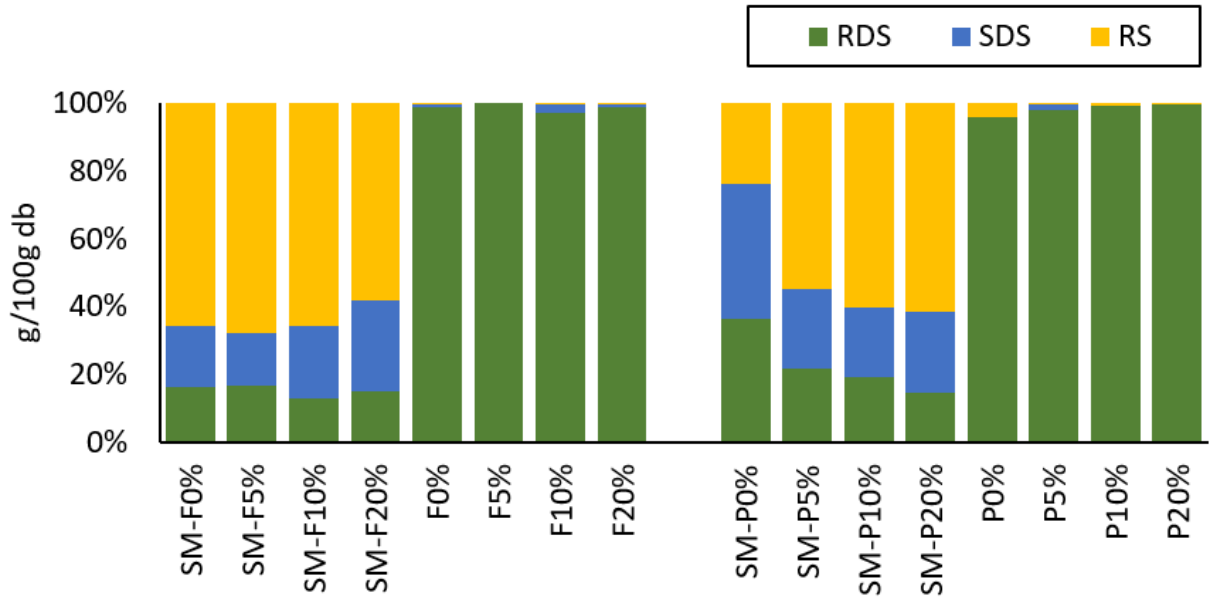

Figure 3.12 Starch digestibility for faba bean and pea starting material and extrudates at 0%, 5%, 10%, and 20% starch inclusion.

branched amylopectin and long linear amylose chains into smaller molecular weight chains, leaving the shorter starch chains open to enzymatic cleavage from digestive amylase, and thus increasing the digestibility of the extrudates (Ye et al., 2018). Conversely, other papers have found extrusion to decrease digestibility of starches because protein competes with starch for water, leaving less water for starch swelling and gelatinization. Starch can also become trapped in the protein matrix, reducing digestibility (Huang et al., 2022). This breakdown of pea starch generally occurs in the melting stage from shear and heat. Generally, an increase in RS and subsequent decrease in starch digestion is desired in the general public for better regulation of blood glucose levels and weight management, though increased starch digestibility can be beneficial for populations seeking high energy dense foods (Guo et al., 2022). The combination of high protein and digestible starch in TVP could benefit populations at risk for malnutrition.

3.3.10 Impact of starch on TVP

The addition of starch improved TVP product characteristics and structure. ER, BD and WHC were improved especially in faba bean TVP overall but specifically between 10%-20% starch inclusion in faba bean and pea TVP. Rheology analysis showed typical starch swelling and gelatinizing characteristics and promoted stabilization of faba bean G' which resulted in increased expansion. Excess starch inclusion between 10%-20% in TVP induced a shift from starch-in-protein network to develop a homogeneous phase which displayed maximum TVP expansion. As starch increased above 10% inclusion, elongated pores became more globular in structure, which had no increased effect on expansion ratio. Starch imparted an increase in pore size which improved water holding capacity on TVP. Extrusion caused the breakdown of starch crystalline regions to form V-type RS complexes but converted most RS and SDS present in the starting material to RDS making the extrudate starches more digestible.

3.3.11 Effect of insoluble and soluble fiber inclusion on faba bean and pea TVP functional properties

The base TVP formulation to which insoluble fiber (5%-10%) and soluble fiber (5%-20%) were added was based on the TVP with the most favorable results from the addition of starch (5%-20%) from previous sections 3.3.1 to 3.3.10. Pea was chosen as the protein source at the 10% starch inclusion rate as the base formulation for fiber addition. This TVP displayed the highest quality of product characteristics overall of ER (1.99), BD (0.34 g/cm^3), WHC (2.77g/g), and OHC (2.38g/g). Moreover, this TVP had an open pore structure at the highest possible protein content for nutritional purposes without losing structural integrity of the TVP. TVPs produced with insoluble pea hull fiber were visually more dense with smaller pores (Fig. 3.13) whereas TVPs

produced with soluble fiber from β-glucan were more open in structure with larger pores and greater expansion (Fig. 3.14).

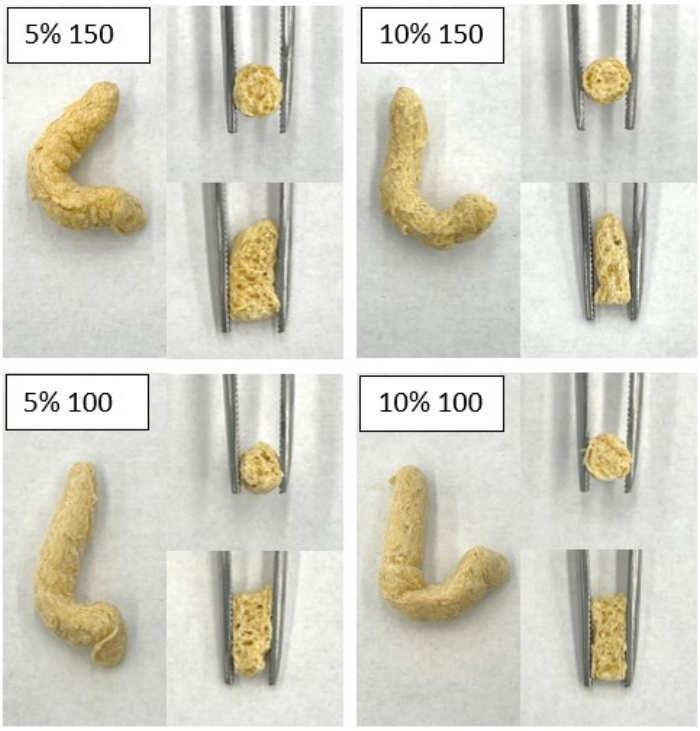

Figure 3.13 Whole (left), cross section (top right), and longitudinal (bottom right) cuts respectively of pea TVP with 5% and 10% inclusion levels of insoluble pea fiber at 150µm and 100µm size.

The starch phase plays an important role in expansion during the extrusion process (Ek et al., 2020b). Low solubility of fibers and incompatibility of insoluble fibers within the starch phase can lead to bubble rupture and may have contributed to lower expansion (Kristiawan et al., 2020). In addition, as insoluble fiber content increases, this difference in solubility between fiber and starch widens and extrapolates the effect of bubble rupture, causing further decrease in expansion between 5% fiber content (1.81, 1.70 ER) and 10% fiber content (1.57-1.54 ER) (Fig 3.15a). Wang et al. (2017) found that an inclusion of insoluble fiber from cherry pomace to expanded corn starch extrudates at 5% increased expansion whereas inclusion at 15% decreased expansion. Although

the addition of pea hull fiber at 5% inclusion did not increase expansion, the results align with previous reports such that as insoluble fiber content increases to 10% there is a decrease in expansion. Since the insoluble fiber acts as a filler, due to its incompatibility, the increase in fiber content to 10% may be too high for the protein phase to hold the protein matrix in a continuous phase, and the additional starch is not enough to support the expanded matrix when cooled (Deng et al., 2023). Collapse or bubble rupture could occur from lack of structural integrity (interruption

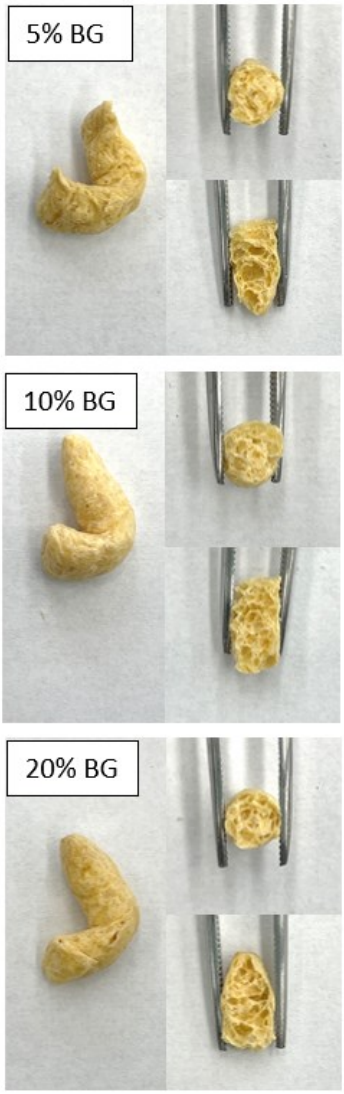

Figure 3.14 Whole (left), cross section (top right), and longitudinal (bottom right) cuts respectively of pea TVP with 5%, 10%, and 20% inclusion levels of soluble β-glucan fiber.

of protein-protein bond formations) or from fibers piercing the protein matrix, resulting in decreased expansion (Deng et al., 2023; Wang et al., 2017). Surprisingly, a decrease in particle size from 150µm (1.81, 1.57 ER) to 100µm (1.70-1.54 ER) at 5% and 10% fiber content respectively resulted in a decrease in expansion. This is contradictory to previous understandings that: (i) larger particle sizes would promote higher probability of bubble membrane rupture based on incompatible solubility of the fiber within the starch phase (Kristiawan et al., 2020) and (ii) larger sized fibers need more space for starch to bind and hold the bubble structure (Wang et al., 2017). Although it should be mentioned that the conclusions made by Kristiawan et al. (2020) and Wang et al. (2017) were based on extrudates where starch was the dominant phase, whereas in this work, the experimental extrudates contain a protein dominant phase with starch and fiber dispersed within the protein matrix. Therefore, assumption of molecular interactions in a starch expanded extrudate should not be extrapolated to a TVP extrudate with higher protein content. ER was lower than that of soy protein based TVP from 50-70% protein levels with inclusion of rice bran insoluble fiber from 2.2-2.27 ER but within range of rice protein based TVP ranging from 1.34-1.97 ER (Pengjun et al., 2023).

β-glucan soluble fiber extrudates have larger expansion values (Fig 3.15A) overall at 5%, 10% and 20% inclusion (1.95-2.07 ER) than the insoluble pea fiber extrudates (1.54-1.81 ER), which may be due to better physiochemical compatibility stemming from higher water solubility of β-glucan closer to the solubility of starches within the starch phase of the melt (Kristiawan et al., 2020). 10% BG was highest in ER compared to 0% and even 5% BG with little difference in expansion when β-glucan was increased to 20%, indicating that an addition of 10% or 20% β-glucan to TVP formulations can improve TVP expansion.

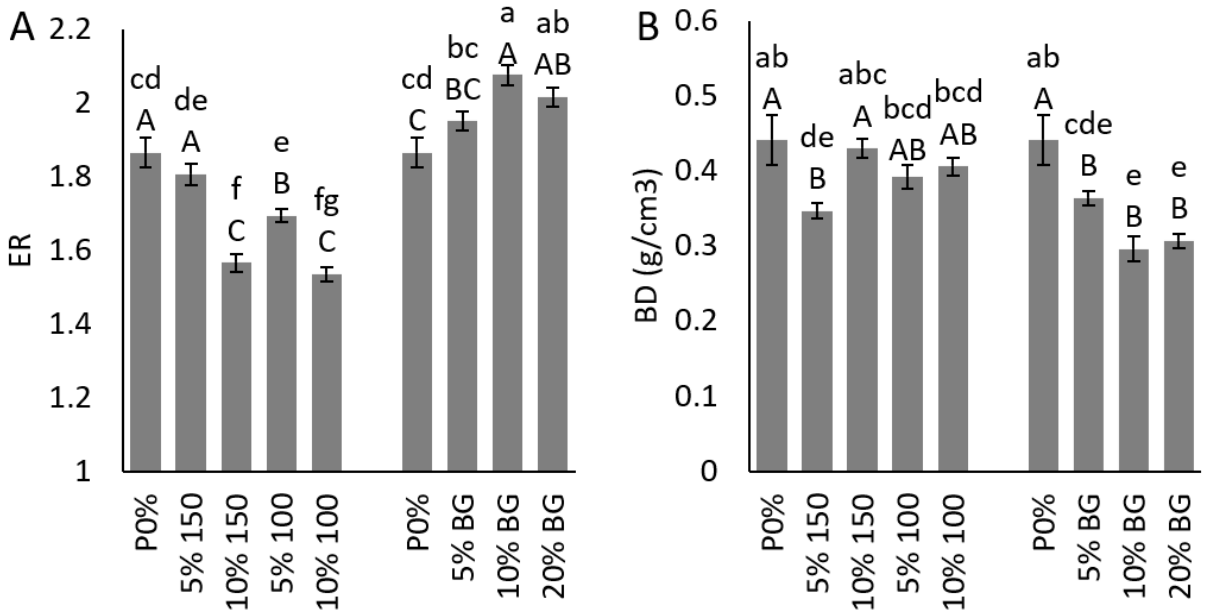

Figure 3.15 Expansion ratio (A) and bulk density (B) of insoluble fiber inclusion at 0%, 5%, and 10% (150μm and 100μm size), soluble fiber inclusion at 0%, 5%, 10% and 20% β-glucan, and TVP at 5% β-glucan. Uppercase letters indicate significant differences within insoluble or soluble fiber content and lowercase letters indicate significant differences among all TVP samples.

BD of insoluble fiber (0.35-0.43g/cm^3) and soluble fiber (0.30-0.44g/cm^3) TVP followed a similar trend to the starch inclusion TVP where an increase in ER resulted in a decrease in bulk density (Fig. 3.15B). It should be mentioned that the insoluble and soluble fibers had a large impact visually (Figures 3.13 and 3.14) on pore cell structure and size which is not fully captured in the BD values. Insoluble fibers from wheat or corn bran have previously been shown to increase in cell density and smaller cell size attributed by an increase in nucleation degree from insoluble fibers in the extruder (Robin et al., 2012), as was found visually in Fig. 3.13 as well. Improvement in BD of soluble fiber TVP indicates either more pores or larger sized pores were formed during

extrusion. According to the TVP photoimaging (Figures 3.13 and 3.14), the driving force of lower BD is larger sized pores, which in turn may lead to thicker cell walls (Esbroeck et al., 2024). Interestingly, the amount of β-glucan inclusion (5%-20%) did not significantly impact the BD among β-glucan inclusion TVP as it did impact the ER. BD of the pea hull fiber TVP are within range of TVP made with soy or rice protein with rice bran inclusion ranging in BD from 0.26-0.34g/cm^3 and 0.63-0.88g/cm^3 respectively (Pengjun et al., 2023). BD of the β-glucan 5%, 10% and 20% TVP were all lower than other TVP made from faba bean protein at 5.6% β-glucan which can range from 0.48-0.52g/cm^3 (Saldanha et al., 2023), whereas the 5% oat TVP was within that reported range.

WHC (Fig. 3.16A) was significantly improved with the addition of insoluble fiber (2.73-3.16g/g) and soluble fiber (2.60-2.98g/g) compared to the TVP with no added fiber (1.41g/g). The insoluble fiber TVP were significantly higher in WHC than their corresponding starting materials most likely due to exposure of hydrophilic groups during extrusion to intrinsically bind water as well as through capillary uptake (Esbroeck et al., 2024). The insoluble fiber TVP tended to have small pores which are more likely to hold more water from capillary action than larger pores (Esbroeck et al., 2024). Whereas the soluble fiber TVP had similar WHC to their starting materials which could be more likely caused by the ability of β-glucan to hold water effectively prior to extrusion when compared to the insoluble fiber (Sayanjali et al., 2017). The β-glucan 5%-20% included treatments had significantly lower BD than the insoluble fibers from larger pore sizes, the WHC between insoluble and soluble proteins remained similar. New insight to TVP WHC by Esbroeck et al. (2024) suggests that along with porosity and cell size, wall thickness may also play a role in WHC when pore size is large as with the β-glucan included TVP. Lower BD could indicate

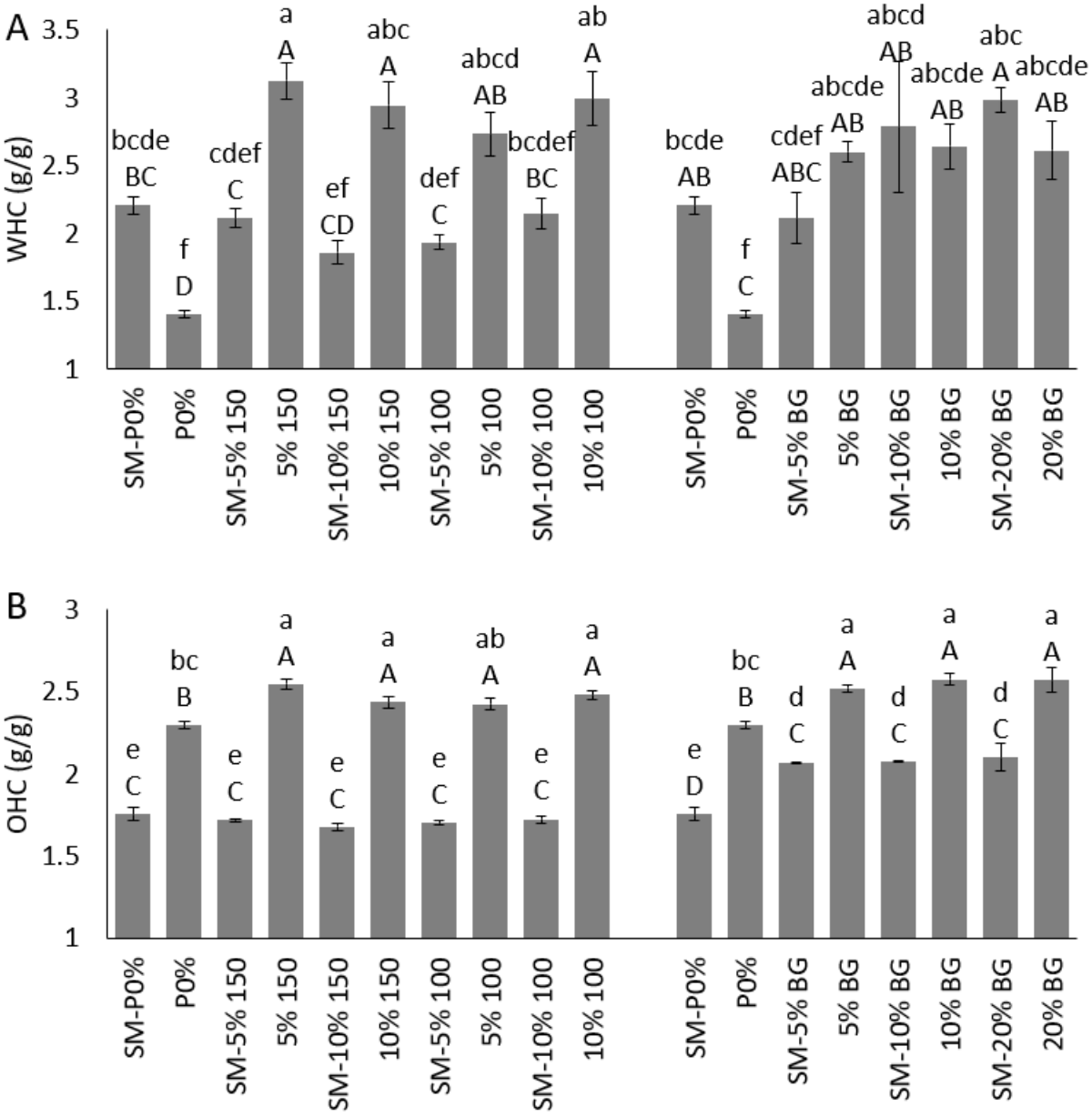

Figure 3.16 Water holding (A) and oil holding capacity (B) of insoluble fiber inclusion at 0%, 5%, and 10% (150 and 100µm size), soluble fiber inclusion at 0%, 5%, 10% and 20% β-glucan, oat protein TVP at 5% β-glucan and their respective starting materials. Uppercase letter indicate significant differences within protein sources and lowercase letters indicate significant differences among all TVP samples.

larger cell size and thinner cell walls, which are slower to uptake water but can hold more water overall (compared to thick walls) since there is room for swelling (Esbroeck et al., 2024). Although cell wall thickness was not measured in this study, this new insight could be a contributing factor to increased WHC with a lower bulk density but cannot be confirmed. All TVP were within range of other reported WHC of TVP from 1.5-2.9g/g of assorted protein sources like soy, pea, gluten, chickpea, and navybean (Hong et al., 2022). WHC was generally higher than the averages for soy (2.1g/g), pea (2.1g/g) and wheat (1.9g/g) TVP (Hong et al., 2022) but within range or lower than WHC with insoluble rice bran in soy (2.9-4.9g/g) and in rice (2.97-3.47g/g) (Pengjun et al., 2023).

Again, OHC was improved from the respective TVP starting materials through extrusion (Fig. 3.16B) but was also improved by the addition of both insoluble pea hull fiber (2.42-2.54g/g) and soluble β-glucan (2.52-2.57g/g) compared to TVP with no fiber added (2.29g/g). Interestingly the increase in OHC in the insoluble fiber TVP may not be due just to capillary action from increased expansion because the insoluble fiber TVP actually had lower expansion than the 0% fiber included TVP. It is possible that the increase in OHC in insoluble fiber TVP may come from increased porosity and increased pore surface area from a rough pore surface (Waliullah et al., 2021), rather than from expansion. Soluble fiber may have improved OHC with increasing β-glucan comes from improved protein network mesh structure from increased expansion, which facilitates the binding of lipids (Xiao et al., 2023) although there was less improvement of OHC compared to starting materials than there was in insoluble fiber TVP compared to their starting materials respectively. All TVP were higher than other reported OHC of TVP from 0.69-1.04g/g of assorted protein sources like soy, pea, gluten, chickpea, and navybean (Hong et al., 2022). Moreover, the WHC of TVP falls within range reported for TVP with rice bran inclusion in soy (2.55-2.73 g/g) and rice (1.91-2.51g/g) (Pengjun et al., 2023).

3.3.12 FTIR protein secondary structure of faba bean and pea dietary fiber inclusion extrudates

The increase in insoluble fiber at different sizes (100µm and 150µm) and soluble fiber had no effect on protein structure in raw materials, but there were changes in TVP in both fiber sources (Fig 3.17). Protein aggregates correlated to the peak at 1618cm^{-1} are the intermolecular β-sheets formed by hydrogen bonds which are more dominant in all extruded TVP compared to the starting material, indicating increased β-sheet formation from protein aggregation (Zhang et al., 2022c; Yang et al., 2021).

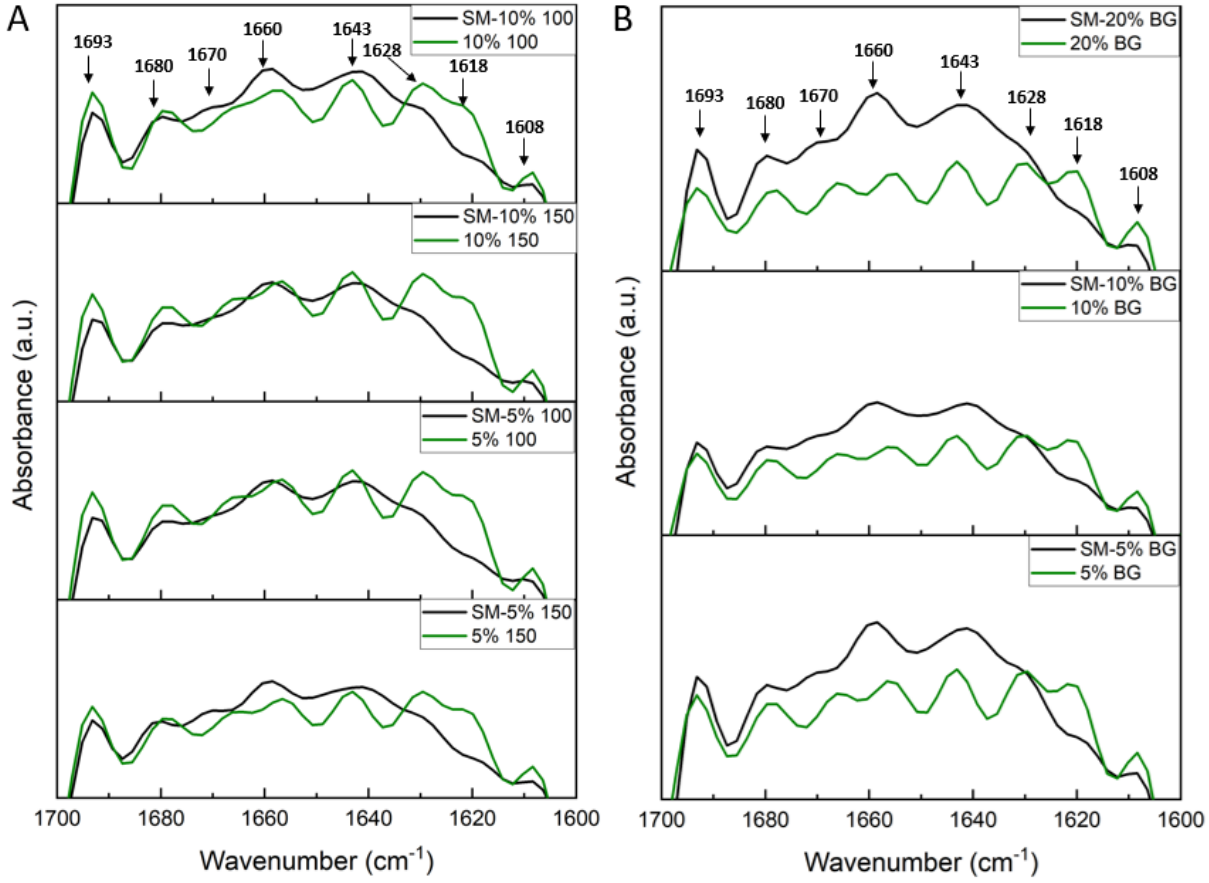

Fig 3.17 FTIR spectra of insoluble fiber inclusion at 5% and 10% at 150µm and 100µm sizes (a) and β-glucan fiber inclusion at 5%, 10%, and 20% (b) TVP with corresponding starting materials in the protein region (1700-1600 cm^{-1}).

3.3.13 Rheological properties of dietary fiber inclusion extrudates

The rheology curve of the storage modulus was higher than the loss modulus for all curves with the inclusion of insoluble and soluble fiber indicating the protein melt was in a solid state (Deng, 2023). The G' of all insoluble fiber TVP (Fig. 3.18A) were lower than TVP with no insoluble fiber added, indicating that fewer or weaker bonds and interactions between protein or starch were formed when insoluble fiber was included. This resulted in a decrease in viscosity which may indicate why ER was lower for TVP with insoluble fiber, since there may have been fewer bonds to hold the air cells when TVP expanded.

β-glucan has been known to display shear-thinning flow behaviors based on a decrease in viscosity relative to an increase in shear (Herrera et al., 2016). Since shear rate and temperature increases on the extrusion melt as it is conveyed down the barrel (especially in the mixing and melting zones), shear-thinning behavior may explain the steady downward G' slope of the viscosity curve as the melt is heated and held until cooling starts (Fig. 3.18B). Ye et al. (2018) suggests that the addition of β-glucan can cause entanglement of β-glucan chains with other components which could reduce the attraction between protein-protein interactions. The inclusion of β-glucan did increase ER in this study, implying that β-glucan positively impacted bond structures from proteins which were indeed able to hold expanded cell structure.

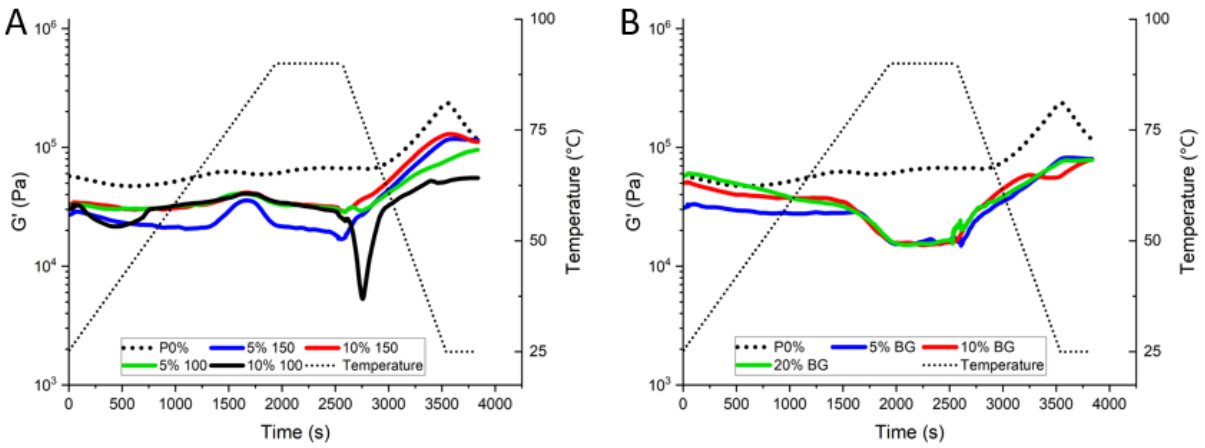

Figure 3.18 Rheological properties of storage modulus (G') for insoluble and soluble fiber extrudates over a temperature ramp 25°C-90°C-25°C.

3.3.14 Effects of dietary fiber distribution on protein matrix phase of extrudates

Confocal imaging of TVP highlights the starch and fiber (dyed blue) size, orientation, and effects on the protein matrix which is dyed red (Figures 3.19 and 3.20). Insoluble carbohydrates such as pea hull fiber may act as a particulate during texturization in the extruder and not as a separate phase, allowing this particulate to also act as a nucleating agent. Since the surface of the particulate is rough, air could be trapped as microscopic cavities on the fiber once all materials are mixed in the extruder barrel and could be inflated at the die when water is flashed off (Twombly et al., 2020). This could cause micro bubble formation effecting the protein matrix structure which is clearly evident when comparing insoluble fiber addition at both 5% and 10% levels for both 150µm and 100µm sized fibers against 0% fiber inclusion TVP structure (Fig. 3.19). The protein matrix is highly disrupted by the insoluble fiber compared to the TVP with no fiber added. A significant decrease in ER of insoluble fiber TVP (Fig. 3.15A) with little change in density (Fig. 3.15B) suggests that there is an increase in small air pockets from many nucleation sites that do not grow in bubble size to cause an increase in expansion, supporting the micronucleation caused

by insoluble pea hull fiber seen in confocal imaging. Particle size of insoluble fiber can impact not only expansion of extrudates but also the structure of the protein such that small particle sized fiber will fill the small gaps within the protein matrix, leaving the structure unimpacted. Though as insoluble particle size increases up to 150µm in this work, the fibers could start to interfere with protein-protein bonding and prevent or cut the protein matrix, causing collapse of structure preventing bubble growth and ultimately a decrease in expansion (Wang et al., 2017). In this work, such increase in size threshold above 150µm was not reached, therefore expansion still occurred in all TVP.

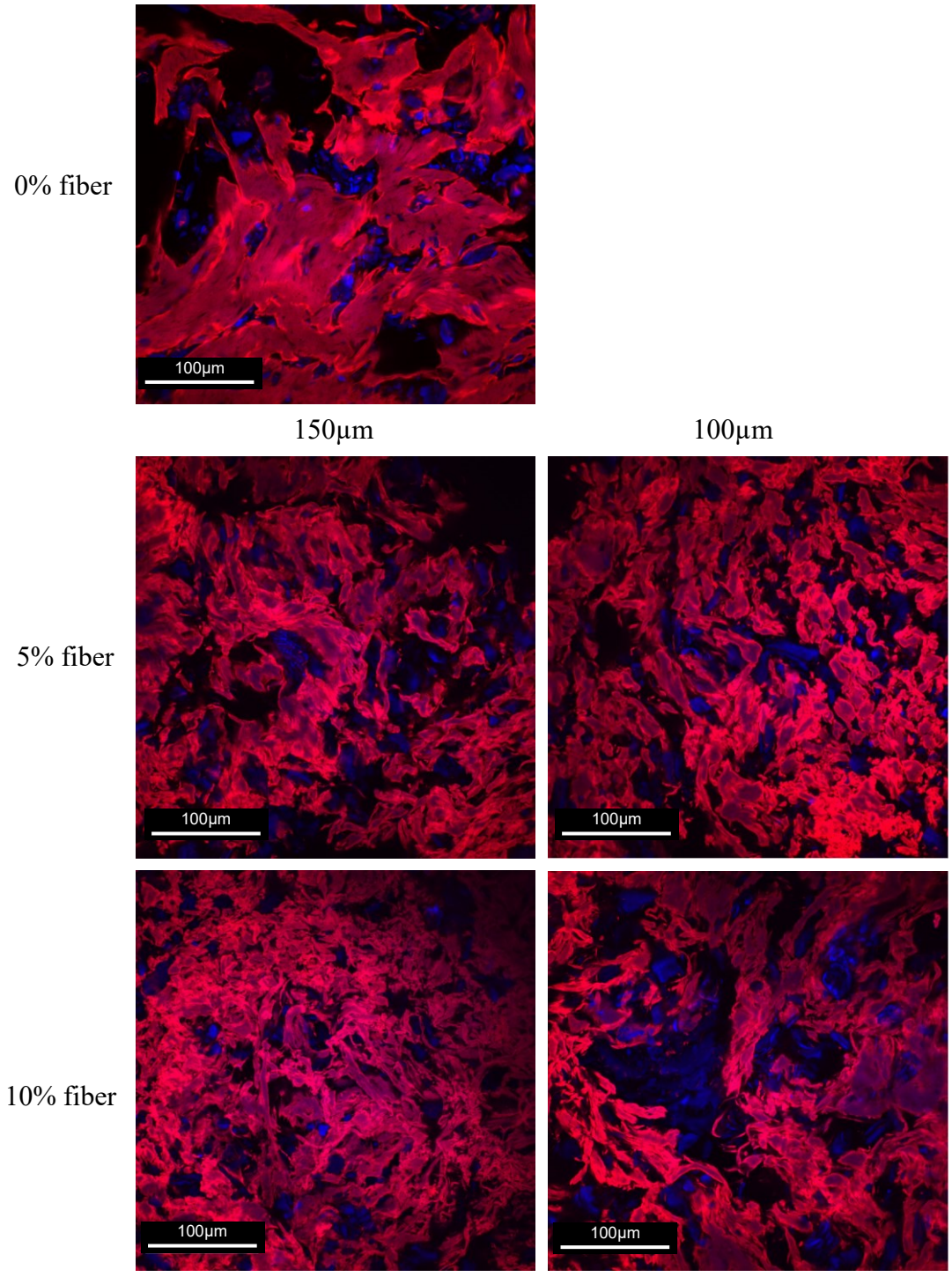

Figure 3.19 Confocal imaging of pea TVP with insoluble fiber inclusion of 150µm and 100µm size at 0%, 5%, and 10%.

Deng et al. (2023) found that between 20%-25% inclusion insoluble dietary fiber in high moisture soy extrudates a bi-continuous phase between the protein and fiber developed which resulted in a crumbly texture with no desired filaments. Insoluble fiber inclusion was not high enough to shift the matrix to a bi-continuous phase in this work as there is a clear defined protein phase with a dispersed insoluble fiber phase throughout the protein matrix (Fig. 3.19). Insoluble fiber is unique from starch or soluble fiber in that it does not undergo phase change from extrusion heat, shear or pressure, but rather acts like a discontinuous filler within the extrudate's protein phase. The rigid structure from additional hydrogen bonds contributes to higher glass transition and melt temperatures (220°C-250°C for dry cellulose), therefore providing resistance to deformation and phase change along with its insolubility providing thermodynamic immiscibility with the dominant protein phase (Deng et al., 2023; Ek et al., 2020b).

Confocal imaging of soluble β-glucan (Fig. 3.20) between protein (red) and fiber (blue) at each fiber inclusion level shows very different protein matrix structure and fiber distribution compared to the insoluble fiber included TVP. At 5%, β-glucan is accumulated as a separate phase from the protein and are dispersed homogenously within the formed air cells of the protein matrix. β-glucan at 10% and 20% inclusion has also blended into the protein phase (shown as purple), indicating a change in protein phase is taking place. β-glucan can solubilize into the protein phase by evidence of previous confocal imaging in noodles where β-glucan was found to overlap with the protein network as β-glucan content increases, whereas the starch remained as a separate phase from the protein network (Nguyen et al., 2022). It is possible that the blending of the soluble fiber into the protein phase helped TVP expansion, leading to a decrease in bulk density. However, the mechanisms will need to be investigated in future studies.

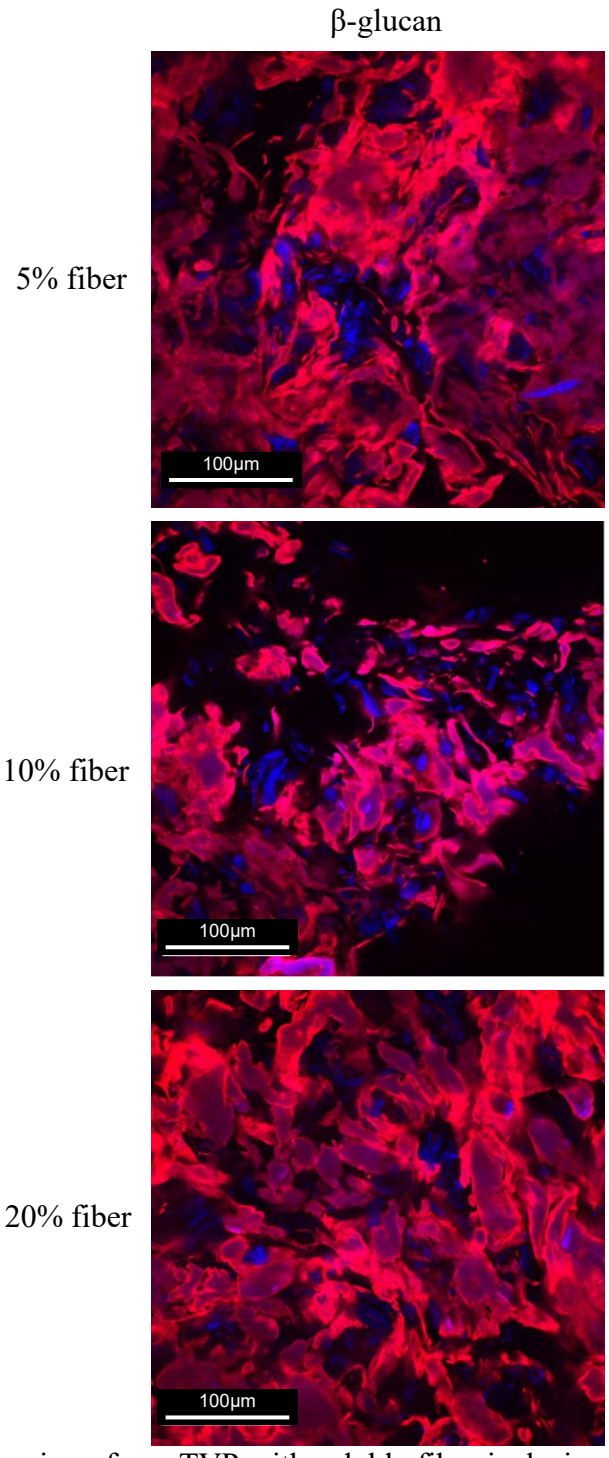

Figure 3.20 Confocal imaging of pea TVP with soluble fiber inclusion of β-glucan at 5%, 10%, and 20%.

3.3.15 Effects dietary fiber on microstructure of extrudates

All TVP with insoluble fiber inclusion had similar microstructures (Fig. 3.21) when viewed under a scanning electron microscope. Insoluble fiber TVP had a rough surface on the air pockets as well as in the protein matrix internally when compared to the TVP with starch included. This rough pore texture may be why the insoluble fiber TVP had higher OHC without an increase in

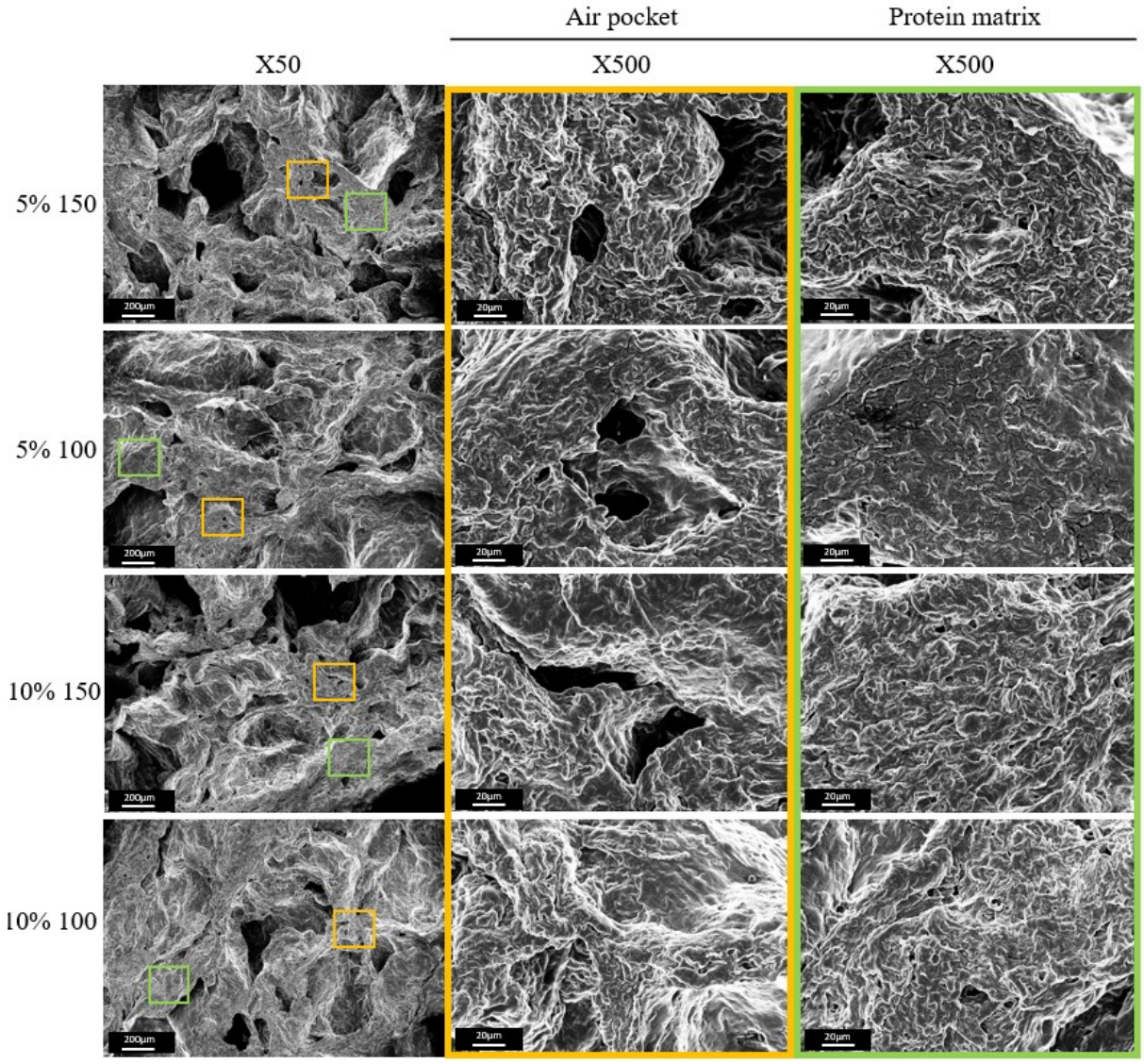

expansion which provides a beneficial function to TVP as a meat alternative (Waliullah et al.,

Figure 3.21 SEM micrographs of insoluble fiber included pea TVP at 5% and 10% of 150µm size and 100µm size pea hull fiber.

2021). Clear bubble expansion is seen in all insoluble fiber TVP (Fig. 3.21 X50 magnification). All insoluble fiber TVP contained distinct micronucleation sites stemming from unhydrated fiber, creating a matrix with many rough ridges dispersed throughout the TVP, which coincides with confocal imaging (Fig. 3.19) (Beck et al., 2018). Both TVP with100µm and 150µm sized insoluble fiber at 10% fiber inclusion had significant decreases in ER that could be caused by excess fiber filling the cell walls and piercing the matrix, causing rupture of air cells and collapse of pockets evident by flattened or misshaped air pockets in the SEM micrographs (Fig. 3.21 X500 magnification) (Wang et al., 2017). Small round craters visible in the protein matrix (Fig. 3.22 X500 magnification) of 10% fiber inclusion TVP indicate micronucleation sites where air bubbles ruptured causing an increase in porosity but not a subsequent increase in expansion (Beck et al., 2018).

Interestingly, SEM at a higher magnification (Fig. 3.22) showed the formation of fibrous bundles within the cross section throughout the extrudate more often as insoluble fiber content increased. High shear could cause degradation of the fiber into smaller bundles (Bhatt et al., 2022; EK et al., 2021), but this was not seen in this study with pea hull fiber. Since the glass transition temperature of cellulose (220°C-250°C) is above the extrusion temperature, the fibrous bundles have not degraded, but rather remain in the TVP (Deng et al., 2023; Ek et al., 2020b). In addition, the fibrous bundles tended to be short and wide rather long strands. The 5% inclusion of 150µm sized fiber TVP tended to have larger fibril bundles which are clearly shown in Fig. 3.22. The protein matrix forms around these fibrous bundles homogenously distributed within the matrix, specifically starches can gelatinize around the fibrous bundles since the fiber has poor interfacial adhesion with starch from lack of hydrogen bonding (Ek et al., 2021). This phenomenon is clearly visible in the micrograph of 5% inclusion of the 150µm sized insoluble pea hull fiber.

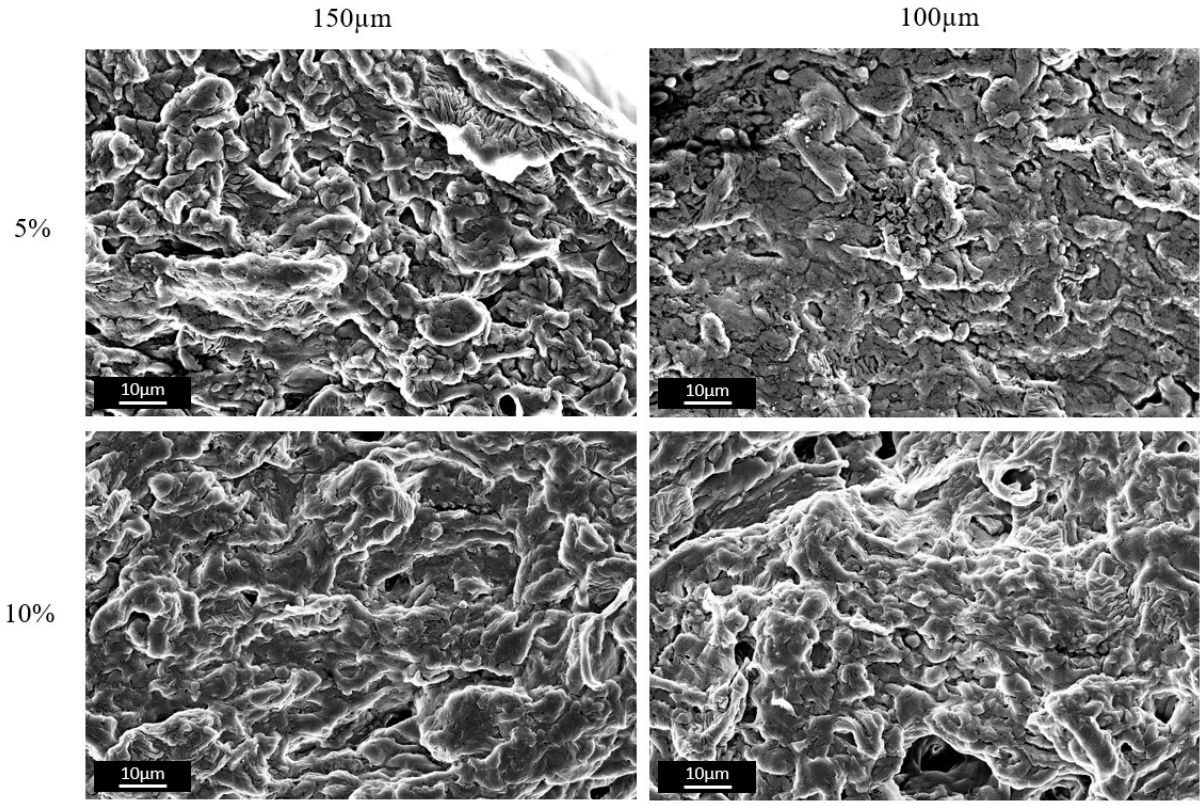

Figure 3.22 SEM micrographs of insoluble fiber included pea TVP at 5% and 10% of 150µm size and 100µm size pea hull fiber at a magnification of 1KX.

The SEM of soluble β-glucan fiber TVP (Fig. 3.23) also have a rougher surface compared to the starch inclusion TVP (Figures 3.8 and 3.9) and larger surface lumps compared to the insoluble fiber TVP (Fig. 3.21). The β-glucan TVP had a dense protein matrix with thicker cell walls and fewer small air pockets than the insoluble fiber (Kour et al., 2019). At lower soluble β-glucan fiber content (5%) the texture of the protein matrix seemed smoother (Fig. 3.23 X500 magnification) implying that soluble fiber has more positive impact on expansion than insoluble fiber (Xiao et al., 2023). Soluble fiber formulation was able to increase up to 20% inclusion whereas insoluble fiber inclusion was only able to increase up to 10% before impacting extrusion processing and the TVP integrity.

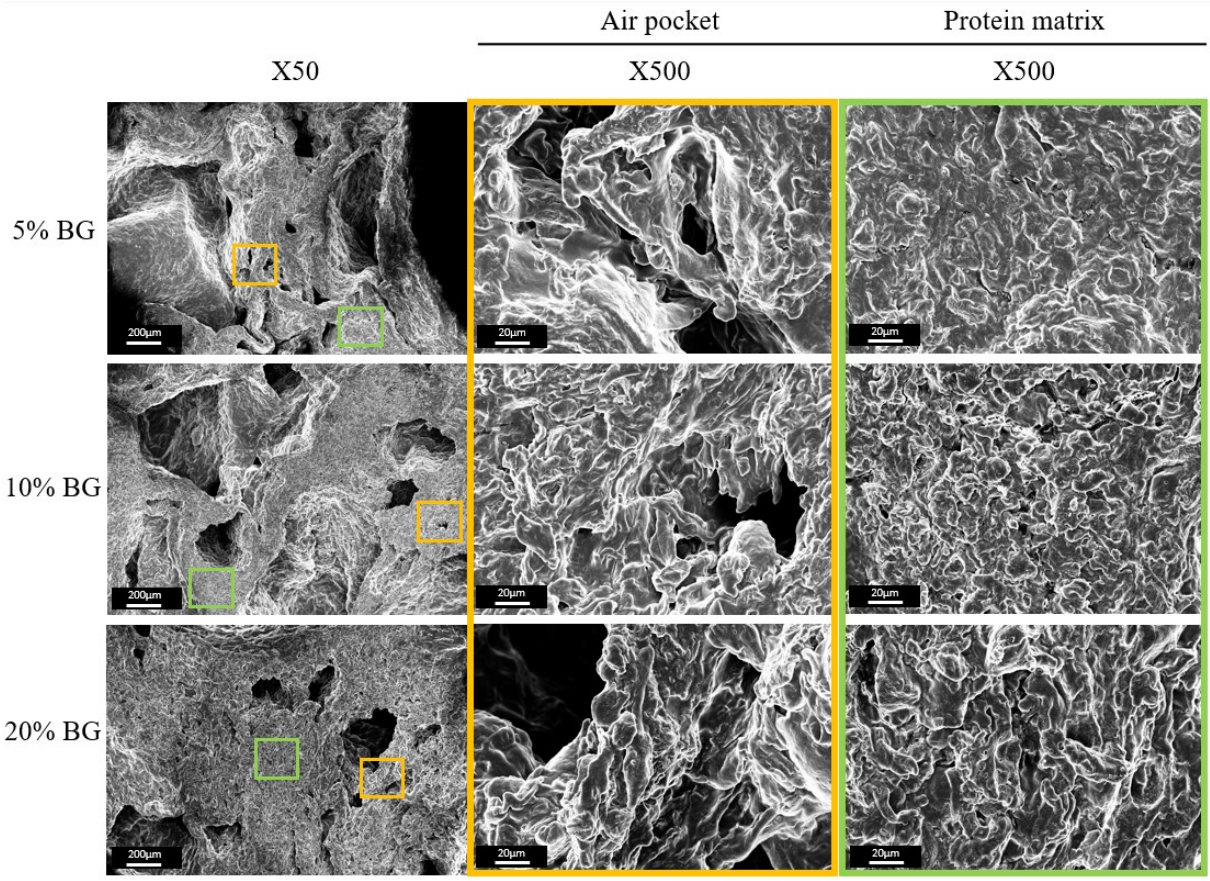

Figure 3.23 SEM micrographs of pea TVP at 5% and 10% inclusion of soluble fiber.

3.3.16 Impact of digestible fiber on TVP

Insoluble pea hull fiber caused a decrease in expansion ratio brought on by a dense TVP structure, but BD was unaffected. Inclusion of insoluble fiber also promoted micro nucleation to form many small air pockets which improved WHC. Soluble β-glucan fiber improved ER, BD, and WHC by promoting larger air pockets with thicker cell walls. The inclusion of soluble fiber at 10% and 20% in TVP induced a shift from starch-in-protein network to develop a homogeneous phase where β-glucan started to blend into the protein phase resulting in improved ER and lower BD.

3.4 Conclusion

By using imaging techniques on protein matrix microstructure to connect the effects of starch and dietary fiber on TVP, this study was able to expand upon concepts from starch expanded products and HME, helping to improve TVP nutrition and quality. This study was able to link changes in chemical components to the extrudate microstructure, and then to the TVP product characterization. Extrusion of pea starch converted all C-type crystallinity to RS V-type complexes in pea and faba bean TVP which decreased in double helical starch structure yet converted the RS and SDS to RDS. Starch inclusion modified faba bean protein network microstructure by creating larger pockets and thicker cell walls, thereby increasing expansion of all faba bean TVP and pea TVP once 10% starch inclusion was met while improving WHC at 7.5-10% in faba bean and at 20% in pea. The addition of appropriate amount of insoluble or soluble fiber to TVP improved WHC and OHC, as did the addition of β-glucan to ER and BD. Insoluble fiber decreased expansion at a higher concentration (10%) due to the formation of fibril bundles which disrupted in the protein network. On the other hand, in the soluble fiber TVP a change in the protein phase occurred within the protein matrix where β-glucan was distributed within the protein phase while being retained as a separate phase to the protein as well. To the best of our knowledge, this study is the first to show how dietary fiber from insoluble pea hulls and soluble β-glucan impact TVP microstructure and the impact of how pea starch can improve faba bean TVP.

Chapter 4: Conclusion and Future work

4.1 Conclusion

This study was able to better describe the pulse protein structure and its interaction with other food components, starch and dietary fiber, within extrusion black box technology by combining spectroscopic and microscopic analytical techniques. And to study the impact of protein melt rheology and structure on the TVP functional quality and starch nutritional value.

The first objective (Chapter 2) showed that TVP microstructure and rheological properties can be modulated by modifying the protein and moisture content, thereby improving TVP functionalities. TVP expansion was improved by a degree of phase separation in the protein matrix at 70% protein and a lower moisture (50%) brought on by increased G' rheological properties resulting in smooth SEM imaging and good WHC and OHC. Faba bean protein had lower yet fairly similar functionality to that of pea protein in TVP. Both faba bean and pea proteins were within ranges of acceptable functionality from traditional TVP protein sources like soy and wheat. Because faba bean and pea are not allergens they could be a replacement for soy and wheat protein in TVP production. This study also showed that TVP can have acceptable functionality and structure when protein concentrates (~60% protein) are used as the raw materials when supplemented with protein isolates to reach higher protein levels. Protein concentrates are less expensive and may contain superior native (less aggregated) proteins compared to protein isolates, due to using a dry fractionation process which is also more environmentally friendly than the wet fractionation process.

The second objective (Chapter 3) was able to show improvement of expansion of faba bean and pea TVP by starch inclusion in the protein matrix. Starch inclusion also improved WHC of pea TVP at 20% inclusion, while WHC of faba bean was improved at an even lower

level of 7.5% by creating larger pores, thickening of cell walls and improving microstructure, thus increasing the quality of TVP. Although extrusion was shown to convert all C-type starch to crystalline V-type RS, almost all RS and SDS were converted to RDS under extrusion conditions. Inclusion of insoluble pea hull fiber decreased ER for all TVP brought on by lower G' rheological properties and disruption of protein matrix showing visible fibril bundles in SEM imaging. On the other hand, inclusion of dietary fiber was shown to improve WHC and OHC of all TVP at all inclusion levels. Soluble fiber improved expansion and density of all pea TVP by imparting a change in the protein phase where β-glucan blends with the proteins in addition to remaining as a separate phase within the protein matrix, specifically at 10% inclusion of β-glucan.

The overall human diet can be improved by the incorporation of TVP to replace animal meats, thereby decreasing total fat intake and cholesterol while providing protein from plant sources along with beneficial starches and fibers (Boukid, 2021). Increased RS in the diet is desired in the general population for regulation of glycemic response and blood glucose levels, and for the fermentation of RS in the gut which can promote the growth of beneficial bacteria. A decrease in starch digestibility is also desired for management of body weight and composition, as well to decrease caloric intake to combat obesity and associated chronic diseases (Guo et al., 2022). Since amylose-lipid complexes are a type of RS and can form from starches high in amylose, the inclusion of other starches higher in amylose like modified or high amylose corn starch (55%-70%), native lentil starch (29%-45%), or native potato starch (25%-31%) could possibly improve the amount of RS in TVP (Zakaria et al., 2017; Bertoft, 2017; El Seoud et al., 2013). Our study found pea starch content in the starting material to be higher in beneficial RS and SDS, but under extrusion conditions were converted to RDS which are more easily digestible. Digestible starch

may actually be desired in populations that require highly digestible energy dense foods such as the elderly or those with poor appetites from malnutrition or other related conditions.

Inclusion of β-glucan improved TVP functionality, but the effect of this β-glucan on human health was outside of the scope of this study and yet to be investigated. Incorporation of the β-glucan containing TVP into a model food system such as a burger patty or alone as a ground beef could provide additional health benefits on human health such as improved laxation, healthier gut microbiota, and lower cholesterol, but will need to be demonstrated by in-vivo and clinical studies in the future (McKeown et al., 2022).

Based on results from this study, there were three TVP from chapter 2 and 3 which displayed the most promising functionality (ER, BD, WHC and OHC) overall without compromising protein content; i) the pea with 70% protein content and 50% moisture content, ii) the pea TVP with 10% starch inclusion and, iii) the pea TVP with 10% β-glucan fiber. The TVP with 20% β-glucan fiber still had acceptable product characteristics. Moreover, the addition of small amounts of pea starch (high in amylose) can improve the structural and functional quality of new or underutilized protein sources as was true for faba bean TVP.

4.2 Study innovations

Results from this study were able to expand beyond current work focused just on optimization of input and output parameters of extrusion by investigating deeper into the effect of protein, starch, and dietary fiber on microstructure and functionality in TVP, to help guide product developers. Chapter 2 was able to show evidence of faba bean protein's capability and potential as another alternative source of plant protein for TVP production in addition to pea protein. As well as the proven capability of TVP production from a protein concentrate base

supplemented with protein isolate, which can reduce energy and costs associated with protein extraction from a TVP ingredient.

Chapter 3 was able to apply concepts from starch expanded LME products to the impact of increasing starch in a starch-in-protein matrix TVP dominant in protein, which has not been fully explored. This study has added value to a protein extraction by-product stream (pea starch) as a quality enhancer to TVP protein sources such as faba bean that have lower expansion capabilities and could be applied to other lower functional protein sources to expand TVP plant protein options. The addition of dietary fiber provided the opportunity to improve TVP for human health while showcasing improved expansion, WHC, and OHC of TVP. In addition, confocal imaging was able to show β-glucan distributed within the protein phase as well as within the protein matrix, which to the best of our knowledge has not been demonstrated in a LME TVP product and could promote a new area of research.

4.3 Future work

i. Continue investigation of TVP for quality attributes associated with food applications including structural integrity and textural attributes.
ii. Implementing TVP into model food systems such as ground meat patty analogues (exposed) and sausage analogues (enclosed by casing) with and without dietary fiber to determine capability and quality in a hybrid or meatless product.
iii. Evaluate sensory qualities (texture, aroma, flavour) of faba bean and pea TVP with starch and dietary fiber inclusion in a model food system for product evaluation correlating to instrumental texture analysis.
iv. Investigate application of pea starch and other starches high in amylose on other plant protein sources to expand viable protein options and enhance quality of TVP.

v. Continue investigation of β-glucan interactions with protein to better understand the physiochemical impact of β-glucan within the TVP protein matrix.

vi. Explore the impact of TVP on health from the inclusion of dietary fiber and digestibility of starch through animal models or by substitution of typical animal meat products with TVP.

References

Adamidou, S., Nengas, I., Grigorakis, K., Nikolopoulou, D. and Jauncey, K. (2011), Chemical Composition and Antinutritional Factors of Field Peas (Pisum sativum), Chickpeas (Cicer arietinum), and Faba Beans (Vicia faba) as Affected by Extrusion Preconditioning and Drying Temperatures. *Cereal Chemistry*, 88(1), 80-86. https://doi.org/10.1094/CCHEM-05-10-0077

Akdogan, H. (1999). Review High moisture food extrusion. *International Journal of Food Science and Technology*, 34(3), 195-207. https://doi.org/10.1046/j.1365-2621.1999.00256.x

Allen, K. E., Carpenter, C. E., & Walsh, M. K. (2007). Influence of protein level and starch type on an extrusion-expanded whey product. *International Journal of Food Science and Technology*, 42(8), 953–960. https://doi.org/10.1111/j.1365-2621.1006.01316.x

Allotey, D. K., Kwofie, E. M., Adewale, P., Lam, E., & Ngadi, M. (2023). Life cycle sustainability assessment outlook of plant-based protein processing and product formulations. *Sustainable Production and Consumption*, 36, 108–125. https://doi.org/10.1016/j.spc.2022.12.021

Altan, A., & Yağci, S. (2023). Physicochemical characteristics and structural changes of fermented faba bean extrudates prepared by twin-screw extrusion. *Food Chemistry*, 411, Article 135502 https://doi.org/10.1016/j.foodchem.2023.135502

Arijaje, E. O., & Wang, Y. J. (2015). Effects of chemical and enzymatic modifications on starch-oleic acid complex formation. *Journal of Agricultural and Food Chemistry*, 63(16), 4202–4210. https://doi.org/10.1021/acs.jafc.5b00125

Basiak, E., Lenart, A., & Debeaufort, F. (2018). How glycerol and water contents affect the structural and functional properties of starch-based edible films. *Polymers*, 10(4), 412. https://doi.org/10.3390/polym10040412

Baune, M. C., Jeske, A. L., Profeta, A., Smetana, S., Broucke, K., van Royen, G., Gibis, M., Weiss, J., & Terjung, N. (2021). Effect of plant protein extrudates on hybrid meatballs – Changes in nutritional composition and sustainability. *Future Foods*, 4, Article 100081. https://doi.org/10.1016/j.fufo.2021.100081

Baune, M. C., Terjung, N., Tülbek, M. Ç., & Boukid, F. (2022). Textured vegetable proteins

(TVP): Future foods standing on their merits as meat alternatives. *Future Foods*, 6, Article 100181. https://doi.org/10.1016/j.fufo.2022.100181

Beck, S. M., Knoerzer, K., & Arcot, J. (2017a). A Review: Protein-Fortified Low Moisture Extrusion. *Reference Module in Food Science*. https://doi.org/10.1016/b978-0-08-100596-5.21101-3

Beck, S. M., Knoerzer, K., & Arcot, J. (2017b). Effect of low moisture extrusion on a pea protein isolate's expansion, solubility, molecular weight distribution and secondary structure as determined by Fourier Transform Infrared Spectroscopy (FTIR). *Journal of Food Engineering*, 214, 166–174. https://doi.org/10.1016/j.jfoodeng.2017.06.037

Beck, S. M., Knoerzer, K., Foerster, M., Mayo, S., Philipp, C., & Arcot, J. (2018). Low moisture extrusion of pea protein and pea fibre fortified rice starch blends. *Journal of Food Engineering*, 231, 61–71. https://doi.org/10.1016/j.jfoodeng.2018.03.004

Beliciu, C. M., & Moraru, C. I. (2011). The effect of protein concentration and heat treatment temperature on micellar casein-soy protein mixtures. *Food Hydrocolloids*, 25(6), 1448–1460. https://doi.org/10.1016/j.foodhyd.2011.01.011

Bello-Perez, L. A., Flores-Silva, P. C., Agama-Acevedo, E., & Tovar, J. (2020). Starch digestibility: past, present, and future. *Journal of the Science of Food and Agriculture,* 100(14), 5009–5016. https://doi.org/10.1002/jsfa.8955

Bertoft, E. (2017). Understanding Starch Structure: Recent Progress. *Agronomy*, 7(3), 56. https://doi.org/10.3390/agronomy7030056

Bhatnagar, S., & Hanna, M. A. (1994). Amylose-Lipid Complex Formation During Single-Screw Extrusion of Various Corn Starches. *Cereal Chemistry*, 71(6), 582-587.

Bhatt, S., & Gupta, M. (2022). Exploration of soluble dietary fiber extraction technique for enhancing physicochemical and structural properties of mango and pomegranate peel. *Biomass Conversion and Biorefinery*, 14, 2545-2560. https://doi.org/10.1007/s13399-022-02545-7

Bobade, H., Gupta, A., & Sharma, S. (2021). Beta-glucan. *Nutraceuticals and Health Care,* (pp. 343–358). Elsevier. https://doi.org/10.1016/B978-0-323-89779-2.00013-2

Boukid, F. (2021). Plant-based meat analogues: from niche to mainstream. *European Food Research and Technology*, 247(2), 297–308. https://doi.org/10.1007/s00217-020-03630-9

Bojarczuk, A., Skąpska, S., Mousavi Khaneghah, A., & Marszałek, K. (2022). Health benefits of

resistant starch: A review of the literature. *Journal of Functional Foods*, 93, Article 105094. https://doi.org/10.1016/j.jff.2022.105094

Brennan, M. A., Derbyshire, E. J., Brennan, C. S., & Tiwari, B. K. (2012). Impact of dietary fibre-enriched ready-to-eat extruded snacks on the postprandial glycaemic response of non-diabetic patients. *Molecular Nutrition and Food Research*, 56(5), 834–837. https://doi.org/10.1002/mnfr.201100760

Brennan, M. A., Derbyshire, E., Tiwari, B. K., & Brennan, C. S. (2013). Integration of β-Glucan Fibre Rich Fractions from Barley and Mushrooms to Form Healthy Extruded Snacks. *Plant Foods for Human Nutrition*, 68(1), 78–82. https://doi.org/10.1007/s11130-012-0330-0

Brishti, F. H., Chay, S. Y., Muhammad, K., Ismail-Fitry, M. R., Zarei, M., & Saari, N. (2021a). Texturized mung bean protein as a sustainable food source: Effects of extrusion on its physical, textural and protein quality. *Innovative Food Science and Emerging Technologies*, 67, Article 102591. https://doi.org/10.1016/j.ifset.2020.102591

Brishti, F.H., Chay, S. Y., Muhammad, K., Rashedi Ismail-Fitry, M., Zarei, M., Karthikeyan, S., Caballero-Briones, F., & Saari, N. (2021b). Structural and rheological changes of texturized mung bean protein induced by feed moisture during extrusion. *Food Chemistry*, 344, Article 128643. https://doi.org/10.1016/j.foodchem.2020.128643

Bühler, J. M., Schlangen, M., Möller, A. C., Bruins, M. E., & van der Goot, A. J. (2022a). Starch in Plant-Based Meat Replacers: A New Approach to Using Endogenous Starch from Cereals and Legumes. *Starch*, 74, Article 2100157. https://doi.org/10.1002/star.202100157

Bühler, J. M., van der Goot, A. J., & Bruins, M. E. (2022b). Quantifying water distribution between starch and protein in doughs and gels from mildly refined faba bean fractions. *Current Research in Food Science*, 5, 735–742. https://doi.org/10.1016/j.crfs.2022.03.013

Cabrera-Ramírez, A. H., Cervantes-Ramírez, E., Morales-Sánchez, E., Rodriguez-García, M. E., Reyes-Vega, M. de la L., & Gaytán-Martínez, M. (2021). Effect of Extrusion on the Crystalline Structure of Starch during RS5 Formation. *Polysaccharides*, 2(1), 187–201. https://doi.org/10.3390/polysaccharides2010013

Carrera Sánchez, C., Rodríguez Niño, M. R., Molina Ortiz, S. E., Añon, M. C., & Rodríguez

Patino, J. M. (2004). Soy globulin spread films at the air-water interface. *Food Hydrocolloids*, 18(2), 335–347. https://doi.org/10.1016/S0268-005X(03)00089-4

Chan, E., Rodas-Gonzalez, A., Tulbek, M., & Koksel, F. (2023). Effects of protein formula and extrusion cooking conditions on the techno-functional properties of texturised pea proteins. *International Journal of Food Science & Technology*. 59(1), 584-595. https://doi.org/10.1111/ijfs.16593

Chen, L., Ren, F., Zhang, Z., Tong, Q., & Rashed, M. M. A. (2015). Effect of pullulan on the short-term and long-term retrogradation of rice starch. *Carbohydrate Polymers*, 115, 415–421. https://doi.org/10.1016/j.carbpol.2014.09.006

Chen, Q., Zhang, J., Zhang, Y., Kaplan, D. L., & Wang, Q. (2022). Protein-amylose/amylopectin molecular interactions during high-moisture extruded texturization toward plant-based meat substitutes applications. *Food Hydrocolloids*, 127, Article 107559. https://doi.org/10.1016/j.foodhyd.2022.107559

Chi, H., Xu, K., Wu, X., Chen, Q., Xue, D., Song, C., Zhang, W., & Wang, P. (2008). Effect of acetylation on the properties of corn starch. *Food Chemistry*, 106(3), 923–928. https://doi.org/10.1016/j.foodchem.2007.07.002

Clifton, P. M. (2011). Protein and coronary heart disease: The role of different protein sources. *Current Atherosclerosis Reports*, 13(6), 493–498. https://doi.org/10.1007/s11883-011-0208-x

Damodaran, S. (2008a) Fennema's food chemistry (4th ed.). Amino Acids, Peptides, and Proteins, (Chapter 5). CRC Press/Taylor & Francis. https://doi.org/10.1201/9781420020526

Damodaran, S. (2008b) Fennema's food chemistry (4th ed.). Carbohydrates, (Chapter 3). CRC Press/Taylor & Francis. https://doi.org/10.1201/9781420020526

Day, L., & Swanson, BG. (2013). Functionality of Protein-Fortified Extrudates. *Comprehensive Reviews in Food Science and Food Safety*, 12(5), 546-564. https://doi: 10.1111/1541-4337.12023

Dekkers, B. L., Boom, R. M., & van der Goot, A. J. (2018a). Structuring processes for meat analogues. *Trends in Food Science and Technology*, 81, 25–36. https://doi.org/10.1016/j.tifs.2018.08.011

Dekkers, B. L., Boom, R. M., & van der Goot, A. J. (2018b). Viscoelastic properties of soy

protein isolate – pectin blends: Richer than those of a simple composite material. *Food Research International*, 107, 281–288. https://doi.org/10.1016/j.foodres.2018.02.037

Deng, Q., Wang, Z., Fu, L., He, Z., Zeng, M., Qin, F., & Chen, J. (2023). High-moisture extrusion of soy protein: Effects of insoluble dietary fiber on anisotropic extrudates. *Food Hydrocolloids*, 141, Atricle 108688. https://doi.org/10.1016/j.foodhyd.2023.108688

Duque-Estrada, P., Hardiman, K., Bøgebjerg Dam, A., Dodge, N., Aaslyng, M. D., & Petersen, I. L. (2023). Protein blends and extrusion processing to improve the nutritional quality of plant proteins. *Food and Function*, 14(16), 7361–7374. https://doi.org/10.1039/d2fo03912e

Ek, P., & Ganjyal, G. M. (2020a). Basics of extrusion processing. Extrusion Cooking, (pg 1–28). *Elsevier*. https://doi.org/10.1016/b978-0-12-815360-4.00001-8

Ek, P., Gu, B. J., Saunders, S. R., Huber, K., & Ganjyal, G. M. (2021). Exploration of physicochemical properties and molecular interactions between cellulose and high-amylose cornstarch during extrusion processing. *Current Research in Food Science*, 4, 588–597. https://doi.org/10.1016/j.crfs.2021.07.001

Ek, P., Kowalski, R. J., & Ganjyal, G. M. (2020b). Raw material behaviors in extrusion processing I (Carbohydrates). In Extrusion Cooking (pg 119–152). *Elsevier*. https://doi.org/10.1016/b978-0-12-815360-4.00004-3

El Seoud, O.A., Nawaz, H., & Areas, E.P.G. (2013). Chemistry and Applications of Polysaccharide Solutions in Strong Electrolytes/Dipolar Aprotic Solvents: An Overview. *Molecules*, 18(1), 1270-1313. https://doi.org/10.3390/molecules18011270

Englyst, H.N., Kingman, S. M., & Cummings, J. H. (1992). Classification and measurement of nutritionally important starch fractions. *European Journal of Clinical Nutrition*, 46(2), 33-50.

Esbroeck, T., Sala, G., Stieger, M., & Scholten, E. (2024). Effect of structural characteristics on functional properties of textured vegetable proteins. *Food Hydrocolloids*, 149, Article 109529. https://doi.org/10.1016/j.foodhyd.2023.109529

Ferawati, F., Zahari, I., Barman, M., Hefni, M., Ahlström, C., Witthöft, C., & Östbring, K. (2021). High-moisture meat analogues produced from yellow pea and faba bean protein isolates/concentrate: Effect of raw material composition and extrusion parameters on texture properties. *Foods*, 10(4), Article 843. https://doi.org/10.3390/foods10040843

Fiorentini, M., Kinchla, A. J., & Nolden, A. A. (2020). Role of sensory evaluation in consumer acceptance of plant-based meat analogs and meat extenders: a scoping review. *Foods*, 9(9), Article 1334. https://doi.org/10.3390/foods9091334

FAO (1985). Food and Agriculture Organization of the United Nations, World Health Organization. Codex https://www.fao.org/fao-who-codexalimentarius/codex-texts/guidelines/en/.

Food and Drug Regulations, CRC, C 870, B.01.503(4) (2024). Dietary Fibre claims. SOR/2022-168, s. 52. https://inspection.canada.ca/food-labels/labelling/industry/nutrient-content/specific-claim-requirements/eng/1627085614476/1627085788924#a12

Grabowska, K. J., Zhu, S., Dekkers, B. L., de Ruijter, N. C. A., Gieteling, J., & van der Goot, A. J. (2016). Shear-induced structuring as a tool to make anisotropic materials using soy protein concentrate. *Journal of Food Engineering*, 188, 77–86. https://doi.org/10.1016/j.jfoodeng.2016.05.010

Grasso, S., & Goksen, G. (2023). The best of both worlds? Challenges and opportunities in the development of hybrid meat products from the last 3 years. *LWT*, 173, Article 114235. https://doi.org/10.1016/j.lwt.2022.114235

Green, A., Blattmann, C., Chen, C., & Mathys, A. (2022). The role of alternative proteins and future foods in sustainable and contextually-adapted flexitarian diets. *Trends in Food Science and Technology*, 124, 250–258. https://doi.org/10.1016/j.tifs.2022.03.026

Grossmann, L. (2023). Structural properties of pea proteins (Pisum sativum) for sustainable food matrices. *Critical Reviews in Food Science and Nutrition*, 1-21. https://doi.org/10.1080/10408398.2023.2199338

Guegun, J., & Cerletti, P. New and Developing Sources of Food Proteins. (1994). In B.J.F Hudson. *Springer US*. https://doi.org/10.1007/978-1-4615-2652-0

Guerrieri, N., & Cavaletto, M. (2017). *Cereals proteins* (Chapter 8). In Proteins in Food Processing, Second Edition (pg 223–244). Elsevier. https://doi.org/10.1016/B978-0-08-100722-8.00009-7

Gulati, P., Brahma, S., & Rose, D. J. (2020). Impacts of extrusion processing on nutritional components in cereals and legumes: Carbohydrates, proteins, lipids, vitamins, and minerals. *Extrusion Cooking,* (pg 415–443). Elsevier. https://doi.org/10.1016/b978-0-12-815360-4.00013-4

Guo, J., Tan, L., & Kong, l. (2022). Multiple levels of health benefits from resistant starch. *Journal of Agriculture and Food Science*, 10, Article 100380. https://doi.org/10.1016/j.jafr.2022.100380

Guy, R. (2001). Raw materials for extrusion cooking. *Extrusion Cooking: Technologies and applications,* (pg 5-28). Woodhead Publishing.

Guyony, V., Fayolle, F., & Jury, V. (2023). High moisture extrusion of vegetable proteins for making fibrous meat analogs: A review. *Food Reviews International*, 39(7), 4262–4287. https://doi.org/10.1080/87559129.2021.2023816

Hall, A. E., & Moraru, C. I. (2021). Structure and function of pea, lentil and faba bean proteins treated by high pressure processing and heat treatment. *LWT*, 152, Article 112349. https://doi.org/10.1016/j.lwt.2021.112349

Han, C., Wang, G., Guo, J., Wang, J., & Yang, X. (2023). Oral oil release improves lubrication and sensory properties of meat analogs with protein-stabilized oleogel. *Food Hydrocolloids*, 142, Article 108788https://doi.org/10.1016/j.foodhyd.2023.108788

He, X., Zhou, L., Gunness, P., Solah, V. A., & Sun, Q. (2024). Lecithin enhances the complexation between pea starch and fatty acids in aqueous system, and affects the starch's structure and enzymatic hydrolysis. *Food Chemistry*, 433. https://doi.org/10.1016/j.foodchem.2023.137326

Herrera, M. P., Gao, J., Vasanthan, T., Temelli, F., & Henderson, K. (2016). β-Glucan content, viscosity, and solubility of Canadian grown oat as influenced by cultivar and growing location. *Canadian Journal of Plant Science*, 96(2), 183–196. https://doi.org/10.1139/cjps-2014-0440

Hidayat, B. T., Wea, & Andriati. (2018). Physicochemical, sensory attributes and protein profile by SDS-PAGE of beef sausage substituted with texturized vegetable protein. *Food Research*, 2(1), 20–31. https://doi.org/10.26656/fr-2017.2(1).106

Hong, S., Shen, Y., & Li, Y. (2022). Physicochemical and Functional Properties of Texturized Vegetable Proteins and Cooked Patty Textures: Comprehensive Characterization and Correlation Analysis. *Foods*, 11(17), Article 2619. https://doi.org/10.3390/foods11172619

Huang, X., Liu, H., Ma, Y., Mai, S., & Li, C. (2022). Effects of Extrusion on Starch Molecular

Degradation, Order–Disorder Structural Transition and Digestibility—A Review. *Foods*, 11(16). Article 2538. https://doi.org/10.3390/foods11162538

Hussain, S. Z., & Singh, B. (2013). Effect of extrusion conditions on pasting behavior and microstructure of refabricated rice: A response surface analysis. *Cereal Chemistry*, 90(5), 480–489. https://doi.org/10.1094/CCHEM-12-12-0170-R

Kesarwani, A., Chiang, P. Y., & Chen, S. S. (2016). Rapid Visco Analyzer Measurements of japonica Rice Cultivars to Study Interrelationship between Pasting Properties and Farming System. *International Journal of Agronomy*, 2016, Article 3595326. https://doi.org/10.1155/2016/3595326

Khatun, A., Waters, D. L. E., & Liu, L. (2019). A Review of Rice Starch Digestibility: Effect of Composition and Heat-Moisture Processing. *Starch*, 71(9-10), Article 1900090. https://doi.org/10.1002/star.201900090

Kimura, A., Takako, F., Meili, Z., Shiori, M., Maruyama, N., & Utsumi, S. (2008). Comparison of physicochemical properties of 7S and 11S globulins from pea, fava bean, cowpea, and French bean with those of soybean-french bean 7S globulin exhibits excellent properties. *Journal of Agricultural and Food Chemistry*, 56(21), 10273–10279. https://doi.org/10.1021/jf801721b

Kong, L., Lee, C., Kim, S. H., & Ziegler, G. R. (2014). Characterization of starch polymorphic structures using vibrational sum frequency generation spectroscopy. *Journal of Physical Chemistry*, 118(7), 1775–1783. https://doi.org/10.1021/jp411130n

Kornet, C., Venema, P., Nijsse, J., van der Linden, E., van der Goot, A. J., & Meinders, M. (2020). Yellow pea aqueous fractionation increases the specific volume fraction and viscosity of its dispersions. *Food Hydrocolloids*, 99, Article 105332. https://doi.org/10.1016/j.foodhyd.2019.105332

Kour, J., Singh, S., & Saxena, D. C. (2019). Effect of nutraceuticals (beta-glucan concentrate, flaxseed lignan concentrate and gamma oryzanol concentrate) on nutritional, textural, pasting, thermal, structural and morphological properties of corn and rice flour blend based RTE extrudates. *Journal of Food Measurement and Characterization*, 13(2), 988–1003. https://doi.org/10.1007/s11694-018-0013-0

Kristiawan, M., & della Valle, G. (2020). Transport phenomena and material changes during

extrusion. *Extrusion Cooking* (pg 179–204). Elsevier. https://doi.org/10.1016/b978-0-12-815360-4.00006-7

Kurek, M. A., Onopiuk, A., Pogorzelska-nowicka, E., Szpicer, A., Zalewska, M., & Półtorak, A. (2022). Novel Protein Sources for Applications in Meat-Alternative Products—Insight and Challenges. *Foods*, 11(7), Article 957. https://doi.org/10.3390/foods11070957

Lambert, J. E., Parnell, J. A., Tunnicliffe, J. M., Han, J., Sturzenegger, T., & Reimer, R. A. (2017). Consuming yellow pea fiber reduces voluntary energy intake and body fat in overweight/obese adults in a 12-week randomized controlled trial. *Clinical Nutrition*, 36(1), 126–133. https://doi.org/10.1016/j.clnu.2015.12.016

Lazou, A. E. (2022). Food extrusion: An advanced process for innovation and novel product development. *Critical Reviews in Food Science and Nutrition*. https://doi.org/10.1080/10408398.2022.2143474

Lazou, A., & Krokida, M. (2010). Structural and textural characterization of corn-lentil extruded snacks. *Journal of Food Engineering*, 100(3), 392–408. https://doi.org/10.1016/j.jfoodeng.2010.04.024

Lee, C. J., Horsley, R. D., Manthey, F. A., & Schwarz, P. B. (1997). Comparisons of β-glucan content of barley and oat. *Cereal Chemistry*, 74(5), 571–575. https://doi.org/10.1094/CCHEM.1997.74.5.571

Lee, J. S., Oh, H., Choi, I., Yoon, C. S., & Han, J. (2022). Physico-chemical characteristics of rice protein-based novel textured vegetable proteins as meat analogues produced by low-moisture extrusion cooking technology. *LWT*, 157, Article 113056. https://doi.org/10.1016/j.lwt.2021.113056

Lee, Y. P., Puddey, I. B., & Hodgson, J. M. (2008). Protein, fibre and blood pressure: Potential benefit of legumes. *Clinical and Experimental Pharmacology and Physiology*, 35(4), 473–476. https://doi.org/10.1111/j.1440-1681.2008.04899.x

Li, C. (2022). Recent progress in understanding starch gelatinization - An important property determining food quality. *Carbohydrate Polymers*, 293, Article 119735. https://doi.org/10.1016/j.carbpol.2022.119735

Li, C., Gong, B., Hu, Y., Liu, X., Guan, X., & Zhang, B. (2020). Combined crystalline, lamellar and granular structural insights into in vitro digestion rate of native starches. *Food Hydrocolloids*, 105, Article 105823. https://doi.org/10.1016/j.foodhyd.2020.105823

Lin, L., Guo, D., Huang, J., Zhang, X., Zhang, L., & Wei, C. (2016). Molecular structure and enzymatic hydrolysis properties of starches from high-amylose maize inbred lines and their hybrids. *Food Hydrocolloids*, 58, 246–254. https://doi.org/10.1016/j.foodhyd.2016.03.001

Liu, K. (2014). Fractionation of oats into products enriched with protein, beta-glucan, starch, or other carbohydrates. *Journal of Cereal Science*, 60(2), 317–322. https://doi.org/10.1016/j.jcs.2014.06.002

Lu, Z. H., Donner, E., & Liu, Q. (2019). The Effect of Various Extracting Agents on the Physicochemical and Nutritional Properties of Pea Starch. *Starch*, 71(11–12), Article 1900123. https://doi.org/10.1002/star.201900123

Lue, S., Hsieh, F., Huff, H.E., (1990). Extrusion cooking of corn meal and sugar beet fiber: effects on expansion properties, starch gelatinization, and dietary fiber content. *Cereal Chemistry*, 68(3), 227-234.

Lyu, J. S., Lee, J. S., Chae, T. Y., Yoon, C. S., & Han, J. (2023). Effect of screw speed and die temperature on physicochemical, textural, and morphological properties of soy protein isolate-based textured vegetable protein produced via a low-moisture extrusion. Food Science and Biotechnology, 32(5), 659–669. https://doi.org/10.1007/s10068-022-01207-8

Magallanes-Cruz, P. A., Flores-Silva, P. C., & Bello-Perez, L. A. (2017). Starch Structure Influences Its Digestibility: A Review. *Journal of Food Science*, 82(9), 2016–2023. https://doi.org/10.1111/1750-3841.13809

Maningat, C., Demeritt, K., Chinnaswamy, R., Bassi, D. (1999). Properties and applications of texturized wheat gluten. *Cereal Foods World*, 44(9), 650-655.

Marcotorchino, J., Roux, J., Bariohay, B., Guerin-Deremaux, L., & Thabuis, C. (2021). Pea Hull Fiber Improves Bowel Regularity in Both a Healthy and Constipated Rat Model. *Food and Nutrition Sciences*, 12(10), 950–961. https://doi.org/10.4236/fns.2021.1210070

Martens, G. L., Nilsen, M. M., & Provan, F. (2017). Pea Hull Fibre: Novel and Sustainable Fibre with Important Health and Functional Properties. *EC Nutrition*, 10(4), 139-148.

Martineau-Côté, D., Achouri, A., Karboune, S., & L'Hocine, L. (2022). Faba Bean: An Untapped Source of Quality Plant Proteins and Bioactives. *Nutrients*, 14(8), 1541. https://doi.org/10.3390/nu14081541

McCready, R. M., Guggolz, J., Silviera, V., & Owens, H. S. (1950). Determination of Starch and

Amylose in Vegetables Application to Peas. *Analytical Chemistry*, 22(9) 1156-1158. https://doi.org/10.1021/ac60045a016

McKeown, N. M., Fahey, G. C., Slavin, J., & van der Kamp, J. W. (2022). Fibre intake for optimal health: how can healthcare professionals support people to reach dietary recommendations? *BMJ*, Article 054370. https://doi.org/10.1136/bmj-2020-054370

Morach, B., Witte, B., Walker, D., von Koeller, E., Grosse-Holz, F., Rogg, J., Brigl, M. (2021). Protein transformation. Boston Consulting Group, Retrieved Feb 4. 2024. https://www.bcg.com/publications/2021/the-benefits-of-plant-based-meats

Morales Alvarez, J. C. (2020). Engineering aspects of extrusion: Extrusion processing as a multiple-input and multiple-output system. *Extrusion Cooking* (pg 29–71). Elsevier. https://doi.org/10.1016/b978-0-12-815360-4.00002-x

Nguyen, T. T. L., Flanagan, B. M., Tao, K., Ni, D., Gidley, M. J., Fox, G. P., & Gilbert, R. G. (2022). Effect of processing on the solubility and molecular size of oat β-glucan and consequences for starch digestibility of oat-fortified noodles. *Food Chemistry*, 372, Article 131291. https://doi.org/10.1016/j.foodchem.2021.131291

Nilsson, K., Sandström, C., Özeren, H. D., Vilaplana, F., Hedenqvist, M., & Langton, M. (2022). Physiochemical and thermal characterisation of faba bean starch. *Journal of Food Measurement and Characterization*, 16(6), 4470–4485. https://doi.org/10.1007/s11694-022-01543-7

Osen, R., Toelstede, S., Wild, F., Eisner, P., & Schweiggert-Weisz, U. (2014). High moisture extrusion cooking of pea protein isolates: Raw material characteristics, extruder responses, and texture properties. *Journal of Food Engineering*, 127, 67–74. https://doi.org/10.1016/j.jfoodeng.2013.11.023

Parmar, P., Bobade, H., Singh, B., & Pathania, S. (2021). Extrusion technologies for cereal–pulses blends. *Pulse Foods* (pg 393–421). Elsevier. https://doi.org/10.1016/b978-0-12-818184-3.00016-7

Pengjun, T., Sringarm, C., Kunanopparat, T., Rungchang, S., Ditudompo, S., & Siriwattanayotin, S. (2023). Effect of defatted rice bran addition on properties of texturized soy and rice protein products. *International Journal of Food Engineering*, 19(10), 435–444. https://doi.org/10.1515/ijfe-2023-0041

Philipp, C., Emin, M. A., Buckow, R., Silcock, P., & Oey, I. (2018). Pea protein-fortified

extruded snacks: Linking melt viscosity and glass transition temperature with expansion behaviour. *Journal of Food Engineering*, 217, 93–100. https://doi.org/10.1016/j.jfoodeng.2017.08.022

Philipp, C., Oey, I., Silcock, P., Beck, S. M., & Buckow, R. (2017). Impact of protein content on physical and microstructural properties of extruded rice starch-pea protein snacks. *Journal of Food Engineering*, 212, 165–173. https://doi.org/10.1016/j.jfoodeng.2017.05.024

Pietsch, V. L., Bühler, J. M., Karbstein, H. P., & Emin, M. A. (2019). High moisture extrusion of soy protein concentrate: Influence of thermomechanical treatment on protein-protein interactions and rheological properties. *Journal of Food Engineering*, 251, 11–18. https://doi.org/10.1016/j.jfoodeng.2019.01.001

Pozo, C., Rodríguez-Llamazares, S., Bouza, R., Barral, L., Castaño, J., Müller, N., & Restrepo, I. (2018). Study of the structural order of native starch granules using combined FTIR and XRD analysis. *Journal of Polymer Research*, 25(12), Article 266. https://doi.org/10.1007/s10965-018-1651-y

Prabha, K., Ghosh, P., S, A., Joseph, R. M., Krishnan, R., Rana, S. S., & Pradhan, R. C. (2021). Recent development, challenges, and prospects of extrusion technology. *Future Foods*, 3, Article 100019. https://doi.org/10.1016/j.fufo.2021.100019

Rajpurohit, B., & Li, Y. (2023). Overview on pulse proteins for future foods: ingredient development and novel applications. *Journal of Future Foods*, 3(4), 340–356. https://doi.org/10.1016/j.jfutfo.2023.03.005

Ralet, M.-C., della Valle, G., & Thibauit, J.-F. (1993). Raw and extruded fibre from pea hulls. Part I: Composition and physico-chemical properties. *Carbohydrate Polymers*, 20(1), 17-23. https://doi.org/10.1016/0144-8617(93)90028-3

Rangira, I., Gu, B. J., Ek, P., & Ganjyal, G. M. (2020). Pea starch exhibits good expansion characteristics under relatively lower temperatures during extrusion cooking. *Journal of Food Science*, 85(10), 3333–3344. https://doi.org/10.1111/1750-3841.15450

Reinkensmeier, A., Bußler, S., Schlüter, O., Rohn, S., & Rawel, H. M. (2015). Characterization of individual proteins in pea protein isolates and air classified samples. *Food Research International*, 76(1), 160–167. https://doi.org/10.1016/j.foodres.2015.05.009

Robin, F., Schuchmann, H. P., & Palzer, S. (2012). Dietary fiber in extruded cereals: Limitations

and opportunities. *Trends in Food Science and Technology*, 28(1), 23–32. https://doi.org/10.1016/j.tifs.2012.06.008

Rodriguez, Y., & Beyrer, M. (2023). Impact of native pea proteins on the gelation properties of pea protein isolates. *Food Structure*, 37, Article 100340. https://doi.org/10.1016/j.foostr.2023.100340

Ryu, G.-H. (2020). Extrusion cooking of high-moisture meat analogues. *Extrusion Cooking* (pg 205–224). Elsevier. https://doi.org/10.1016/b978-0-12-815360-4.00007-9

Sadat, A., & Joye, I. J. (2020). Peak fitting applied to fourier transform infrared and raman spectroscopic analysis of proteins. *Applied Sciences*, 10(17), Article 5918. https://doi.org/10.3390/app10175918

Sahu, C., Patel, S., & Tripathi, A. K. (2022). Effect of extrusion parameters on physical and functional quality of soy protein enriched maize based extruded snack. *Applied Food Research*, 2(1), Article 100072. https://doi.org/10.1016/j.afres.2022.100072

Saldanha do Carmo, C., Rieder, A., Varela, P., Zobel, H., Dessev, T., Nersten, S., Gaber, S. M., Sahlstrøm, S., & Knutsen, S. H. (2023). Texturized vegetable protein from a faba bean protein concentrate and an oat fraction: Impact on physicochemical, nutritional, textural and sensory properties. *Future Foods*, 7, Article 100228. https://doi.org/10.1016/j.fufo.2023.100228

Sayanjali, S., Ying, D., Sanguansri, L., Buckow, R., Augustin, M. A., & Gras, S. L. (2017). The effect of extrusion on the functional properties of oat fibre. *LWT*, 84, 106–113. https://doi.org/10.1016/j.lwt.2017.05.025

Schmid, E. M., Farahnaky, A., Adhikari, B., & Torley, P. J. (2022). High moisture extrusion cooking of meat analogs: A review of mechanisms of protein texturization. *Comprehensive Reviews in Food Science and Food Safety*, 21(6), 4573–4609. https://doi.org/10.1111/1541-4337.13030

Scott, G., & Awika, J. M. (2023). Effect of protein–starch interactions on starch retrogradation and implications for food product quality. *Comprehensive Reviews in Food Science and Food Safety*, 22(3), 2081–2111. https://doi.org/10.1111/1541-4337.13141

Sha, L., & Xiong, Y. L. (2020). Plant protein-based alternatives of reconstructed meat: Science, technology, and challenges. *Trends in Food Science and Technology*, 102, 51–61. https://doi.org/10.1016/j.tifs.2020.05.022

Shi, D., & Nickerson, M. T. (2022). Comparative evaluation of the functionality of faba bean protein isolates with major legume proteins in the market. *Cereal Chemistry*, 99(6), 1246–1260. https://doi.org/10.1002/cche.10589

Singh, N. (2021). Functional and physicochemical properties of pulse starch. *Pulse Foods* (pg 87–112). Elsevier. https://doi.org/10.1016/b978-0-12-818184-3.00005-2

Sokolowski, C. M., Higgins, S., Vishwanathan, M., & Evans, E. M. (2020). The relationship between animal and plant protein intake and overall diet quality in young adults. *Clinical Nutrition*, 39(8), 2609–2616. https://doi.org/10.1016/j.clnu.2019.11.035

Sridhar, K., & Kaur, R. (2023). β-Glucan. In Valorization of Biomass to Bioproducts. *Biochemicals and Biomaterials*, 27–43. https://doi.org/10.1016/B978-0-12-822887-6.00006-1

Stone, A. K., Nosworthy, M. G., Chiremba, C., House, J. D., & Nickerson, M. T. (2019). A comparative study of the functionality and protein quality of a variety of legume and cereal flours. *Cereal Chemistry*, 96(6), 1159–1169. https://doi.org/10.1002/cche.10226

Svanes, E., Waalen, W., & Uhlen, A. K. (2022). Environmental impacts of field peas and faba beans grown in Norway and derived products, compared to other food protein sources. *Sustainable Production and Consumption*, 33, 756–766. https://doi.org/10.1016/j.spc.2022.07.020

Tas, A. A., & Shah, A. U. (2021). The replacement of cereals by legumes in extruded snack foods: Science, technology and challenges. *Trends in Food Science and Technology*, 116, 701–711. https://doi.org/10.1016/j.tifs.2021.08.016

Timm, M., Offringa, L. C., van Klinken, B. J. W., & Slavin, J. (2023). Beyond Insoluble Dietary Fiber: Bioactive Compounds in Plant Foods. *Nutrients*, 15(19), Article 4138. https://doi.org/10.3390/nu15194138

Todica, M., Nagy, E. M., Niculaescu, C., Stan, O., Cioica, N., & Pop, C. V. (2016). XRD investigation of some thermal degraded starch based materials. *Journal of Spectroscopy*, 2016, Article 9605312. https://doi.org/10.1155/2016/9605312

Tolstoguzov, V. B. (1993). Thermoplastic Extrusion-the Mechanism of the Formation of Extrudate Structure and Properties. *Journal of the American Oil Chemists' Society*, 70, 417-424. https://doi.org/10.1007/BF02552717

Torres, F. G., Mayorga, J. P., Vilca, C., Arroyo, J., Castro, P., & Rodriguez, L. (2019).

Preparation and characterization of a novel starch–chestnut husk biocomposite. *SN Applied Sciences*, 1(10), Article 1158. https://doi.org/10.1007/s42452-019-1204-y

Tripathi, A., Iswarya, V., Rawson, A., Singh, N., Oomah, B. D., & Patras, A. (2021). Chemistry of pulses-macronutrients. *Pulse Foods* (pg 31–59). Elsevier. https://doi.org/10.1016/b978-0-12-818184-3.00003-9

Tsoukala, A., Papalamprou, E., Makri, E., Doxastakis, G., & Braudo, E. E. (2006). Adsorption at the air-water interface and emulsification properties of grain legume protein derivatives from pea and broad bean. *Colloids and Surfaces B: Biointerfaces*, 53(2), 203–208. https://doi.org/10.1016/j.colsurfb.2006.08.019

Twombly, W. (2020). Raw material behaviors in extrusion processing II; Proteins, lipids, and other minor ingredients. *Extrusion Cooking* (pg 153–178). Elsevier. https://doi.org/10.1016/b978-0-12-815360-4.00005-5

Tzitzikas, E. N., Vincken, J. P., de Groot, J., Gruppen, H., & Visser, R. G. F. (2006). Genetic variation in pea seed globulin composition. *Journal of Agricultural and Food Chemistry*, 54(2), 425–433. https://doi.org/10.1021/jf0519008

United Nations. World Population Prospects 2022 Summary of Results. Department of Economics and Social Affairs. (New York: United Nations, 2022), available from file:///C:/Users/17809/Downloads/undesa_pd_2022_WPP_summary_of_results.pdf

Van Loo, E. J., Caputo, V., & Lusk, J. L. (2020). Consumer preferences for farm-raised meat, lab-grown meat, and plant-based meat alternatives: Does information or brand matter? *Food Policy*, 95, Article 101931. https://doi.org/10.1016/j.foodpol.2020.101931

Vatansever, S., Tulbek, M.C., & Riaz, M.N. (2020). Low- and High-Moisture Extrusion of Pulse Proteins as Plant-Based Meat Ingredients: A Review. *Cereal Foods World*, 65(4). https://doi.org/10.1094/cfw-65-4-0038

Vatansever, S., Whitney, K., Ohm, J. B., Simsek, S., & Hall, C. (2021). Physicochemical and multi-scale structural alterations of pea starch induced by supercritical carbon dioxide + ethanol extraction. *Food Chemistry*, 344, Article 128699. https://doi.org/10.1016/j.foodchem.2020.128699

Verbeek, C. J. R., & van den Berg, L. E. (2010). Extrusion processing and properties of protein-based thermoplastics. *Macromolecular Materials and Engineering*, 295(1), 10–21. https://doi.org/10.1002/mame.200900167

Von Kaufmann, F., & Skafida, V. (2023). Captive school markets, industry self-regulation, and public-private partnerships: Narratives shaping the development of alternative proteins in the United States, 1965–1982. *Food Policy*, 116, Article 102437. https://doi.org/10.1016/j.foodpol.2023.102437

Waliullah, M. H., Mu, T., & Ma, M. (2021). Recovery of total, soluble, and insoluble dietary fiber from potato (Solanum tuberosum) residues and comparative evaluation of their structural, physicochemical, and functional properties. *Journal of Food Processing and Preservation*, 45(7), Article 15650. https://doi.org/10.1111/jfpp.15650

Wang, B., Dong, Y., Fang, Y., Gao, W., Kang, X., Liu, P., Yan, S., Cui, B., & Abd El-Aty, A. M. (2022). Effects of different moisture contents on the structure and properties of corn starch during extrusion. *Food Chemistry*, 368, Article 130804. https://doi.org/10.1016/j.foodchem.2021.130804

Wang, N., Warkentin, T. D., Vandenberg, B., & Bing, D. J. (2014). Physicochemical properties of starches from various pea and lentil varieties, and characteristics of their noodles prepared by high temperature extrusion. *Food Research International*, 55, 119–127. https://doi.org/10.1016/j.foodres.2013.10.043

Wang, S., Kowalski, R. J., Kang, Y., Kiszonas, A. M., Zhu, M. J., & Ganjyal, G. M. (2017). Impacts of the Particle Sizes and Levels of Inclusions of Cherry Pomace on the Physical and Structural Properties of Direct Expanded Corn Starch. *Food and Bioprocess Technology*, 10(2), 394–406. https://doi.org/10.1007/s11947-016-1824-9

Wang, S., Sharp, P., & Copeland, L. (2011). Structural and functional properties of starches from field peas. *Food Chemistry*, 126(4), 1546–1552. https://doi.org/10.1016/j.foodchem.2010.11.154

Wang, T. L., Bogracheva, T. Y., & Hedley, C. L. (1998). Starch: as simple as A, B, C? *Journal of Experimental Botany*, 49(320), 481-502. https://academic.oup.com/jxb/article/49/320/481/514900

Wang, Y., Guldiken, B., Tulbek, M., House, J.D., & Nickerson, M., (2020). Impact of alcohol washing on the flavour profiles, functionality and protein quality of air classified pea protein enriched flour. *Food Research International*, 132, Article 109085. https://doi.org/10.1016/j.foodres.2020.109085

Warren, F. J., Gidley, M. J., & Flanagan, B. M. (2016). Infrared spectroscopy as a tool to

characterise starch ordered structure - A joint FTIR-ATR, NMR, XRD and DSC study. *Carbohydrate Polymers*, 139, 35–42. https://doi.org/10.1016/j.carbpol.2015.11.066

Webb, D., Li, Y., & Alavi, S. (2023). Chemical and physicochemical features of common plant proteins and their extrudates for use in plant-based meat. *Trends in Food Science and Technology*, 131, 129–138. https://doi.org/10.1016/j.tifs.2022.11.006

Webb, D., Plattner, B. J., Donald, E., Funk, D., Plattner, B. S., & Alavi, S. (2020). Role of chickpea flour in texturization of extruded pea protein. *Journal of Food Science*, 85(12), 4180–4187. https://doi.org/10.1111/1750-3841.15531

Wittek, P., Karbstein, H. P., Azad Emin, M., José, M., & Apesteguía, B. (2021b). Blending Proteins in High Moisture Extrusion to Design Meat Analogues: Rheological Properties, Morphology Development and Product Properties. *Foods*, 10(7), Article 1509. https://doi.org/10.3390/foods

Wittek, P., Walther, G., Karbstein, H. P., & Emin, M. A. (2021a). Comparison of the rheological properties of plant proteins from various sources for extrusion applications. *Foods*, 10(8), Article 1700. https://doi.org/10.3390/foods10081700

Xiao, T., Su, X., Jiang, R., zhou, H., & Xie, T. (2023). Low moisture extrusion of soybean protein isolate: Effect of β-glucan on the physicochemical properties of the product. *LWT*, 179, Article 114660. https://doi.org/10.1016/j.lwt.2023.114660

Xie, F., Liu, H., Chen, P., Xue, T., Chen, L., Yu, L., & Corrigan, P. (2006). Starch gelatinization under shearless and shear conditions. *International Journal of Food Engineering*, 2(5), Article 6. https://doi.org/10.2202/1556-3758.1162

Xie, L., Chen, N., Duan, B., Zhu, Z., & Liao, X. (2008). Impact of proteins on pasting and cooking properties of waxy and non-waxy rice. *Journal of Cereal Science*, 47(2), 372–379. https://doi.org/10.1016/j.jcs.2007.05.018

Xu, B., Zhang, C., Liu, Z., Xu, H., Wei, B., Wang, B., Sun, Q., Zhou, C., & Ma, H. (2023). Starches modification with rose polyphenols under multi-frequency power ultrasonic fields: Effect on physicochemical properties and digestion behavior. *Ultrasonics Sonochemistry*, 98, Article 106515. https://doi.org/10.1016/j.ultsonch.2023.106515

Xu, X., Sharma, P., Shu, S., Lin, T. S., Ciais, P., Tubiello, F. N., Smith, P., Campbell, N., & Jain,

A. K. (2021). Global greenhouse gas emissions from animal-based foods are twice those of plant-based foods. *Nature Food*, 2(9), 724–732. https://doi.org/10.1038/s43016-021-00358-x

Yacu, W. (2020). Extruder screw, barrel, and die assembly: General design principles and operation. *Extrusion Cooking* (pg 73–117). Elsevier. https://doi.org/10.1016/b978-0-12-815360-4.00003-1

Yang, J., Liu, G., Zeng, H., & Chen, L. (2018). Effects of high pressure homogenization on faba bean protein aggregation in relation to solubility and interfacial properties. *Food Hydrocolloids*, 83, 275–286. https://doi.org/10.1016/j.foodhyd.2018.05.020

Yang, J., Zamani, S., Liang, L., & Chen, L. (2021). Extraction methods significantly impact pea protein composition, structure and gelling properties. *Food Hydrocolloids*, 117, Article 106678. https://doi.org/10.1016/j.foodhyd.2021.106678

Ye, J., Hu, X., Luo, S., Liu, W., Chen, J., Zeng, Z., & Liu, C. (2018). Properties of Starch after Extrusion: A Review. *Starch*, 70(11–12), Article 1700110. https://doi.org/10.1002/star.201700110

Zakaria, N.H., Muhammad, N., & Abdullah, M.M.A.B. (2017) Potential of Starc Nanocomposites for Biomedical Applications. *Materials Science and Engineering*, 209, Article 012087. https://doi:10.1088/1757-899X/209/1/012087

Zhang, G., Venkatachalam, M., & Hamaker, B. R. (2006). Structural basis for the slow digestion property of native cereal starches. *Biomacromolecules*, 7(11), 3259–3266. https://doi.org/10.1021/bm060343a

Zhang, J., Chen, Q., Kaplan, D. L., & Wang, Q. (2022b). High-moisture extruded protein fiber formation toward plant-based meat substitutes applications: Science, technology, and prospect. *Trends in Food Science and Technology*, 128, 202–216. https://doi.org/10.1016/j.tifs.2022.08.008

Zhang, J., Liu, L., Liu, H., Yoon, A., Rizvi, S. S. H., & Wang, Q. (2019). Changes in conformation and quality of vegetable protein during texturization process by extrusion. *Critical Reviews in Food Science and Nutrition*, 59(20), 3267–3280. https://doi.org/10.1080/10408398.2018.1487383

Zhang, S., Huang, W., Roopesh, M. S., & Chen, L. (2022c). Pre-treatment by combining

atmospheric cold plasma and pH-shifting to prepare pea protein concentrate powders with improved gelling properties. *Food Research International*, 154, Article 111028. https://doi.org/10.1016/j.foodres.2022.111028

Zhang, Z., Zhang, L., He, S., Li, X., Jin, R., Liu, Q., Chen, S., & Sun, H. (2022a). High-moisture Extrusion Technology Application in the Processing of Textured Plant Protein Meat Analogues: A Review. *Food Reviews International*, 39(8), 4873-4908. https://doi.org/10.1080/87559129.2021.2024223

Appendix

Table A1. Full factorial optimization trial WHC, OHC, and ER results of pea (P) at protein content of 60% and 70%, temperatures of 160°C, 170°C and 180°C, at moisture contents of 45%, 50% and 55%.

Sample	Protein (%)	Temperature (°C)	Moisture (%)	WHC (g/g)	OHC (g/g)	ER
P60-160-45	60	160	45	2.39	1.91	1.39
P60-160-50	60	160	50	2.86	2.02	1.56
P60-160-55	60	160	55	2.99	1.99	1.46
P60-170-45	60	170	45	3.54	2.07	1.43
P60-170-50	60	170	50	3.60	2.08	1.54
P60-170-55	60	170	55	2.60	2.00	1.38
P60-180-45	60	180	45	3.30	2.20	1.63
P60-180-50	60	180	50	3.43	2.23	1.63
P60-180-55	60	180	55	3.00	2.17	1.75
P70-160-45	70	160	45	3.19	2.06	1.50
P70-160-50	70	160	50	2.88	2.09	1.60
P70-160-55	70	160	55	3.20	2.10	1.65
P70-170-45	70	170	45	1.30	2.03	1.52
P70-170-50	70	170	50	1.48	2.13	1.58
P70-170-55	70	170	55	1.35	2.17	1.96
P70-180-45	70	180	45	1.26	2.13	1.68
P70-180-50	70	180	50	1.29	2.03	1.74
P70-180-55	70	180	55	2.29	2.21	1.50